Aus dem Pathologischen Institut der Ludwig-Maximilians-Universität München

Direktor: Prof. Dr. med. Thomas Kirchner

Arbeitsgruppe Experimentelle und Molekulare Pathologie

Leiter: Prof. Dr. rer. nat. Heiko Hermeking

Integrated Analysis of p53 Targets

Dissertation zum Erwerb des

Doktorgrades der Naturwissenschaften (Dr. rer. nat.)

an der Medizinischen Fakultät

der Ludwig-Maximilians-Universität München

vorgelegt von

Sabine Hünten

aus Schweinfurt

2015

Gedruckt mit der Genehmigung der Medizinischen Fakultät
der Ludwig-Maximilians-Universität München

Betreuer:	Prof. Dr. rer. nat. Heiko Hermeking
Zweitgutachter:	Prof. Dr. Roland Kappler
Dekan:	Prof. Dr. med. dent. Reinhard Hickel

Tag der mündlichen Prüfung:
07. Oktober 2016

Ich erkläre hiermit an Eides statt, dass ich die vorliegende Dissertation mit dem Thema

„Integrated Analysis of p53 Targets“

selbständig verfasst, mich außer der angegebenen keiner weiteren Hilfsmittel bedient und alle Erkenntnisse, die aus dem Schrifttum ganz oder annähernd übernommen sind, als solche kenntlich gemacht und nach ihrer Herkunft unter Bezeichnung der Fundstelle einzeln nachgewiesen habe.

Ich erkläre des Weiteren, dass die hier vorgelegte Dissertation nicht in gleicher oder in ähnlicher Form bei einer anderen Stelle zur Erlangung eines akademischen Grades eingereicht wurde.

München, den

Sabine Hünten

Parts of this thesis have been published in:

Original article:

- Siemens H*, Jackstadt R*, **Hünten S***, Kaller M*, Menssen A*, Götz U and Hermeking H (2011). *miR-34* and *SNAIL* form a double-negative feedback loop to regulate epithelial-mesenchymal transitions. Cell Cycle 10 (24), 4256-71. [1] *equally contributing authors

- **Hünten S**, Kaller M*, Drepper F*, Oeljeklaus S, Bonfert T, Erhard F, Dueck A, Eichner N, Friedel CC, Meister G, Zimmer R, Warscheid B and Hermeking H (2015). p53-Regulated Networks of Protein, mRNA, miRNA and lncRNA Expression Revealed by Integrated Pulsed Stable Isotope Labeling With Amino Acids in Cell Culture (pSILAC) and Next Generation Sequencing (NGS) Analyses. Mol Cell Proteomics, 2015 Jul 16. pii: mcp.M115.050237. [2]
  *equally contributing authors

- **Hünten S** and Hermeking H. p53 directly activates cystatin D/CST5 to mediate mesenchymal-epithelial transition: a possible link to tumor suppression by vitamin D3. Oncotarget, 2015. **6**(18): p. 15842-56. [3]

Review/book chapter:

- **Hünten S***, Siemens H*, Kaller M*, Hermeking H (2013). The p53/microRNA Network in Cancer: Experimental and Bioinformatics Approaches. Advances in Experimental Medicine and Biology 2013; 774: 77-101. [4]
  *equally contributing authors

In addition, I made contributions to the following publication that is not further described in this work:

Original article:

- Hahn S, Jackstadt R, Siemens H, **Hünten S** and Hermeking H (2013). SNAIL and miR-34a feed-forward regulation of ZNF281/ZBP99 promotes epithelial-mesenchymal transition. *EMBO J.*; 32(23): 3079–3095. [5]

1. INTRODUCTION 1
1.1 Cancer 1
1.2 The tumor suppressor p53 1
1.3 Non-coding RNAs 4
1.3.1 microRNAs and cancer 4
1.3.2 p53 and the miRNA-network 5
1.3.3 Long non-coding RNAs 8
1.3.4 p53 and the lncRNA-network 8
1.4 Epithelial-mesenchymal transition in cancer progression 9
1.5 The role of vitamin D3 in cancer 10
2. AIMS OF THE STUDY 12
3. MATERIALS 13
3.1 Chemicals and reagents 13
3.2 Enzymes 14
3.3 Kits 14
3.4 Antibodies 14
3.4.1 Primary antibodies 14
3.4.2 Secondary antibodies 15
3.5 Vectors and oligonucleotides 15
3.5.1 Vectors 15
3.5.2 Oligonucleotides 15
3.5.2.1 Oligonucleotides used for qPCR 15
3.5.2.2 Oligonucleotides used for qChIP 16
3.5.2.3 Oligonucleotides used for cloning and mutagenesis 17
3.5.3 miRNA mimics and antagomiRs 18
3.6 Buffers and solutions 18
3.7 Laboratory equipment 19
4. METHODS 20
4.1 Bacterial cell culture 20
4.1.1 Propagation and seeding 20
4.1.2 Transformation 20
4.1.3 Purification of plasmid DNA from E.coli 20
4.2 Cell culture of human cell lines 20
4.2.1 Propagation of human cell lines 20

4.2.2 Transfection of oligonucleotides and vector constructs 21
4.2.3 Conditional expression in cell pools 21
4.2.4 Cryo-preservation of mammalian cell lines 21
4.3 Chromatin immunoprecipitation (ChIP) assay 21
4.4 Episomal vectors for ectopic protein-expression 22
4.5 Flow cytometry 22
4.5.1 Determination of the transfection efficiency (eGFP) 22
4.5.2 Cell cycle analysis by propidium iodide staining 22
4.6 Immunofluorescence and confocal-laser scanning microscopy 23
4.7 Isolation of RNA and reverse transcription 23
4.8 Luciferase assay 23
4.9 Migration and invasion analysis in Boyden-chambers 24
4.10 PCR methods 24
4.10.1 Colony PCR 24
4.10.2 Cloning of 3´-UTR sequences 25
4.10.3 qPCR using SYBR Green 25
4.10.4 qPCR using TaqMan/Exiqon Probes 25
4.11 Protein isolation, SDS-PAGE and Western blot 25
4.12 pSILAC 26
4.13 Real-time impedance measurement 28
4.14 RNA interference 29
4.15 Sequencing 29
4.15.1 DNA-sequencing 29
4.15.2 RNA-sequencing 29
4.15.3 miRNA-sequencing 30
4.15.4 ChIP-sequencing 31
4.16 Site directed mutagenesis 31
4.17 Statistical analysis 32
4.18 Web-based expression analyses and algorithms 32
4.19 Wound healing assay 32

5. RESULTS 34

5.1 *miR-34* and *SNAIL* form a double-negative feedback loop to regulate epithelial-mesenchymal transitions 34
5.1.1 p53-dependent regulation of SNAIL is mediated by miR-34a 34

5.1.2 miR-34a regulates markers of mesenchymal-epithelial transition 38
5.1.3 miR-34a dependent regulation of MET-like changes 38
5.1.4 Relevance of SNAIL as a miR-34a target 40
5.1.5 Direct repression of *miR-34* by SNAIL 40
5.2 p53-regulated networks of protein, mRNA, miRNA and lncRNA expression revealed by integrated pSILAC and NGS analyses 42
5.2.1 NGS and pSILAC analyses after p53 activation 43
5.2.2 pSILAC analysis of protein expression after p53 activation 44
5.2.3 RNA-Seq analysis of differential RNA expression after p53 activation 47
5.2.4 miR-Seq analysis after p53 activation 50
5.2.5 Genome-wide mapping of p53 DNA-binding 52
5.2.6 Identification and confirmation of novel putative p53 target genes 55
5.2.7 Comparison of p53 and miR-34a effects on *de novo* protein synthesis 59
5.2.8 miRNA-mediated repression by p53 61
5.2.9 p53-induced miRNAs regulate putative prognostic markers 63
5.3 p53 directly activates *CST5* to mediate mesenchymal-epithelial transition 69
5.3.1 p53 induces *CST5* expression 69
5.3.2 *CST5* is a direct p53 target 71
5.3.3 Role of CST5 in p53-mediated MET 73
5.3.4 Combined treatment with calcitriol and DOX enhances *CST5* induction 74
5.3.5 Opposing regulation of *CST5* by SNAIL and VDR activation 75

6. DISCUSSION 77
6.1 p53-induced *miR-34* targets SNAIL to repress EMT and stemness 77
6.2 Genome-wide analysis of the p53-induced transcriptome and proteome 81
6.3 The p53 target gene *CST5* mediates in part p53´s tumor suppressive functions 88

7. SUMMARY 92

8. ZUSAMMENFASSUNG 93

9. ABBREVIATIONS 94

10. REFERENCES 97

11. ACKNOWLEDGMENT 122

1. INTRODUCTION

1.1 Cancer

Cancer is one of the leading causes of death worldwide accounting for 8.2 million deaths in 2012 (Globocan 2012, IARC). It is a multistep process involving genetic as well as epigenetic changes that result in the activation of oncogenic pathways and/or the inactivation of tumor suppressive mechanisms. Two seminal reviews by Hanahan and Weinberg described several fundamental traits that are necessary for a cancer cell to survive, proliferate and disseminate, known as the hallmarks of cancer [6, 7] (Fig. 1). In brief, tumor cells are able to sustain proliferative signaling, are insensitive to growth-inhibitory signals and evade cell death. Furthermore, they show a limitless replicative potential, enhanced angiogenesis, invasion and metastasis. In addition, tumors are characterized by genomic instability and mutability and tumor-associated inflammation promotes tumorigenesis and progression. Moreover, tumor cells acquire a deregulated cellular energy metabolism and the ability to actively evade the immune system.

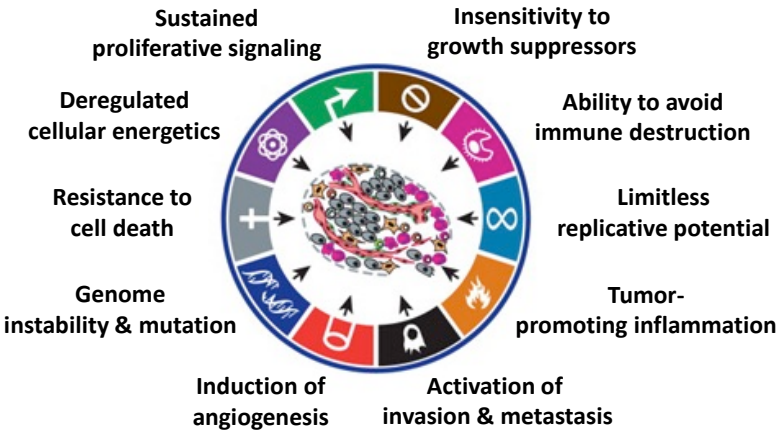

Figure 1: **The hallmarks of cancer**. The 10 fundamental traits acquired during tumor development that enable a cancer cell to survive, proliferate and disseminate. Modified from [7].

1.2 The tumor suppressor p53

p53, also known as the guardian of the genome, is one of the most important tumor suppressor proteins protecting against tumor development [8]. It acts as a tetrameric transcription factor controlling the expression of various target genes in response to diverse stimuli including DNA damage, oncogene activation or other types of cellular stresses and induces tumor suppressive processes, such as cell cycle arrest, DNA repair, senescence or apoptosis [9, 10]. The frequency of p53 mutations

in human cancer is very high ranging from 50 to 70% in for example colorectal, ovarian or head and neck cancer [11-13]. Most of the mutations that arise in the p53 gene are missense mutations with 80% affecting p53´s DNA binding domain, most often at the six hot-spot amino acid residues 175, 245, 248, 249, 273, 282 [14]. p53 mutations in one allele are usually followed by loss of heterozygosity i.e. the remaining wild-type allele is inactivated by deletion, which results in the complete loss of p53 function [15]. Interestingly, mutant p53 proteins may lose their tumor suppressive abilities and gain new tumor-promoting functions, thereby undergoing a „gain-of-function" (reviewed in [16]). In tumors retaining wild type p53, p53´s activity is often decreased by deregulations of genes directly or indirectly controlling its degradation, such as *MDM2* or $p14^{ARF}$ [17].

p53 levels are posttranslationally controlled by its main negative regulators, MDM2 and MDM4. MDM2 acts as an E3 ligase and polyubiquitinates p53, leading to its proteasomal degradation [18-20]. MDM2 and MDM4 bind to the transactivation domain (TAD) of p53 thereby inhibiting its transcriptional functions [21-23]. p53 directly induces the transcription of *MDM2* which results in a negative autoregulatory feedback loop that limits the activity of p53 in response to its activating stimuli [24, 25]. MDM2-deficient mice display embryonic lethality which is rescued by p53 knockout highlighting the tight control of p53 by MDM2 [26]. In addition, the tumor-suppressor ARF, which is activated by hyperproliferative signals, interrupts the p53-MDM2 interaction by inhibiting MDM2´s E3 ligase activity or sequestering MDM2 to nucleoli [27-29].

In unstressed, normal cells, p53 is kept at low levels. Acute DNA damage leads to the activation of the kinases ATM and ATR, which in turn phosphorylate the kinases CHK1 and/or CHK2 [30]. Once activated, these kinases phosphorylate p53 predominantly at its amino terminus to disrupt the binding of MDM2 and MDM4, resulting in increased p53 levels [31, 32]. Phosphorylation of p53´s TAD not only results in the disruption of MDM2/4 binding, but also initiates the interaction with different p53 binding proteins necessary for the initiation of transcription [33]. Upon DNA damage, the histone acetyltransferases CBP/p300, pCAF, GCN5 and TIP60 are recruited near p53 binding sites via interaction with p53´s TAD which results in the acetylation of nearby histones and chromatin unwinding [34-42]. Moreover, CBP and p300 also acetylate p53 itself at its C-terminus which leads to further stabilization and activation of p53 [43, 44]. Though acetylation is the most well-documented p53-dependent histone modification, histone methyltransferases such as PRMT1 and CARM1 cooperate with CBP/p300 to facilitate transcription of *GADD45* [45]. Additionally, the recruitment of chromatin remodeling factors such as SWI/SNF facilitates promoter opening [46]. Moreover, p53 facilitates the formation of the preinitiation complex (PIC) including RNA polymerase II and different basal transcription factors [47, 48] and assists in the recruitment of TFIID, TFIIA as well as TFIIH [49-55].

p53 is widely known as a transcriptional inducer that binds to specific response elements in a sequence-specific manner. Upon activation, p53 translocates to the nucleus where it binds as a tetramer to the sequence RRRCWWGYYY (R = purine, W = A or T, Y = pyrimidine), arranged as two palindromes with a 0 – 13 base pair (bp) long spacer [56, 57]. A large number of genes that are transcriptionally activated by p53 have been described up to date [58, 59].

In contrast to that, the mechanism for p53-mediated gene repression remained largely elusive. Several different direct and indirect mechanisms have been proposed (reviewed in [60]). It has been shown that p53 directly represses target genes by binding to a p53 binding site that, however, differs from the consensus binding site described above. In some cases it has been demonstrated that the orientation of the p53 binding site is important for the effect on gene expression and that a head-to-tail formation (RRRCWYYYGW) instead of the common head-to-head formation (RRRCWWGYYY) switches the p53 effect from activation to repression [61, 62]. Furthermore, the two bases located in the core of the p53 binding site, normally AT, AA or TT, are changed to TC, GA, CA, GC, GG, CC or CG and p53 response elements associated with down-regulated genes show a weaker affinity compared to those associated with up-regulated genes [63]. In addition, differences in the spacer length have been observed within p53 binding sites for repressed genes showing longer spacers than those of induced ones [64]. However, a recent study also reported that the p53 response element associated with down-regulated genes hardly differs from the one linked to transcriptional up-regulation [65]. p53 may also compete with other transcription factors such as E2F1 or BRN3A that show overlapping or neighboring binding sites [66, 67]. Another mechanism proposed for direct repression by p53 is the recruitment of chromatin-modifying factors, such as HDACs, as described for the p53-mediated repression of *c-Myc* [68].

Apart from direct repression, several indirect mechanisms for gene repression by p53 have been documented. p53 is able to bind and thereby inactivate specific transactivation factors, such as SP1 or the glucocorticoid receptor, required for the transcriptional repression of *Sgk* [69] and *hTERT* [70], respectively. In addition, the known p53-target p21 indirectly represses the expression of different genes involved in the cell cycle [71-73]. Increased levels of p21, an inhibitor of cyclin-dependent kinases, result in hypophosphorylation of RB which in turn remains complexed with E2F. This results in decreased E2F-dependent gene expression. Furthermore, p53 directly induces non-coding RNAs, including microRNAs (miRNAs) or lncRNAs (long non-coding RNAs), or interacts with the miRNA-processing machinery to indirectly down-regulate mRNA- and protein-expression (reviewed in [60]).

1.3 Non-coding RNAs

The Human Genome Project revealed 20,000 – 25,000 protein-coding genes which occupy only 1% of the human genome [74]. However, recent advances in sequencing analyses demonstrated that about 70% of the human genome is transcribed into non-coding RNAs (ncRNAs) [75, 76]. In general, two main groups of ncRNAs are known – long ncRNAs defined as RNA molecules longer than 200 nucleotides and small ncRNAs including tRNAs, snRNAs, snoRNAs and miRNAs.

1.3.1 microRNAs and cancer

miRNAs are a class of endogenously expressed, 20 – 25 nucleotides long, ncRNAs that mediate gene repression on a posttranslational level [77]. They regulate various processes, such as cell growth, differentiation, apoptosis or tumorigenesis acting as tumor suppressors or oncogenes [78]. Aberrant miRNA expression patterns are characteristic for different kinds of human cancers [79-82]. Furthermore, a general loss of miRNA expression has been observed in different tumor cells indicating that miRNAs may have an important function in tumor suppression [82, 83]. In addition, more than 60% of all human mRNAs are miRNA targets highlighting the regulatory importance of this group of small ncRNAs [84]. miRNAs are located in introns or exons of non-coding and protein-coding genes [85]. miRNA-encoding genes are transcribed by RNA polymerase II to form primary miRNA transcripts (pri-miRNAs) [78] (Fig. 2).

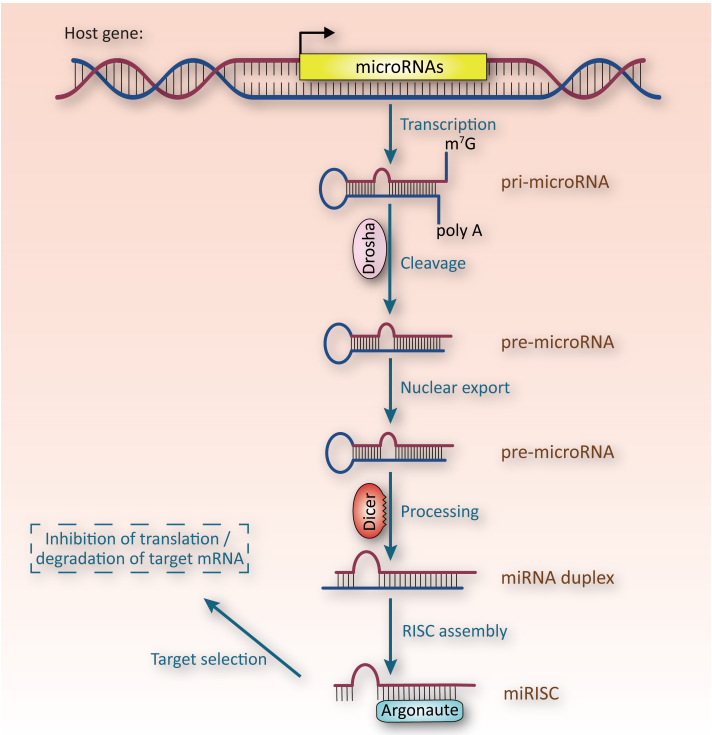

Figure 2: **miRNA generation and function**. miRNA genes are transcribed in the nucleus by RNA polymerase II to form primary miRNA transcripts that are further processed by the RNase III Drosha. The precursor miRNA is transported out of the nucleus by Exportin 5. In the cytoplasm the RNase III Dicer generates a ~22 nucleotide long miRNA-antisense - miRNA duplex that is unwound and one strand, the mature miRNA, is loaded into the RNA-induced silencing complex (RISC). The miRNA guides the RISC to specific target mRNAs. miRNAs bind to specific seed-matching regions in the 3´-UTR of mRNAs, thereby inducing either mRNA degradation or translational repression. Figure modified from [86].

Pri-miRNAs are further processed in the nucleus by the RNase III complex of Drosha and DGCR8 generating ~65 nucleotide long precursor miRNAs (pre-miRNAs) with a stem-loop structure, which are transported out of the nucleus by Exportin 5. In the cytoplasm the pre-miRNAs are further processed by the RNase III Dicer, which cleaves off the double-stranded part of the hairpin. Subsequently the miRNA-duplex is unwound and one of the two strands – the mature miRNA - is incorporated into the RNA-induced silencing complex (RISC). The mature miRNA guides this complex to (partially) complementary seed-matching sites in the 3´-UTR of its target mRNAs resulting in mRNA destabilization and/or translational repression depending on the grade of complementarity of the seed region [87, 88].

1.3.2 p53 and the miRNA-network

The tumor suppressor p53 regulates miRNA-expression and -processing but is also known to be under the control of several miRNAs (reviewed in [4, 86]).

As a transcription factor, p53 directly controls the expression of several miRNAs. In 2007, the miR-34 family were the first miRNA-encoding genes that were found to be directly up-regulated by p53 and to mediate diverse tumor suppressive effects such as apoptosis, differentiation as well as inhibition of invasion, cell cycle, epithelial-mesenchymal transition (EMT) and metabolism by inhibiting the expression of key regulators of these processes [89-96]. In addition, members of the miR-200 genes, namely *miR-200c/141* and *miR-200a/200b/429* have been identified as direct p53 targets. Their products down-regulate the EMT transcription factors (TFs) ZEB1 and ZEB2 and consequently inhibit EMT [97, 98]. Moreover, miR-200c has been shown to inhibit the stemness factors KLF4 and BMI1 [98]. The miR-192 family, encoded by the two clusters *miR-194-1/215* and *miR-192/194-2*, is another direct p53 target repressing regulators of DNA synthesis, cell cycle and metastasis [99-103]. Furthermore, miR-107, which inhibits tumor angiogenesis and cell cycle regulators [104, 105], as well as miR-145, which targets the oncogenes *c-MYC*, *KRAS* and pluripotency regulators, were demonstrated to be directly regulated by p53 [106-108]. Recently, also the *miR-15a/16-1* cluster was shown to be induced by p53 [109]. These miRNAs inhibit the cell cycle regulators *CDK6* and *CCND1*, induce apoptosis and also down-regulate *AP4*, thereby inhibiting EMT, invasion and metastasis [110-113]. Further up-regulated miRNAs by p53 are miR-29 [114], -605 [115], -149* [116], -22 [117], -23b [118], -1246 [119] and -1204 [120].

p53 also directly represses miRNAs with oncogenic functions. But only three examples of direct p53-mediated miRNA-repression are known up to now: the miR-17-92 cluster, which is known to exert different pro-tumorigenic functions [121-123] and the miRNAs-224 and -502, which inhibit autophagy and tumor growth in colon cancer cells [124, 125].

Besides functioning as a transcription factor, p53 also regulates miRNA-levels by influencing miRNA-processing (Fig. 3). The processing of specific primary miRNAs is increased by p53 via its association with the DEAD-box RNA helicase p68 enhancing the interaction with the Drosha complex [126]. Furthermore, a conditional Dicer knockout mouse model with decreased miRNA maturation shows reduced p53-mediated growth-arrest and premature senescence [127]. In addition, the p53 family member p63 induces Dicer which leads to reduced metastasis [128]. This effect is inhibited by mutant p53. Another mechanism by which p53 affects miRNA-mediated processes is the regulation of the RNA-binding-motif protein RBM38 [129]. RBM38 is directly induced by p53 and selectively inhibits the binding of miRNAs to its targets, thereby enhancing certain p53 functions.

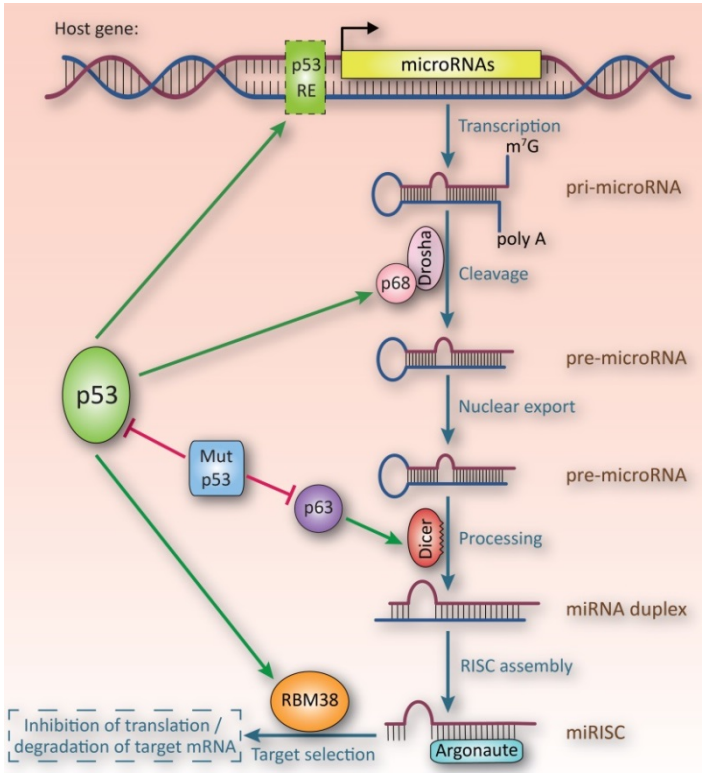

Figure 3: **p53 in the control of miRNA expression and processing**. p53 interacts with the miRNA-network via different mechanisms. As a transcription factor it directly induces or represses the expression of several miRNAs and influences miRNA processing by interacting with the RNA helicase p68 which is part of the Drosha complex. Furthermore, p53 induces the RNA-binding-motif protein RBM38 leading to the inhibition of miRNA-mediated processes to enhance p53`s function. Mutant p53 inhibits all those functions. Furthermore, mutant p53 inhibits p63 which then negatively affects Dicer and consequently miRNA-processing. Figure from [86].

On the other hand, p53 itself is targeted by several miRNAs (see Fig. 4). Since targeting of p53 reduces its tumor-suppressive functions, those miRNAs are predominantly oncomirs that are often overexpressed in human tumors. The first miRNA found to repress p53 and to negatively regulate p53-induced apoptosis was miR-125b [130]. miR-125b is a prognostic marker in colorectal cancer which is associated with poor prognosis and increased tumor size [131]. Also miR-504 targets p53 [132]. This miRNA was shown to inhibit apoptosis and to lead to increased tumorigenicity of colon cancer cells. miR-25 and miR-30d represent p53-regulating miRNAs that show enhanced expression in different types of tumors [133-135]. Additionally, miR-33 and miR-380-5p were shown to target the 3´-UTR of p53 [136,

137]. Moreover, p53 is down-regulated by miR-1285 [138]. Further miRNAs directly inhibiting p53 are miR-150 [139], -214 [140] and -375 [141].

Several tumor suppressive miRNAs regulate p53 indirectly via p53-modifying enzymes (see Fig. 4). *MDM2*, the main negative regulator of p53, is a target of the miRNAs miR-145, miR-192/194/215, miR-29b and miR-605 [103, 115, 142]. Consequently, induction of those miRNAs leads to repression of *MDM2* and induction of p53. In the case of the p53-induced miR-192/194/215 and miR-605 this results in a positive feedback loop. In addition, miR-122 indirectly suppresses *MDM2* levels by targeting *CCNG1* [143, 144]. Furthermore, it is known that the miR-34a target SIRT1 negatively regulates p53 expression and that miR-29 down-regulates the PI3K/AKT pathway which indirectly leads to increased p53-levels [145-147].

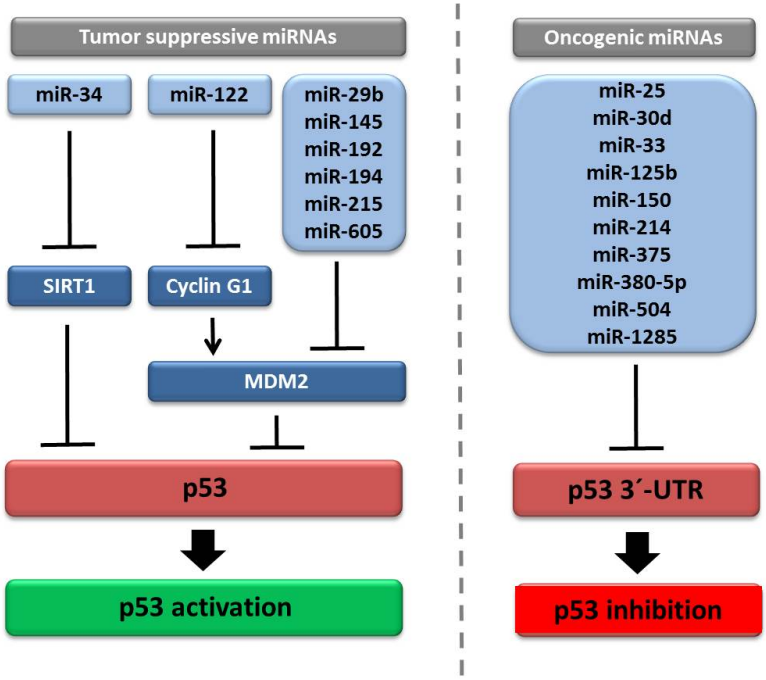

Figure 4: **miRNAs that directly or indirectly regulate p53**. Several tumor suppressive miRNAs regulate p53 indirectly via p53-modifying enzymes which results in enhanced p53 activation. Some oncogenic miRNAs directly target p53´s 3´-UTR to suppress p53 activity. Figure modified from [4].

1.3.3 Long non-coding RNAs

lncRNAs are defined as RNA transcripts larger than 200 nucleotides with no protein-coding functions. The NONCODE database currently lists more than 30,000 human lncRNA transcripts [148]. They are known to be transcribed from their own promoters and are often under the control of key transcription factors, such as p53, NFκB, Sox2, Oct4 or Nanog [149]. Different types of lncRNAs have been described including long intergenic ncRNAs (lincRNAs), transcribed pseudogenes, antisense RNAs or enhancer RNAs [150]. lncRNAs were described to play a role in cancer with either tumor-suppressive or oncogenic functions and to regulate gene expression by diverse mechanisms [150]. Many lncRNAs bind histone-modifying or chromatin-remodeling proteins, such as the polycomb repressive complexes PRC1 and PRC2, to mediate the repression of gene transcription [151]. In addition, lncRNAs act as enhancer RNAs (eRNAs), that are transcribed from enhancer regions and regulate their activity [152]. Furthermore, they influence tumor suppressor activity by epigenetic silencing or activating the expression of tumor suppressor target genes [153, 154]. Moreover, lncRNAs affect posttranscriptional mRNA processing as described for MALAT1 and NEAT1 [155, 156] and act as competitive endogenous RNAs (ceRNA) that function as miRNA sponges [157].

1.3.4 p53 and the lncRNA-network

In 2009, Guttman *et al.* described a number of lncRNAs, which are significantly up-regulated in a p53-dependent manner in mouse embryonic fibroblasts after DNA damage [149]. The p53-inducible, tumor-suppressive lincRNA-p21 is located about 15 kbp upstream of the gene encoding p21 and facilitates p53-mediated repression as well as posttranscriptional regulation of p53 [153, 158, 159]. In addition, *PANDA*, which is transcribed from the *CDKN1A* promoter, is directly induced by p53 and suppresses the expression of pro-apoptotic genes, thereby controlling apoptosis [160]. Furthermore, the lncRNA *loc285194* was found to be regulated by p53 [161]. It is located in a region with frequent focal copy number alterations and loss of heterozygosity in different kinds of cancer and its deletion promotes proliferation and is associated with poor survival in osteosarcoma patients [162]. In particular, *loc285194* acts as a ceRNA to repress miR-211´s oncogenic functions [157, 161]. *RoR* represents another lincRNA, which is transcriptionally induced by p53 [163]. Similar to MDM2, RoR suppresses p53´s translation which results in an autoregulatory feedback loop. Moreover, the maternally imprinted gene *H19* is negatively regulated by p53 [164]. *H19* seems to have opposing roles in cancer. It was described as an oncogene in hepatocellular carcinoma and bladder cancer but displays tumor-suppressive functions in a colorectal cancer mouse model [165, 166].

In addition to lincRNA-p21 and RoR, there are several lncRNAs that are involved in the (in-)direct transcriptional regulation of the tumor suppressor p53. *MALAT1*,

which is overexpressed in several types of cancers, controls cell cycle progression and its depletion results in a G1 arrest and the activation of p53 [167]. Moreover, *MALAT1* influences alternative mRNA splicing by modulating the activity of SR splicing factors [156]. In contrast, the imprinted lncRNA *MEG3* negatively regulates MDM2 expression which leads to an accumulation of p53 [168]. p53 has a natural antisense transcript, *Wrap53*, that is located on the opposite strand immediately upstream of *p53* and partly overlaps with *p53* in an antisense fashion [169]. *Wrap53* positively regulates p53 on the posttranscriptional level. Moreover, several enhancer RNAs (eRNAs) are transcribed from p53-bound enhancer regions and thereby contribute to the long-distance regulation of *DUSP4*, *PAPPA* and *IER5* by p53 [170].

1.4 Epithelial-mesenchymal transition in cancer progression

The epithelial-mesenchymal transition (EMT) represents a reversible switch that allows immotile, polarized, epithelial cells to acquire mesenchymal traits characterized by the loss of polarity, the reduction of intercellular adhesions and an increase in motility (Fig. 5).

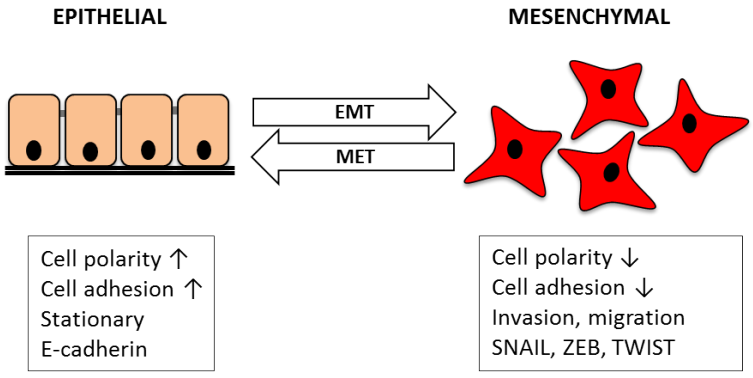

Figure 5: **Model of EMT**. Epithelial cells are characterized by cell polarity, cell adhesion, a stationary phenotye and high expression of the adherens junction protein E-cadherin. During EMT, epithelial cells switch to a mesenchymal phenotype characterized by the loss of cell polarity and adhesion, the ability to invade and migrate and the expression of the EMT-promoting transcription factors SNAIL, ZEB and TWIST.

Initially, the transition between an epithelial and mesenchymal phenotype was identified as an embryonal program involved in developmental processes, such as gastrulation, neural crest formation and heart morphogenesis [171]. Moreover, EMT is associated with tissue regeneration and fibrosis [172, 173]. Furthermore, it is also widely accepted by now that EMT plays an important role in tumorigenesis. It enables cancer cells to acquire invasive and stem-cell like traits, which allow cells to disseminate from the primary tumor to form metastases in distant organs [174].

EMT is induced via several different stimuli, including hypoxia, deregulated TGF-β-, Wnt-, Notch- and/or receptor tyrosine kinase signaling, which activates the

expression of canonical EMT-activating transcription factors, such as SNAIL, ZEB1/2 and TWIST, as well as the Krüppel-like factor KLF8 or the bHLH factor E47 [175, 176]. EMT-TFs are known to repress the adherens-junction protein E-cadherin*/CDH1* via binding to so-called E(enhancer)-boxes in its promoter. Repression of *CDH1* is considered as a hallmark during EMT [177]. Furthermore, mesenchymal-specific markers such as the intermediate filament Vimentin and the extracellular matrix glycoprotein Fibronectin are up-regulated.

More recently also miRNAs have been implicated in the control of EMT. The miR-200 family for example was shown to target the EMT transcription factors *ZEB1* and *ZEB2* [97] and miR-34a to down-regulate *SNAIL* [1, 178].

Interestingly, the EMT-inducing transcription factors have not only been implicated in promoting invasion and migration but also in inducing stemness [179-181]. This allows cancer cells to acquire stem cell traits such as the capacity for self-renewal which is necessary for metastasis formation [182].

It has been shown that disseminated cancer cells regain their epithelial phenotype by reversing EMT in a process called mesenchymal-epithelial transition (MET). MET allows cells to form tumors at the metastatic site [174].

1.5 The role of vitamin D3 in cancer

Vitamin D3 is synthesized in skin exposed to sunlight or is derived from the diet. Two hydroxylation steps mediated by the hydroxylases CYP27A1 and CYP27B1 in the liver and in the kidney, respectively, convert vitamin D3 to the active metabolite calcitriol (1,25-dihydroxy-vitamin D3) [183]. The catabolic hydroxylase CYP24A1 mediates the degradation of calcitriol and the intermediate metabolite 25-hydroxyvitamin D_3 ($25(OH)D_3$) [183]. Interestingly, CYP27B1 is also expressed at extrarenal sites including brain, colon, pancreas or skin, which allows local conversion of the intermediate metabolite 25-hydroxyvitamin D_3 ($25(OH)D_3$) to calcitriol [184].

Calcitriol regulates intestinal calcium- and phosphate-absorption and controls bone mineralization [185]. Moreover, it increases differentiation and apoptosis and has been shown to inhibit proliferation, inflammation, angiogenesis and invasion/metastasis [186]. There is increasing evidence that vitamin D3 acts as an anticancer agent [187]. Alterations in the synthesis and catabolism of vitamin D3 metabolites often occur during cancer progression. Elevated expression levels of *CYP27B1* were detected in breast and prostate cancer, and during early stages of colorectal cancer [188-192]. However, *CYP24A1* is up-regulated in a variety of cancer types and limits the anti-tumorigenic effect of vitamin D3 by catabolising $25(OH)D_3$ and calcitriol [193-195]. Several small-molecule inhibitors for CYP24A1 act as anticancer agents and enhance the antiproliferative effect of calcitriol [196-198].

The genomic response to calcitriol results from its binding to the vitamin D receptor (VDR), which regulates gene expression via sequence-specific binding sites. Several direct VDR target genes, such as *CDKN1A* or *CDH1,* have been identified in colorectal cancer cells (reviewed in [199]). Among these, *CST5*, which codes for the cysteine protease inhibitor cystatin D, has been described as a tumor suppressive factor in colorectal cancer [200]. In addition, calcitriol indirectly affects the expression of a large number of genes by antagonizing Wnt/β-catenin signaling via different mechanisms [201]. Calcitriol promotes VDR/β-catenin interaction which results in reduced binding of β-catenin to TCF4 [202]. Additionally, it induces E-cadherin which leads to the inhibition of Wnt signaling by nuclear export of β-catenin and its relocalization to the plasma membrane [202]. Moreover, calcitriol-induced DKK-1, an extracellular inhibitor of Wnt signaling, binds to the Wnt co-receptor LRP6 thereby preventing Wnt-Frizzled-LRP6 complex formation [203].

Several epidemiological studies have revealed a negative correlation between sunlight exposure and the incidence for colon and prostate cancer suggesting a potential role of vitamin D3 in reducing cancer risk [204]. Furthermore, high circulating 25(OH)D_3 levels are associated with a 30 – 40% lower risk to develop colorectal cancer and an increased overall survival in colorectal cancer patients [205, 206]. Moreover, prostate cancer patients with low prediagnostic 25(OH)D_3-levels have a 60% higher risk to die from cancer [207]. However, no or only a weak positive correlation between circulating 25(OH)D_3-levels and lower cancer risk for breast [208] or prostate cancer [209] has been shown.

Several *in vitro* and *in vivo* studies have confirmed the role of calcitriol as an anticancer agent. It has been shown that calcitriol inhibits proliferation, inflammation and angiogenesis and leads to the induction of apoptosis, differentiation and reduced invasion and migration in several different types of cancer cells [187]. Furthermore, a tumor-inhibiting effect of dietary calcitriol uptake was detected in several different animal models [199]. Meta-analyses of randomized clinical studies show a significant impact of vitamin D3 on the reduction of cancer mortality [210-214]. Several large-scale and long-term randomized clinical trials studying the effect of vitamin D3 are expected to be completed within the next five years [215].

2. AIMS OF THE STUDY

The present work had the following aims:

1) Characterization of the regulatory network between p53, miR-34a and its target SNAIL during mesenchymal-epithelial transition of colorectal cancer cell lines.

2) Genome-wide identification and characterization of p53-regulated proteins, mRNAs, miRNAs and lncRNAs in colorectal cancer cells.

3) Characterization of the newly identified p53 target gene *CST5* and determination of its role in p53-mediated mesenchymal-epithelial transition.

3. MATERIALS

3.1 Chemicals and reagents

Chemical	Supplier
Ammonium peroxodisulfate (APS)	Carl Roth GmbH, Karlsruhe, Germany
Ampicillin	Sigma-Aldrich, St.Louis, MD, USA
BD Matrigel™ Basement Membrane Matrix	BD Bioscience, Heidelberg, Germany
Calcitriol	Sigma-Aldrich, St.Louis, MD, USA
Complete mini protease inhibitor cocktail	Roche Diagnostics GmbH, Mannheim, Germany
Dimethyl-sulfoxide (DMSO)	Carl Roth GmbH, Karlsruhe, Germany
dNTPs (deoxynucleotides triphosphate)	Thermo Fisher Scientific, Inc., Waltham, MA, USA
Doxycycline hyclate	Sigma-Aldrich, St.Louis, MD, USA
DAPI (2-(4-Amidinophenyl)-6-indolecarbamidine-dihydrochloride)	Carl Roth GmbH, Karlsruhe, Germany
ECL/HRP substrate	Immobilon, Merck Millipore, Billerica, MA, USA
Ethidium bromide	Carl Roth GmbH, Karlsruhe, Germany
Etoposide	Sigma-Aldrich, St.Louis, MD, USA
Fast SYBR® Green Master Mix	Applied Biosystems, Foster City, CA, USA
Fast SYBR Green Master Mix Universal RT	Exiqon A/S, Vedbaek, Denmark
FCS (Fetal calf serum)	Gibco®, Life Technologies GmbH, Darmstadt, Germany
FuGENE®6 Transfection Reagent	Promega, Madison, WI, USA
Hi-Di™ Formamide	Applied Biosystems, Foster City, CA, USA
HiPerFect Transfection Reagent	Qiagen GmbH, Hilden, Germany
Immobilon-P Transfer Membrane	Immobilon, Merck Millipore, Billerica, MA, USA
LB-Agar (Lennox)	Carl Roth GmbH, Karlsruhe, Germany
LB-Medium (Luria/Miller)	Carl Roth GmbH, Karlsruhe, Germany
Mitomycin C	Sigma-Aldrich, St.Louis, MD, USA
Nonidet®P40 substitute	Sigma-Aldrich, St.Louis, MD, USA
Nutlin-3a	Sigma-Aldrich, St.Louis, MD, USA
Opti-MEM® Reduced Serum Medium	Life Technologies GmbH, Darmstadt, Germany
Paraformaldehyde	Merck KgaA, Darmstadt, Germany
ProLong Gold antifade	Invitrogen GmbH, Karlsruhe, Germany
Propidium iodide	Sigma-Aldrich, St.Louis, MD, USA
Puromycin dihydrochloride	Sigma-Aldrich, St.Louis, MD, USA
Rotiphorese gel 30 (37,5:1)	Carl Roth GmbH, Karlsruhe, Germany
Sea plaque® agarose	Lonza Ltd, Basel, Switzerland
Skim milk powder	Fluka, Sigma-Aldrich, St.Louis, MD, USA
Sodium dodecyl sulfate (SDS)	Carl Roth GmbH, Karlsruhe, Germany
Temed (tetramethylethylendiamin,1,2-bis (dimethylamino) –ethan)	Carl Roth GmbH, Karlsruhe, Germany
TritonX 100	Carl Roth GmbH, Karlsruhe, Germany
Tween 20	Sigma-Aldrich, St.Louis, MD, USA
Water (molecular biological grade)	Gibco®, Life Technologies GmbH, Darmstadt, Germany

3.2 Enzymes

Enzyme	Supplier
DNase I (RNase-free)	Sigma-Aldrich, St.Louis, MD, USA
FIREPol® DNA Polymerase	Solis BioDyne, Tartu, Estonia
Platinum® *Taq* DNA polymerase	Invitrogen GmbH, Karlsruhe, Germany
Proteinase K	Sigma-Aldrich, St.Louis, MD, USA
Restriction endonucleases	New England Biolabs GmbH, Frankfurt, Germany
RNase A	Sigma-Aldrich, St.Louis, MD, USA
T4 DNA ligase	Thermo Fisher Scientific, Inc., Waltham, MA, USA
Trypsin (10x, phenol-red free)	Invitrogen GmbH, Karlsruhe, Germany

3.3 Kits

Kit	Supplier
BCA Protein Assay Kit	Pierce, Thermo Fisher Scientific, Inc., Waltham, MA, USA
BigDye® Terminator v3.1 Cycle Sequencing Kit	Life Technologies GmbH, Darmstadt, Germany
DyeEx® 2.0 Spin Kit	QIAGEN GmbH, Hilden, Germany
High Pure RNA Isolation Kit	Roche Diagnostics GmbH, Mannheim, Germany
High Pure miRNA Isolation Kit	Roche Diagnostics GmbH, Mannheim, Germany
miRCURY LNA™ Universal RT microRNA PCR – Universal cDNA Synthesis Kit II	Exiqon A/S, Vedbaek, Denmark
Pure Yield™ Plasmid Midiprep System	Promega GmbH, Mannheim, Germany
TaqMan® MicroRNA Reverse Transcription Kit	Applied Biosystems, Life Technologies GmbH, Darmstadt,Germany
TaqMan® PreAmp Master Mix	Applied Biosystems, Life Technologies GmbH, Darmstadt,Germany
TaqMan® Universal Master Mix	Applid Biosystems, Life Technologies GmbH, Darmstadt, Germany
QIAprep Spin Miniprep Kit	QIAGEN GmbH, Hilden, Germany
QIAquick Gel Extraction Kit	QIAGEN GmbH, Hilden, Germany
QuikChange II Site-Directed Mutagenesis Kit	Stratagene, Agilent Technologies GmbH & Co.KG, Waldbronn, Germany
Verso cDNA Kit	Thermo Fisher Scientific, Inc., Waltham, MA, USA

3.4 Antibodies

3.4.1 Primary antibodies

Epitope	Clone	Ordering no.	Company	Use	Dilution	Source
β-actin		# A2066	Sigma	WB	1:1000	rabbit
CST5	N-19	# sc-46890	Santa Cruz	WB; IF	1:200; 1:50	goat
E-cadherin	4A2C7	# 334000	Invitrogen	WB; IF	1:1000; 1:50	mouse
mouse IgG			Santa Cruz	ChIP		mouse
p21	CP-74		Neomarkers	WB	1:1000	mouse
p53	DO-1	# sc-126	Santa Cruz	WB; ChIP	1:1000	mouse
rabbit IgG		# R-5506	Sigma	ChIP		rabbit
SNAIL		# 3879S	Cell Signaling	WB	1:200	rabbit
SNAIL		# AF3639	R&D Systems	WB	1:500	goat
SLUG	H-140	# sc-15391x	Santa Cruz	WB	1:2000	rabbit
VSV		# V4888	Sigma	WB; ChIP	1:7500	rabbit

WB = Western blot, IF = immunofluorescence, ChIP = chromatin immunoprecipitation

3.4.2 Secondary antibodies

Name	Source	Application	Supplier
anti-goat HRP	donkey	WB	Jackson Immuno Reseach, Ltd., Newmarket, Suffolk, UK
anti-goat Cy3	donkey	IF	Jackson Immuno Reseach, Ltd., Newmarket, Suffolk, UK
anti-mouse HRP	goat	WB	Promega GmbH, Mannheim, Germany
anti-mouse-Alexa Fluor-555	goat	IF	Invitrogen GmbH, Karlsruhe, Germany
anti-rabbit HRP	goat	WB	Sigma-Aldrich, St.Louis, MD, USA

WB = Western blot, IF = immunofluorescence

3.5 Vectors and oligonucleotides

3.5.1 Vectors

Name	Insert	Reference
pBV-Luc		[216]
pBV-Luc miR-486 p53 BS	miR-486 p53 BS	this work
pcDNA		
pcDNA-p53-VSV	p53	
pGL3-control-MCS		[217, 218]
pGL3-KLF12 3´-UTR, miR-34a BS	KLF12 3´-UTR, miR-34a BS	this work
pGL3-KLF12 3´-UTR, miR-34a BS mut	KLF12 3´-UTR, miR-34a BS mutated	this work
pGL3-KLF12 3´-UTR, miR-205 BS	KLF12 3´-UTR, miR-205 BS	this work
pGL3-KLF12 3´-UTR, miR-205 BS mut	KLF12 3´-UTR, miR-205 BS mutated	this work
pGL3-HMGB1 3´-UTR, miR-205 BS	HMGB1 3´-UTR, miR-205 BS	this work
pGL3-HMGB1 3´-UTR, miR-205 BS mut	HMGB1 3´-UTR, miR-205 BS mutated	this work
pGL3-CIT 3´-UTR, miR-486 BS	CIT 3´-UTR, miR-486 BS	this work
pGL3-CIT 3´-UTR, miR-486 BS mut	CIT 3´-UTR, miR-486 BS mutated	this work
pRL	Renilla	[219]
pRTR		[220]
pRTR-p53-VSV	p53	[1]
pRTR-SNAIL-VSV	SNAIL	[1]

BS: binding site; UTR: untranslated region; mut: mutated

3.5.2 Oligonucleotides

3.5.2.1 Oligonucleotides used for qPCR

Name	Sequence (5´→ 3´)
β-actin Fwd	TGACATTAAGGAGAAGCTGTGCTAC
β-actin Rev	GAGTTGAAGGTAGTTTCGTGGATG
β-catenin Fwd	AGCTGACCAGCTCTCTCTTCA
β-catenin Rev	CCAATATCAAGTCCAAGATCAGC
CIT Fwd	TGGAAGGTGATGACCGTCTA

Name	Sequence (5´→ 3´)
CIT Rev	ACGTCCACAAGACACAGTGC
CST5 Fwd	CCTCTGCAGGTGATGGCTG [200]
CST5 Rev	GGACTTGGTGCATGTGGTTC [200]
CDH1 Fwd	CCCGGGACAACGTTTATTAC
CDH1 Rev	GCTGGCTCAAGTCAAAGTCC
HMGB1 Fwd	ATATGGCAAAAGCGGACAAG
HMGB1 Rev	GCAACATCACCAATGGACCAG
LINC01021 Fwd	TGTTTTCCTTTTTGCCCAAT
LINC01021 Rev	CGCCTGGTAAAACAACCAGT
MDFI Fwd	AAATCCACCACCTCCCAGA
MDFI Rev	CAGGAACTCGCAGAACAGG
pri-miR-200b Fwd	CGCAGCAGTGGAACCTGT
pri-miR-200b Rev	GTGAGGAGGTGCTGGGATG
pri-miR-200c Fwd	CTTAAAGCCCCTTCGTCTCC
pri-miR-200c Rev	AGGGGTGAAGGTCAGAGGTT
pri-miR-205 Fwd	CCACCTTTCCTCAGGAGTCA
pri-miR-205 Rev	CCAAGATGGGTACTTGAGAGATG
pri-miR-34a Fwd	CGTCACCTCTTAGGCTTGGA
pri-miR-34a Rev	CATTGGTGTCGTTGTGCTCT
pri-miR-34b/c Fwd	GAGCTGCCTGTGCATCATC
pri-miR-34b/c Rev	GGATGAAATCAGCATTTTCCA
pri-miR-486 Fwd	CTCCTTGGAGTAGCCTCTCG
pri-miR-486 Rev	CCAGCTCTCCTCCTGTGTG
p21 Fwd	GGCGGCAGACCAGCATGACAGATT
p21 Rev	GCAGGGGGCGGCCAGGGTAT
SLUG Fwd	TGGTTGCTTCAAGGACACAT
SLUG Rev	GTTGCAGTGAGGGCAAGAA
SNAIL Fwd	GCACATCCGAAGCCACAC
SNAIL Rev	GGAGAAGGTCCGAGCACA
ST14 Fwd	CTTCCCTCATCTCTCCCAACT
ST14 Rev	GCGTGGGGTCTGAGTACCT
Vimentin Fwd	TACAGGAAGCTGCTGGAAGG
Vimentin Rev	ACCAGAGGGAGTGAATCCAG

Fwd: forward; Rev: reverse

3.5.2.2 Oligonucleotides used for qChIP

Name	Sequence (5´→ 3´)
p53 BS CST5 Fwd	TAAGAGACCGGAAAGGTTGAGA
p53 BS CST5 Rev	AGGGCCTTTGCACTGACTATT
SNAIL BS CST5 Fwd	GGGGACACCCAAGTAGGATAA
SNAIL BS CST5 Fwd	GGAGCTGGATCTCCCAGAG
SNAIL BS CDH1 Fwd	TAGAGGGTCACCGCGTCTAT
SNAIL BS CDH1 Rev	TCACAGGTGCTTTGCAGTTC
ELF1α Fwd	CACACGGCTCACATTGCAT
ELF1α Rev	CACGAACAGCAAAGCGACC
p53 BS MDFI Fwd	CAAGCCCTGTGGTTTTTCC
p53 BS MDFI Rev	CCATGTGGGAAGCACAGA
p53 BS miR-205 Fwd	AGGATCTAGCATCAGCAAAACAT
p53 BS miR-205 Rev	CCATTGCAGTTTGAATTCCTT
p53 BS miR-486 Fwd	GAACAGTCCACAGGCACAGA
p53 BS miR-486 Rev	AACAGAATTTTCCATTGCCG
p53 BS LINC01021 Fwd	CATGAGGAATTCATGCCTTG

Name	Sequence (5´→ 3´)
p53 BS LINC01021 Rev	TCCCAGGTCACCACAAGAG
p53 BS ST14 Fwd	GAATGACCTGGAGCACTTGAAT
p53 BS ST14 Rev	CCCTGGAGGTGCTGATGT

BS: binding site; Fwd: forward; Rev: reverse

3.5.2.3 Oligonucleotides used for cloning and mutagenesis

Name	Sequence (5´→ 3´)
CIT 3´-UTR miR-486 BS Fwd	TTTGGTACCGGTAACTTGCCCAGACATGC
CIT 3´-UTR miR-486 BS Rev	TTTGAATTCGGCATCAATGAGGCTGGTAG
CIT 3´-UTR miR-486 BS mut Fwd	CTAGGTCTCCAAAACTACCCCCTTTTTCTTCATTACCTTTT
CIT 3´-UTR miR-486 BS mut Rev	AAAAGGTAATGAAGAAAAAGGGGGTAGTTTTGGAGACCTAG
HMGB1 3´-UTR miR-205 BS Fwd	TTTGAATTCATGAATTATTACAGTGTTTATCCT
HMGB1 3´-UTR miR-205 BS Rev	TTTACTAGTGCTGGCCCAATTAATTAAAAATA
HMGB1 3´-UTR miR-205 BS mut Fwd	CATTTTGAAAGTCTGTCCTTCACCCACTAATAGAAAAGTATG
HMGB1 3´-UTR miR-205 BS mut Rev	CATACTTTTCTATTAGTGGGTGAAGGACAGACTTTCAAAATG
KLF12 3´-UTR miR-34a BS Fwd	TTTGAATTCCCTTAATATTCATAGTTCATAATCCA
KLF12 3´-UTR miR-34a BS Fwd	TTTACTAGTGAAACTGTGAAAATATAGCAATTT
KLF12 3´-UTR miR-34a BS mut Fwd	TTCTACTCATCCCCACAGTCGGTTCCACTTAACCTGTACAG
KLF12 3´-UTR miR-34a BS mut Rev	CTGTACAGGTTAAGTGGAACCGACTGTGGGGATGAGTAGA
KLF12 3´-UTR miR-205 BS Fwd	TTTGAATTCATTTCTCCAGTTTATCTAAAGACC
KLF12 3´-UTR miR-205 BS Rev	TTTACTAGTTTTTGTTCCATACAAAATGCTTTATTTA
KLF12 3´-UTR miR-205 BS mut Fwd	GTATAATTATCTGACCCAAGGCCCGAAGGTTAAATAAAGCATTTG
KLF12 3´-UTR miR-205 BS mut Rev	CAAATGCTTTATTTAACCTTCGGGCCTTGGGTCAGATAATTATAC
miR-486 p53 BS Fwd	TTTGGTACCGGTAACTTGCCCAGACATGC
miR-486 p53 BS Rev	TTTGAATTCGGCATCAATGAGGCTGGTAG
LINC01021_A Fwd	TTTACTAGTCTGGGAATCAATGTGTGAGGT
LINC01021_A Rev	TTTGAGCTCTTAAGCCCCTCATTCGTTATATTTT
Oligonucleotides used for the generation of a small RNA library (miR-Seq)	
adenylated 3’ adapter	Phospho-TGGAATTCTCGGGTGCCAAGG-(C7amino)
5’ RNA adapter	GUUCAGAGUUCUACAGUCCGACGAUC
specific oligonucleotide for reverse transcription	GCCTTGGCACCCGAGAATTCCA
5’ PCR oligonucleotide	AATGATACGGCGACCACCGAGATCTACACGTTCAGAGTTCTACAGTCCGA
3’ PCR oligonucleotide	CAAGCAGAAGACGGCATACGAGAT-6nt Barcode-GTGACTGGAGTTCCTTGGCACCCGAGAATTCCA

BS: binding site; UTR: untranslated region; Fwd: forward; Rev: reverse, mut: mutated

3.5.3 miRNA mimics and antagomiRs

The following pre-microRNA mimics and antagomiRs were purchased from Ambion:

- pre-miR-control
- pre-miR-34a
- pre-miR-205
- pre-miR-486-5p
- anti-miR-control
- anti-miR-34a

3.6 Buffers and solutions

- 2x Laemmli buffer:
  125 mM TrisHCl (pH 6.8), 4% SDS, 20% glycerol, 0.05% bromophenol blue (in H_2O), 10% β-mercaptoethanol (added right before use)
- 10x „Vogelstein“ PCR buffer:
  166 mM NH_4SO_4, 670 mM Tris (pH 8.8), 67 mM $MgCl_2$, 100 mM β-mercaptoethanol
- Propidium iodide staining solution:
  800 µl propidium iodide (1.5 mg/ml), 1000 µl RNase A (10 mg/ml), add 20 ml PBS 0.1% TritonX 100
- RIPA buffer:
  1% NP40, 0.5% sodium deoxycholate, 0.1% SDS, 250 mM NaCl, 50 mM TrisHCl (pH 8.0)
- SDS buffer:
  50 mM Tris (pH 8.1), 100 mM NaCl, 0.5 % SDS, 5 mM EDTA
- 10x Tris-glycine-SDS running buffer:
  720 g Glycin, 150 g Tris base, 50 g SDS, pH 8.3-8.7, add 5 l ddH_2O
- Triton dilution buffer:
  100 mM Tris-HCl (pH 8.6), 100 mM NaCl, 5 mM EDTA (pH 8.2), 0.2% NaN_3, 5% TritonX-100
- Towbin buffer:
  200 mM glycine, 20% methanol, 25 mM Tris base (pH 8.6)
- 10x TBS-T:
  500 ml 1M Tris (pH 8.0), 438.3 g NaCl, 50 ml Tween20, add 5l ddH_2O
- Urea lysis buffer:
  30 mM Tris Base, 7 M Urea, 2 M Thio-Urea, pH 8.5

3.7 Laboratory equipment

Device	Supplier
5417C table-top centrifuge	Eppendorf AG, Hamburg, Germany
ABI 3130 genetic analyzer capillary sequencer	Applied Biosystems, Foster City, USA
Axiovert 25 microscope	Carl Zeiss GmbH, Oberkochen, Germany
BD Accuri™ C6 Flow Cytometer Instrument	Accuri, Erembodegem, Belgium
Biofuge *fresco*	Heraeus; Thermo Fisher Scientific, Inc., Waltham, MA, USA
Biofuge *pico* table top centrifuge	Heraeus; Thermo Fisher Scientific, Inc., Waltham, MA, USA
Boyden chamber transwell membranes (pore size 8.0 µm)	Corning Inc., Corning, NY, USA
CF40 Imager	Kodak, Rochester, New York, USA
Falcons, dishes and cell culture materials	Schubert & Weiss OMNILAB GmbH & Co. KG
Fisherbrand FT-20E/365 transilluminator	Fisher Scientific GmbH, Schwerte, Germany
Forma scientific CO_2 water jacketed incubator	Thermo Fisher Scientific, Inc., Waltham, MA, USA
GeneAmp® PCR System 9700	Applied Biosystems, Foster City, USA
Herasafe KS class II safety cabinet	Thermo Fisher Scientific, Inc., Waltham, MA, USA
HTU SONI130	G. Heinemann Ultraschall- und Labortechnik, Schwäbisch Gmünd
Megafuge 1.0R	Heraeus; Thermo Fisher Scientific, Inc., Waltham, MA, USA
Mini-PROTEAN®-electrophoresis system	Bio-Rad, München, Germany
MultiImage Light Cabinet	Alpha Innotech, Johannesburg, South Africa
ND 1000 NanoDrop Spectrophotometer	NanoDrop products, Wilmington, DE, USA
Neubauer counting chamber	Carl Roth GmbH & Co, Karlsruhe, Germany
Orion II luminometer	Berthold Technologies GmbH & Co. KG, Bad Wildbad, Germany
PerfectBlue™ SEDEC 'Semi-Dry' blotting system	Peqlab Biotechnologie GmbH, Erlangen, Germany
Varioscan Flash Multimode Reader	Thermo Scientific, Inc., Waltham, MA, USA
Waterbath	Memmert GmbH, Schwabach, Germany

4. METHODS

4.1 Bacterial cell culture

4.1.1 Propagation and seeding

The bacterial *E.coli* strain XL1-blue was used for cloning procedures and the replication of plasmids that harbored a resistance against ampicillin. The bacteria were propagated in LB-medium (agitation, 225 rpm) or on LB-agar plates at 37°C overnight. To select for those cells with an antibiotic resistance, 100 µg/ml ampicillin was added to the LB-medium.

4.1.2 Transformation

To transform plasmid DNA, competent *E.coli* XL1-blue strains that were kept at -80°C were carefully thawed on ice and the plasmid DNA was added. Afterwards, the cells were kept on ice for 30 minutes followed by a heat shock at 42°C for 90 seconds. Subsequently, the bacteria were placed on ice for 2 minutes and incubated in 1 ml LB-medium without antibiotics at 37°C for 1 hour. Finally, the cells were centrifuged at 2000 rpm for 5 minutes, the supernatant was discarded and the bacteria were resuspended and plated on a LB agar plate containing ampicillin for overnight incubation.

4.1.3 Purification of plasmid DNA from E.coli

Small amounts of plasmid DNA were generated inoculating a single bacterial clone in 5 ml of LB-medium that was supplemented with ampicillin. After overnight incubation at 37°C, 225 rpm the plasmid DNA was isolated according to the manufacturer´s protocol using the QIAprep Spin Miniprep Kit (Qiagen). To prepare a bigger volume with a higher plasmid concentration, 150 ml of LB-medium (with ampicillin) were incubated overnight at 37°C, 225 rpm and the plasmid DNA was isolated the next day following the instructions of the Pure Yield™ Plasmid Midiprep System (Promega).

4.2 Cell culture of human cell lines

4.2.1 Propagation of human cell lines

The colorectal cancer cell lines HCT116 and RKO and their derivatives were kept in McCoy´s medium (Invitrogen) supplemented with 10% fetal calf serum (FCS, Invitrogen) and 1% Penicillin/Streptavidin (Invitrogen). The cell lines SW480, H1299, HEK293T were cultured in DMEM (Dulbecco´s modified Eagles medium, Invitrogen)

that was supplemented with 10% FCS and 1% Penicillin/Streptavidin. All cell lines were passaged twice a week or at a confluency of ~80% and kept in a humified incubator, at 37°C and 5% CO_2.

4.2.2 Transfection of oligonucleotides and vector constructs

For the transfection of oligonucleotides and vector constructs, cells were trypsinized, counted and seeded into 6-well or 12-well plates. Transfection was carried out immediately after seeding so that the cells were not yet attached to the surface of the cell culture plates. For oligonucleotide transfection, 100 µl Opti-MEM (Invitrogen) was mixed with 10 µl of the respective oligonucleotide [10 µM] (Ambion/Applied Biosystems) for a final concentration of 100 nM and with 10 µl HiPerFect (Qiagen). For the transfection of vector constructs, 150 µl Opti-MEM was supplemented with 4 µg of plasmid DNA and 5 µl FuGENE6 (Promega). The transfection reagent mix was incubated for 20 minutes at room temperature and added drop-wise to the cells.

4.2.3 Conditional expression in cell pools

The episomal vector pRTR [220] was used to generate cell pools with a conditional expression vector. After transfection with FuGENE6 (Promega), those cells containing the pRTR vector were selected using 2 µg/ml Puromycin (Sigma; stock solution: 2 mg/ml in H_20) for 10 days. To determine the percentage of cells that were positive for *eGFP*-expression, 100 ng/ml doxycycline (DOX) (Sigma; stock solution 100 µg/ml in H_20) was added to the medium and *eGFP*-positive cells were determined by FACS analysis after 48 hours (see 4.5.1).

4.2.4 Cryo-preservation of mammalian cell lines

For cryo-preservation of mammalian cells, ~80% confluent cells were trypsinized, pelleted by centrifugation (1200 rpm, 5 minutes) and resuspended in a prepared mixture of 50% FCS, 10% of the respective growth medium and 10% DMSO (Roth). 1 ml aliquots of the resuspended cells were slowly cooled down to -80°C in cryo vials using a freezing device and stored in liquid nitrogen. For cell recovery, cells were thawed quickly at 37°C in a water bath, resuspended in the respective medium and centrifuged for 5 minutes at 1200 rpm. Afterwards, the pelleted cells were resupended and seeded in a cell culture flask for cultivation.

4.3 Chromatin immunoprecipitation (ChIP) assay

SW480/pRTR-p53-VSV and SW480/pRTR were cultured as described above. Cells were treated with DOX for 16 hours before cross-linking to induce ectopic expression of p53. Cross-linking was performed using 1% formaldehyde (Merck) and stopped after five minutes by adding 0.125 M glycine. Cells were harvested with SDS buffer

(50 mM Tris pH 8.1, 0.5% SDS, 100 mM NaCl, 5 mM EDTA) and pelleted and resuspended in IP buffer (2/3 SDS buffer and 1/3 Triton dilution buffer (100 mM Tris-HCl pH 8.6, 100 mM NaCl, 5 mM EDTA, pH 8.0, 0.2% NaN_3, 5% Triton X-100). Chromatin was sheered by sonication to generate DNA fragments with an average size of 500 bp. Preclearing and incubation with polyclonal VSV antibody (V4888, Sigma) or IgG control (M-7023, Sigma) for 16 hours was performed as previously described [94]. Washing and reversal of cross-linking was performed as described in [221]. Immunoprecipitated DNA was analyzed by qRT-PCR and the enrichment was expressed as percentage of the input for each condition [221]. qChIP primers used are listed in 3.5.2.2.

4.4 Episomal vectors for ectopic protein-expression

The pRTR vector is an improved version of the pRTS vector and its generation is described in [220]. The pRTR-p53-VSV vector was generated by excising the p53-VSV sequence from a pcDNA-p53-VSV vector and subsequent ligation into a pUC19 shuttle vector harboring SfiI restriction sites. After that, the C-terminally cDNA sequence of p53 was excised and ligated into the pRTR vector via its SfiI restriction sites.

4.5 Flow cytometry

4.5.1 Determination of the transfection efficiency (eGFP)

The pRTR vector has a DOX-inducible bidirectional promoter expressing the gene of interest in one and *eGFP* in the other direction. To verify the transfection efficiency of cell lines transfected with the pRTR vector, the cells were treated with and without DOX for 48 hours and the percentage of cells showing *eGFP* expression was measured using a BD Accuri™ C6 Flow Cytometer instrument (Accuri). The associated CFlow® software was used to determine the proportion of fluorescent cells.

4.5.2 Cell cycle analysis by propidium iodide staining

The supernatant of sub-confluent cells, that were cultured under the indicated conditions, was transferred into a falcon tube, cells were washed once with HBSS-/- and trypsinized. When the cells were fully detached from the surface of the cell culture flask, trypsin was inactivated using the transferred supernatant and the cell suspension was pelleted by centrifugation (1200 rpm, 5 minutes). Afterwards, the cells were washed once in HBSS+/+, pelleted and resuspended in ice-cold ethanol (70%) that was added dropwise to the cells. Next, the cells were stored overnight at -20°C, washed with PBS the next day, centrifuged and resuspended in propidium iodide (PI) staining solution (filtered using a 0.22 µm filter, Millipore). After

incubation at 37°C for 30 minutes, the cell cycle distribution of the cells was measured using a BD Accuri™ C6 Flow Cytometer Instrument (Accuri) and the corresponding Cflow® software.

4.6 Immunofluorescence and confocal-laser scanning microscopy

Cells were seeded on glass cover-slides and treated as indicated. Subsequently, the cells were washed three times using PBS, fixed with 4% paraformaldehyde (solved in PBS) for 10 minutes, permeabilized with 0.2% TritonX 100 for 20 minutes and blocked for 30 minutes using filtered 100% FCS. After incubation with the pre-blocked first antibody in a solution of 50% FCS (in PBS) and 0.05% PBS-T for one hour, the glass slides were washed three times with 0.05% PBS-T. The secondary antibody (diluted in 0.05% PBS-T and 50% FCS in PBS) was applied for 30 minutes and the cells were washed again three times with 0.05% PBS-T. To stain nucleic chromatin, DAPI (Roth) was added to the last washing step. In the end, the glass slides were placed on an object plate and covered with ProLong® Gold antifade (Invitrogen). The laser scanning microscopy LSM 700, Zeiss, was used to take the respective pictures. A Plan Apochromat 20x/0.8 M27 objective, ZEN 2009 software (Zeiss) and the following settings were used: image size 2048x2048 and 16 bit, pixel/dwell of 25.2 µs, pixel size 0.31 µm, laser power 2% and master gain 600 - 1000.

4.7 Isolation of RNA and reverse transcription

To isolate total RNA, the High Pure RNA Isolation Kit (Roche) was used and the isolation was performed according to the manufacturer´s protocol. RNA was eluted in 50 µl elution buffer. The amount and quality of the RNA was determined using a Nanodrop spectrophotometer and 1 µg of RNA was used for reverse transcription. For cDNA generation, the Verso cDNA Synthesis Kit (Thermo Fisher Scientific) was applied according to the manufacturer´s instructions using anchored oligo(dT) primers. To isolate miRNAs the High Pure miRNA Isolation Kit (Roche) was used according to the manufacturer´s protocol. For cDNA generation the Universal cDNA Synthesis Kit from the miRCURY LNA Universal RT microRNA PCR Kit (Exiqon) and the TaqMan MicroRNA Reverse Transcription Kit (Applied Biosystems) were used.

4.8 Luciferase assay

$3x10^4$ cells/well of the colorectal cancer cell line H1299 were seeded into a 12-well plate. After 24 hours, the cells were transfected with 100 ng of an empty firefly luciferase reporter plasmid (pGL3) or the pGL3 vector containing the respective miRNA binding sequence, 20 ng of Renilla reporter plasmid as a normalization

control and the respective pre-miRNA [25 nM] or its negative control [25 nM]. For antagomiR-transfection a concentration of 50 nM was used. After incubation for 48 hours, the Dual Luciferase Reporter assay kit (Promega) was used according to the manufacturer´s protocol. The Orion II luminometer (Berthold) was used to measure the luminescence intensities in a 96-well format and the SIMPLICITY software package (DLR) was applied for data-analyses.

4.9 Migration and invasion analysis in Boyden-chambers

SW480 cells stably transfected with the pRTR-p53-VSV vector were treated with DOX for 96 hours. Uninduced cells served as a negative control. During the last 24 hours, the cells were serum deprived (0.1% FCS). For migration analysis $5x10^4$ cells were counted and seeded in the upper compartment of a Boyden chamber (pore size 8.0 µm; Corning) in serum free medium. The lower chamber contained medium with 10% FCS as a chemo-attractant. For invasion analysis, $7x10^4$ cells were seeded on a Matrigel (BD Bioscience; 3.3 ng/ml in serum-free medium) coated membrane.

For migration and invasion, the cells were cultured for 48 hours in a Boyden chamber and subsequently fixed in ice-cold methanol for 10 minutes. Cells that remained in the upper compartement of the chamber were removed and those at the lower side of the membrane were stained with DAPI [1 µg/ml]. The pictures were taken with an AxioCam MRm camera using an Axiovert Observer Z.1 microscope. In addition, the Axiovision software (Zeiss) was used. For each condition pictures of three different fields were taken and the cell number was determined by using fluorescence microscopy. The relative migration was expressed as the number of treated to control cells with the control cells set as one.

For CST5-mediated effects, SW480/pRTR-p53-VSV cells were seeded in triplicates into 6-well plates and transfected with siRNA against *CST5* or the respective control for 48 hours. For the last 24 hours previous to the analysis, cells were serum deprived (0.1%). To analyze migration, $3x10^5$ cells were seeded in the upper chamber of a Boyden chamber (8.0 µm pore size; Corning) in serum free medium. After 42 hours, p53 expression was induced by adding DOX to the indicated samples.

4.10 PCR methods

4.10.1 Colony PCR

For the identification of bacterial clones harboring a vector insert in the right orientation, single colonies from the LB agar plate were picked and transferred into a 20 µl reaction mix (dNTPs, 10 x PCR buffer, FIREPol® DNA polymerase and primers specific for the vector or insert). The PCR reaction had the following cycling conditions: 5 minutes at 95°C, 25 cycles (95°C for 20 seconds, 58°C for 30 seconds

and 72°C for X minute/s (1 minute per 1 kbp length of the expected PCR product)). Finally the product size was checked on an agarose gel whose percentage was adapted to the length of the expected PCR product.

4.10.2 Cloning of 3´-UTR sequences

Shortened versions of the 3´-UTRs of the human *KLF12*, *HMGB1* and *CIT* mRNAs were amplified by PCR from cDNA of SW480 cells. The resulting PCR product was ligated into the pGL3 vector [218] and verified by sequencing. All primers that were used for cloning are listed in chapter 3.5.2.3.

4.10.3 qPCR using SYBR Green

A LightCycler 480 (Roche) was used for quantitative real-time PCR (qPCR). Experiments were conducted using the Fast SYBR Green Master Mix (Applied Biosystems) and the expression level of β-*actin* was used for normalization. All qPCR primers are listed in 3.5.2.1. Only those primers that showed a single peak in their melting curves were used.

4.10.4 qPCR using TaqMan/Exiqon Probes

For detection of mature miR-34a, RNA was reverse transcribed using the miRCURY LNA Universal RT microRNA PCR-Kit (Exiqon) and qRT-PCR was performed with the SYBR Green master mix provided using Exiqon LNA primer (Exiqon 204486). U6 primer were used for normalization (Exiqon 203903). For detection of mature miR-486-5p (Applied Biosystems, Catalog # 4427975, 001278) and miR-205 (Applied Biosystems, Catalog # 4427975, 000509), cDNA was generated using the TaqMan MicroRNA Reverse Transcription Kit (Applied Biosystems), qRT-PCR was performed using the TaqMan Universal Master Mix (Applied Biosystems) and values were normalized to RNU48 (Applied Biosystems, Catalog # 4373383, 001006). For miR-486-5p detection RNA had to be preamplified using the TaqMan PreAmp Master Mix (Applied Biosystems).

4.11 Protein isolation, SDS-PAGE and Western blot

For protein isolation, cells were washed two times with cold PBS and lysed in RIPA buffer. Lysates were sonicated using the HTU SONI130 (G. Heinemann Ultraschall- und Labortechnik) for three pulses (~3 seconds per pulse) with an intensity of 85%. Next, the lysates were centrifuged (16,060 g, 4°C, 15 minutes) and the supernatant was transferred into a new tube. For the determination of the protein-concentration the BCA Protein Assay Kit (Pierce, Thermo Scientific) was used according to the manufacturer´s protocol and the concentration was measured using the Varioskan Flash Multimode Reader and the SkanIt RE for Varioskan 2.4.3 software (Thermo Scientific). Afterwards, up to 100 µg of the protein lysates were

supplemented with 2x Laemmli buffer and denatured at 95°C for 5 minutes. After denaturation, the protein lysates were loaded on a 10% or 12% SDS acrylamide gel together with a pre-stained protein ladder (Fermentas). A voltage of 90 – 120 V was applied for electrophoresis in a Mini-PROTEAN®-electrophoresis system (Bio-Rad) with Tris-glycine-SDS running buffer. Next, the proteins were transferred on an Immobilion PVDF membrane (Millipore) using Towbin buffer, the PerfectBlue™ SEDEC blotting system (Peqlab) and a EPS 600 power supply (Pharmacia Biotech) running constantly at 125 mA per gel with a maximum voltage of 10 V. The blotting time varied according to the size of the proteins to be detected (25 – 65 minutes). To prevent unspecific binding of antibodies, the membrane was blocked for 1 hour in 5% skim milk/TBS-Tween20 (TBS-T). Thereafter, the membrane was incubated overnight at 4°C with a primary antibody dilution in TBS-T. The next day, the membrane was incubated with the secondary horseradish-peroxidase (HRP)-conjugated antibody for 1 hour at room temperature. After washing (2x15 minutes in TBS-T) the ECL/HRP substrate was added to the membrane and ECL-signals were detected using a CF440 Imager (Kodak). All antibodies used are listed in 3.4.

4.12 pSILAC

Sample Preparation

pSILAC was performed as described previously [217]. In brief, $5x10^5$ SW480/pRTR-p53-VSV cells were seeded on 10 cm dishes and grown in light DMEM supplemented with light L-arginine (84 mg/l) and L-lysine (40 mg/l), 10% dialyzed FBS, 100 units/ml penicillin and 0.1 mg/ml streptomycin. After p53 induction for 16 hours with 100 ng/ml DOX, cells were shifted to heavy SILAC medium (84 mg/l $^{13}C_6$ $^{15}N_4$-L-arginine and 40 mg/l $^{13}C_6$ $^{15}N_2$-L-lysine). The noninduced control samples were shifted to medium-heavy media (84 mg/l $^{13}C_6$-L-arginine, 40 mg/l $^{2}H_4$-L-lysine). To minimize arginine-to-proline conversion the light, medium-heavy and heavy medium was supplemented with 100 mg/l of unlabeled proline. All reagents (DMEM, dialyzed FBS and amino acids) were purchased from Cambridge Isotope Laboratories. After 24 hours cells were harvested with urea buffer (30 mM Tris base, 7 M urea, 2 M thiourea, pH 8.5). In total, six independent pSILAC analyses were performed, including two with a label-swap, and subjected to further proteomic analysis which was performed by Friedel Drepper, Silke Oeljeklaus and Bettina Warscheid.

Gel Electrophoresis and Tryptic Digestion of Proteins

Following cell lysis, proteins (30 µg per replicate) were separated by SDS-PAGE using 4 – 12% NuPage Bis-Tris gradient gels (Life Technologies) and visualized by colloidal Coomassie Brilliant Blue. Gel lanes were cut into 20 slices. Proteins were subjected to in-gel digestion using trypsin and prepared for LC-MS/MS analyses as described [222].

Mass Spectrometric Analyses

LC/MS analyses were performed using an UltiMate 3000 RSLCnano HPLC system (Thermo Scientific, Dreieich, Germany) and an Orbitrap Elite mass spectrometer (Thermo Scientific, Bremen, Germany). Peptide mixtures were washed and pre-concentrated for 5 min on a 5 mm × 0.3 mm PepMap™ C18 µ-precolumn (Thermo Scientific) followed by separation on a 50 cm × 75 µm C18 reversed-phase nano LC column (Acclaim PepMap™ RSLC column; 2 µm particle size; 100 Å pore size; Thermo Scientific) at a temperature of 40°C using a 45 min linear gradient ranging from 4 to 36% (v/v) acetonitrile [ACN; in 0.1% (v/v) formic acid] followed by 36 to 82% (v/v) ACN in 5 min and 5 min at 82% ACN at a flow rate of 250 nl/min. The mass spectrometer was operated using a Nanospray Flex ion source with stainless steel emitters (Thermo Scientific) and externally calibrated using standard compounds. Full MS scans (*m/z* 370 – 1,700) were acquired in the orbitrap at a resolution of 60.000 (at *m/z* 400) with an automatic gain control (AGC) of 1×10^6 ions and a maximum fill time of 200 ms. Up to 25 of the most intense multiple charged precursor ions above a signal threshold of 2.500 were fragmented by collision-induced dissociation in the linear ion trap at a normalized collision energy of 35%, an activation q of 0.25, an activation time of 10 ms, an AGC of 5×10^3 ions, and a maximum fill time of 150 ms. The dynamic exclusion time for previously fragmented precursor ions was 45 s.

Mass Spectrometric Data Analysis

Mass spectrometric raw data were processed with Andromeda/Max-Quant (version 1.3.0.5) [223, 224]. Peaklists of MS/MS spectra were generated by MaxQuant using default settings and searched against the organism-specific UniProt human protein database including protein isoforms (version 2013_05; 88,817 entries) [225] and the set of common contaminants provided by MaxQuant. The species was restricted to human since all experiments were performed with the human cell line SW480. Database searches were performed with tryptic specificity allowing two missed cleavages, mass tolerances of 20 ppm for the first, 6 ppm for the main search of precursor ions and 0.5 Da for fragment ions; oxidation of methionine and acetylation of protein N-termini as variable modification; carbamidomethylation of cysteine as fixed modification. A false discovery rate of 1% calculated as described previously [223] was applied for filtering both the peptide identifications and the list of proteins. For protein identification, at least one unique peptide with a minimum length of seven amino acids was required. Proteins identified by the same set of peptides were combined to a single protein group by MaxQuant. SILAC-based relative protein quantification was based on unique peptides, Arg6 and Lys4 as medium-heavy (M) and Arg10 and Lys8 as heavy (H) labels. The variability of individual protein abundance ratios was calculated by

MaxQuant and is the standard deviation of the natural logarithms of all peptide ratios used to determine the protein ratio multiplied by 100 [223]. Only proteins quantified in at least two biological replicates were included in the statistical analysis. Protein abundance ratios reported as induced/non-induced (H/M or M/H) and normalized to the median of the respective replicate by MaxQuant to account for systematic deviations such as mixing errors were log_2-transformed and the mean log_2 ratios and p-values were calculated across all replicates with valid values for individual protein groups. Reproducibility of the results was further assessed by correlating log_2 ratios and computing p-values for pairs of replicates. In nine out of 15 pairwise comparisons, a set of proteins appeared to be down-regulated in one replicate but unregulated in the other. In order to account for this effect, proteins exhibiting log_2 fold changes ≤ -0.3 or ≥ 0.3 with a p-value ≤ 0.05 across all replicates but showing p-values > 0.3 in more than half of the pairwise comparisons of replicates indicative of a heterogeneous regulation were separately marked in the list of candidates (class II hits that are marked with an asterisk (*) in Figure 35, Table 2).

The mass spectrometry proteomics data have been deposited to the ProteomeXchange Consortium (http://proteomecentral.proteomexchange.org) via the PRIDE partner repository [226] with the dataset identifier PXD001976.

4.13 Real-time impedance measurement

Cellular impedance was measured using a xCelligence real-time cell analyzer (RTCA) (Roche) according to the manufacturer´s protocol. 5000 cells per well were seeded into an E-plate 16 and were allowed to equilibrate for 30 minutes at room temperature. Subsequently the E-plate 16 was placed into the xCelligence device and the impedance of the cells was measured every 60 minutes for a period of 96 hours. After 24 hours DOX was added to the respective wells. The electrical impedance is represented as a dimension/unit-less parameter termed cell-index, which represents the relative change in electrical impedance that occurs in the presence and absence of cells in the wells. This change is calculated based on the following formula: CI = (Zi−Z0)/15, where Zi determines the impedance at an individual experimental time point and Z0 is the impedance measured at the beginning of the experiment. The impedance is measured at three different frequencies (10, 25 or 50 kHz) (ref: Roche Diagnostics GmbH. Introduction of the RTCA DP Instrument. RTCA DP Instrument Operator‘s Manual, A. Acea Biosciences, Inc.; 2008.). To validate the results of the impedance measurement, the cells were simultaneously seeded in triplicates into a 96-well plate and the number of living cells was counted using trypan blue after 96 hours.

4.14 RNA interference

For RNA interference siRNAs (Ambion silencer siRNA negative control: #1 ID#4611; siCST5 AM16708 ID#10755) were transfected at a final concentration of 10 nM for the indicated time points using HiPerfect transfection reagent (Qiagen).

4.15 Sequencing

4.15.1 DNA-sequencing

To verify a specific DNA sequence, Sanger sequencing was performed. The BigDye® Terminator v3.1 Cycle Sequencing Kit (Life Technologies) was used according to the manufacturer´s instructions. The reaction mix contained 1 µg of DNA, 5 pmol of primer, the BigDye Terminator and the 5x Sequencing buffer. The following conditions for PCR-amplification were applied: 15x (10 seconds at 96°C, 90 seconds at 60°C). Afterwards, the PCR product was purified using the DyeEx 2.0 Spin Kit (Qiagen) in a 5417C centrifuge (Eppendorf). 4 µl of purified DNA was then mixed with 16 µl of Hi-Di Formamide (Applied Biosystems) and sequenced in an ABI3130 genetic analyzer capillary sequencer (Applied Biosystems). Finally, data were analyzed applying the 3130 Data Collection Software v3.0 and the sequencing analysis software 5.2 (Applied Biosystems).

4.15.2 RNA-sequencing

$3x10^5$ SW480/pRTR-p53-VSV as well as SW480/pRTR were seeded on 10 cm plates and total RNA was isolated after 48 hours DOX treatment. Total RNA was isolated using the High Pure RNA Isolation Kit (Roche) and its quality was determined with a Bioanalyzer (Agilent Technologies). Library preparation was done using an RNA-Seq Sample Prep Kit (Illumina) according to the manufacturer´s instructions and sequenced on a HiSeq 2000 (Illumina). The analysis of the RNA-Seq data was performed by Thomas Bonfert. 101-nt sequence reads from SW480/pRTR-p53-VSV and SW480/pRTR cells were aligned separately in a three-step mapping procedure described recently [227] using the short read alignment program Bowtie (version 0.12.7) [228]. In step 1, reads were aligned to pre-rRNA sequences (18S, 5.8S, 28S and spacer regions). In step 2, the remaining unmapped reads were aligned to Ensembl transcripts (ENSEMBL version 60), with the exclusion of pseudogenes and haplotypes. Finally, in step 3, reads that could not be aligned to known transcripts were aligned to the human reference genome (hg19). Reads that could be mapped equally well to more than one location were discarded. Bowtie was configured for all three steps in the following way: The first 60 nucleotides were chosen as the seed region. Three mismatches were allowed in the seed and 10 mismatches in the overall alignment. Expression levels of Ensembl genes were determined using the rpkm (number of reads per kilobase of gene per million mapped reads) measure [229].

Only reads mapped to an exon or exon-exon junction were included in the number of reads mapped to a gene. Log_2 fold changes between the two samples (SW480/pRTR-p53-VSV and SW480/pRTR cells) were calculated from gene rpkm values and used to define induced (log_2 fold change ≥ 1) and repressed (log_2 fold change ≤ -1) genes. The RNA-Seq data can be accessed in the GEO database using the accession number GSE67109.

4.15.3 miRNA-sequencing

The miRNA-sequencing was performed by Anne Dueck, Norbert Eichner and Gunter Meister. Total RNA from SW480/pRTR-p53-VSV and SW480/pRTR cells was isolated using the Trizol reagent (Life Technologies) following the manufacturer´s protocol. 10 µg of the total RNA was run on a 12% Urea-PAGE (National Diagnostics) to purify the small RNA fractions of each sample. Gel pieces were isolated corresponding to a size of about 15 - 30 nt and the contained RNA was collected by crushing the gel, elution over night in elution buffer (300 mM NaCl, 2 mM EDTA) and precipitation with 2.5V 100% ethanol. The small RNA fraction was solved in 12 µl of RNAse-free water, 10 µl were used for the generation of a small RNA library. Cloning was performed as described before [230]. In short, an adenylated adapter was ligated to the 3' end of the RNA by a truncated T4 RNA Ligase 2 [231], followed by the ligation of the 5' adapter by T4 RNA Ligase 1 (NEB). After reverse-transcription with a specific primer, the cDNA was amplified by PCR. The correct PCR product was gel-purified, eluted in elution buffer, precipitated and solved in water. The quality of the libraries was assessed by qPCR and Bioanalyzer measurements. Libraries were sequenced on a HiScan by the KFB (Kompetenzzentrum für fluoreszente Bioanalytik, Regensburg, Germany).

The analysis of the miR-Seq data was performed by Florian Erhard. Fastq files were processed with an in-house pipeline consisting of adapter trimming, read alignment, read counting and normalization. Adapters were trimmed by computing a suffix-prefix alignment of each read against the Illumina 3´ adapter sequence. Trimmed reads were then aligned to the reference genome (hg19) using bowtie 0.12.7 [228] allowing for up to 2 mismatches. All best matches were retained and multi-mapping reads were equally divided among all mapping sites. To compute miRNA read counts all reads mapping to annotated mature miRNA positions (according to mirbase v16 [232]) were considered. At their 3´ end, a tolerance of +/- 3 bp was allowed, but no tolerance at their 5´ end. Normalization was performed by fitting a robust linear model to the quantile-quantile plot of log miRNA counts and taking the offset as normalization factor. The miR-Seq data can be accessed in the GEO database using the accession number GSE67181.

4.15.4 ChIP-sequencing

ChIP assays were performed as described in 4.15. The immunoprecipitated DNA-fragments were quantified using a Bioanalyzer (Agilent Technologies). Libraries were generated using a ChIP-Seq Sample Prep Kit (Illumina Part # 11257047) according to the manufacturer´s instructions and sequenced on a HiSeq 2000 (Illumina). The analysis of the ChIP-Seq data was performed by Thomas Bonfert. 101-nt sequence reads were aligned separately for the two samples (SW480/pRTR-p53-VSV and SW480/pRTR cells) with the same three-step mapping procedure as for RNA-Seq analysis. Peaks were identified using MACS (version 1.4.2) [233] with default parameters. The output of MACS contains the genomic start and stop coordinates for every called peak, as well as the coordinate of the peak maximum (denoted as peak summit). For every called peak, the Ensembl gene with minimum distance between peak summit and respective transcription start site was determined. The ChIP-Seq data can be accessed in the GEO database using the accession number GSE67108.

Analysis of Sequence Motifs

Genomic sequences +/- 250 bp around the called peak summits were extracted for every peak with an associated gene within 20 kbp from the peak summit. If the peak start or end was less than 250 bp away from the summit, the extracted sequence started or ended with the peak start or end, respectively. MEME (version 4.7.0) [234] was applied on the generated sequences in order to discover p53 binding site motifs. The default parameter settings were used. The maximum number of motifs to find was set to 3. This step was repeated separately for sequences of peaks associated with induced and repressed genes, respectively. SpaMo (version 4.7.0) [235] was used to search for enriched transcription factor binding motifs located in direct proximity to the best predicted motif by MEME. The input of SpaMo were peak sequences, the output of the MEME run and the JASPAR core database [236] as source for secondary motifs. All other parameters were set to default.

4.16 Site directed mutagenesis

For site directed mutagenesis of miRNA binding sites in the 3´-UTR of their respective target genes, the 3´-UTR fragments were ligated into the pGEM T Easy vector (Promega). Afterwards, the QuikChange II Site-Directed Mutagenesis Kit was used according to the manufacturer´s instructions. All primers used for the mutagenesis PCR are listed in 3.5.2.3. To verify successful mutagenesis, the mutated plasmids were sequenced.

4.17 Statistical analysis

A Student´s t-test (unpaired, two-tailed) was used to determine significant differences between two groups of samples. A Kolmogorov-Smirnov test was applied to calculate the significance of cumulative distribution analyses. For correlation analyses a two-tailed Pearson´s correlation was applied. p-values < 0.05 were considered as significant (*: $p < 0.05$; **: $p < 0.01$; ***: $p < 0.001$).

4.18 Web-based expression analyses and algorithms

The Oncomine database [237] was used to analyze the differential mRNA expression of *HMGB1, KLF12 and CIT* in human cancer versus normal tissue datasets. The threshold for the p-value and fold change was set to 0.05 and 1.5, respectively.

The PROGgene database [238] was used to analyze the clinical significance of the target gene set *HMGB1*, *KLF12* and *CIT*. To analyze overall and metastasis free survival, the colorectal cancer datasets GSE15736 and GSE11121 were used, respectively.

miRNA target prediction of up-regulated miRNAs was performed combining the results from the public databases TargetScan (http://www.targetscan.org) and Pictar (http://pictar.mdc-berlin.de) [239, 240]. Only conserved target sites were considered for further analysis.

A KEGG pathway enrichment analysis of differentially up- and down-regulated mRNAs and proteins was perfomed using the DAVID bioinformatics database [241, 242].

To visualize p53-binding signals the ChIP-Seq results were uploaded in wig-format to the UCSC genome browser [243].

Data from the TCGA (The Cancer Genome Atlas) database [244] were used for differential mRNA expression analyses in different tumor stages in the colorectal cancer dataset (n = 424). Only those differences that showed a p-value ≤ 0.05 were taken into account.

4.19 Wound healing assay

SW480/pRTR-p53-VSV cells were seeded into 12-well plates and the scratch was applied when cells were grown to a confluent cell layer using a pipet tip. Two hours before applying the scratch, the cells were treated with Mitomycin C [10 ng/ml]. After scratching, the cells were washed three times with HBSS+/+ and medium with or without DOX was added. In addition, images of the initial wound area were taken with an Axiovert Observer Z.1 microscope connected to an AxioCam MRm camera using the Axiovision software (Zeiss). Afterwards, cells were allowed to close the wound for a time period of 48 hours and images were captured with the above mentioned device.

To investigate the impact of CST5 on p53-mediated inhibition of migration, SW480/pRTR-p53-VSV cells were seeded into culture inserts (IBIDI, 80241) and transfected with siRNA against *CST5* or the respective control for 48 hours. After 42 hours, p53 expression was induced by adding DOX to the indicated samples and Mitomycin C was added for 2 hours before applying the scratch by taking out the culture insert. Cells were washed three times with HBSS +/+, medium with or without DOX was added and the pictures showing the initial wound area were taken. After 48 hours final pictures were taken. The experiment was performed in triplicates and three pictures of different wound areas were captured for each well.

5. RESULTS

5.1 *miR-34* and *SNAIL* form a double-negative feedback loop to regulate epithelial-mesenchymal transitions

The following results are published in:

Siemens H*, Jackstadt R*, Hünten S*, Kaller M*, Menssen A*, Götz U and Hermeking H (2011). *miR-34* and *SNAIL* form a double-negative feedback loop to regulate epithelial-mesenchymal transitions. Cell Cycle 10 (24), 4256-71. [1]
* Equally contributing authors.

All figures shown in this section are exclusively based on my experimental work. Figures from contributing authors have deliberately not been included in the following section as they are only adjacent to the scope of this thesis. However, to provide a comprehensive picture of the published findings the text refers to results from contributing authors of the publication above. The respective name of the contributing author is clearly stated in the text.

5.1.1 p53-dependent regulation of SNAIL is mediated by miR-34a

p53 has been described to suppress tumorigenesis by the inhibition of epithelial-mesenchymal transition [98, 245]. To study p53-dependent regulations and processes related to mesenchymal-epithelial transitions, we used the colorectal cancer cell line HCT116 *p53+/+* and its isogenic clone harboring a homozygous deletion of p53 [246] and treated those cells with Nutlin-3a, an inhibitor of the E3-ligase MDM2 [247], to activate p53 expression. Expectedly, Nutlin-3a treatment resulted in p53 activation on protein level in the HCT116 *p53+/+* but not in HCT116 *p53-/-* cells (Fig. 6).

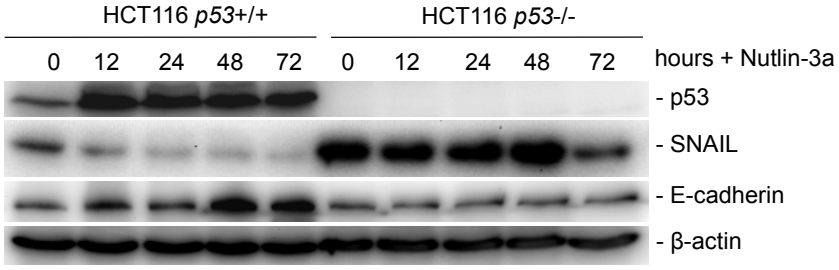

Figure 6: **p53-dependent regulation of SNAIL- and E-cadherin protein levels in the colorectal cancer cell line HCT116**. HCT116 *p53+/+* and HCT116 *p53-/-* were treated with the MDM2-inhibitor Nutlin-3a for the indicated timepoints. Western blot analysis of the indicated proteins. ß-actin served as a loading control.

Furthermore, we detected a robust induction of the adherens junction protein E-cadherin upon p53 expression in the HCT116 *p53+/+* cells whereas no change was observed in the HCT116 cell line carrying the p53 deletion (Fig. 6). This induction was confirmed by an immunofluorescence analysis showing the p53-dependent localization of E-cadherin to the outer cell membrane (Fig. 7).

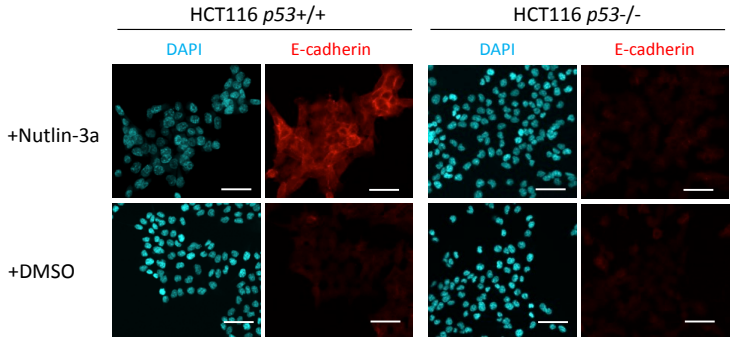

Figure 7**: p53-dependent regulation of E-cadherin expression and localization in the colorectal cancer cell line HCT116**. HCT116 *p53+/+* and HCT116 *p53-/-* were treated with the MDM2-inhibitor Nutlin-3a for 72 hours and subsequently subjected to an immunofluorescence analysis of E-cadherin protein-expression and localization. DAPI was used to stain nuclear DNA. 200x magnification.

Moreover, Nutlin-3a treatment resulted in increased *E-cadherin* mRNA levels as well as decreased expression of the mesenchymal marker *Vimentin* in HCT116 *p53+/+* cells (Fig. 8).

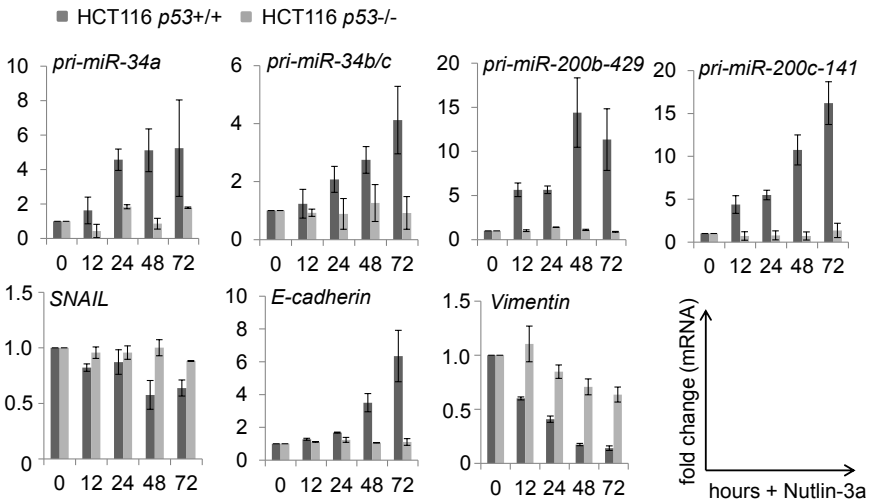

Figure 8: **p53-dependent regulation of EMT-related factors as well as primary miRNA-transcripts in the colorectal cancer cell line HCT116**. HCT116 *p53+/+* and HCT116 *p53-/-* were treated with the MDM2-inhibitor Nutlin-3a for the indicated timepoints and the indicated mRNAs were measured by qPCR analysis. *ß-actin* served as a normalization control. Fold changes represent mean values of triplicate analyses of Nutlin-3a versus DMSO treated cells and error bars represent standard deviations.

Since the mesenchymal marker SNAIL is known to repress E-cadherin expression, we investigated the effect of p53 on SNAIL protein- and mRNA-level. Interestingly, SNAIL was repressed in a p53-dependent manner on both, protein- and mRNA-level (Fig. 6, 8). It was striking that SNAIL protein levels were lower in untreated HCT116 *p53+/+* cells when compared to HCT116 *p53-/-* cells.

As p53 is known to induce MET-like processes through the regulation of miRNAs [98, 245], we checked for the expression of the primary transcripts of miR-34a, miR-34b/c and the miR-200 family members, miR-200b-429 and miR-200c-141 (Fig. 8). All primary miRNA transcripts were induced in a p53-dependent manner in the HCT116 *p53+/+* cell line but not in HCT116 *p53-/-* cells after Nutlin-3a treatment.

To further interrogate the p53-dependency of those EMT-related factors, I established the DOX-inducible colorectal cancer cell line SW480/pRTR-p53-VSV, which is described in detail on page 42. Upon activation of p53 by treatment with DOX, SNAIL was down-regulated on protein- and mRNA-level (Fig. 9).

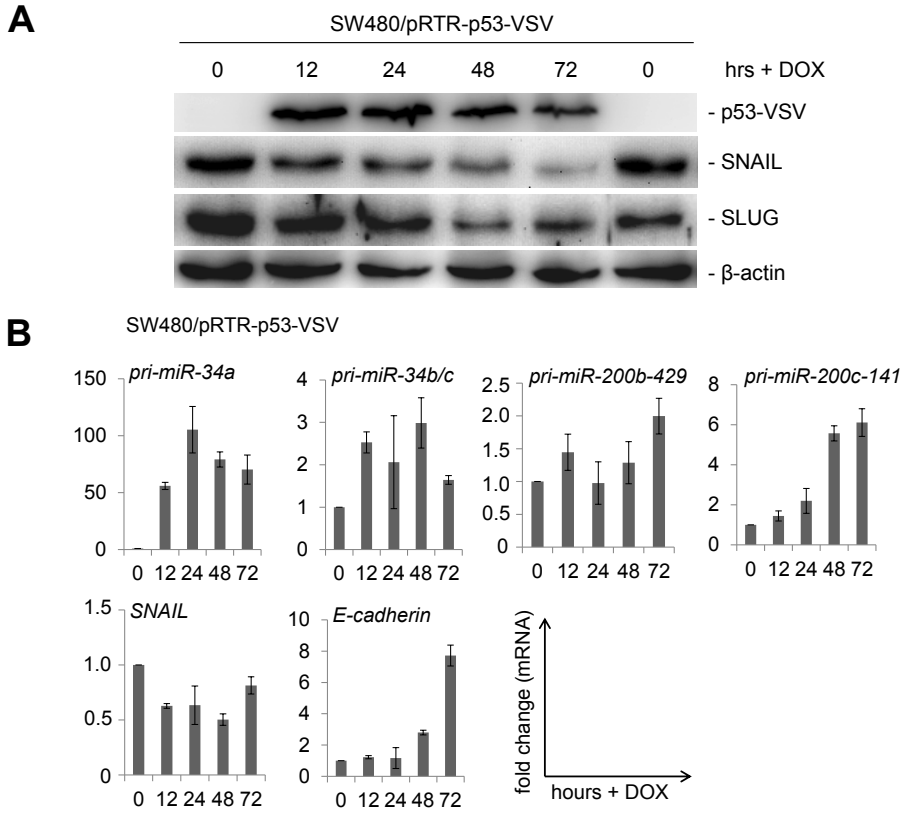

Figure 9**: p53-induced regulation of EMT-related factors in the colorectal cancer cell line SW480/pRTR-p53-VSV**. SW480/pRTR-p53-VSV cells were treated with DOX for the indicated timepoints. (A) Western blot analysis of the indicated proteins. ß-actin served as a loading control. (B) The indicated mRNAs were measured by qPCR analysis. *ß-actin* served as a normalization control. Fold changes represent mean values of triplicate analyses of DOX-treated versus untreated cells and error bars represent standard deviations.

As seen before in the HCT116 cells, the SNAIL target *CDH1* showed a prominent up-regulation upon ectopic p53 expression (Fig. 9B). Furthermore, the mesenchymal marker SLUG was down-regulated on protein level in the SW480/pRTR-p53-VSV cells after DOX treatment (Fig. 9A), which could possibly be explained by the MDM2-mediated degradation of SLUG upon p53 induction [248]. In addition, the primary miRNA transcripts of the miR-34 and miR-200 families were induced upon ectopic p53 expression (Fig. 9B). *pri-miR-34a* showed the most pronounced induction whereas *pri-miR-34b/c*, *-miR-200b/429* and *-miR-200c/141* were moderately induced.

To check whether the down-regulation of SNAIL is causally linked to the robust induction of miR-34a upon p53 expression, we treated the SW480/pRTR-p53-VSV cells with an antagomir-*miR-34a* and simultaneously induced p53 expression (Fig. 10). As shown before, treatment with DOX led to the induction of p53 protein levels and a repression of the mesenchymal marker SNAIL. The same effect was demonstrated when the cells were simultaneously treated with an antagomir control-oligonucleotide. However, when the cells were treated with an antagomir against *miR-34a* the repression of SNAIL was less pronounced compared to the control transfection. This indicates that SNAIL repression after induction of p53 is - at least in part - mediated by miR-34a.

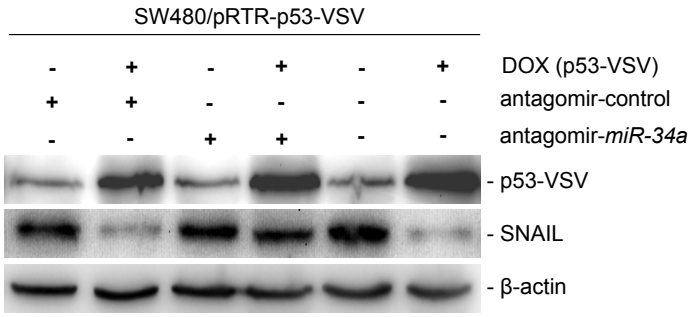

Figure 10: **p53-dependent down-regulation of SNAIL is mediated by miR-34a in the colorectal cancer cell line SW480**. Western blot analysis of the indicated proteins, ß-actin served as a loading control. SW480/pRTR-p53-VSV cells were transfected with the indicated oligonucleotides for 48 hours and treated with or without DOX for 24 hours before harvesting. Antagomir-*miR-34a* represents an oligonucleotide specifically targeting *miR-34a* and antagomir-control is the respective control.

Next, we addressed the question whether SNAIL is a direct miR-34a target. My colleague Dr. Markus Kaller inspected the 3´-UTR of *SNAIL* for putative miR-34a seed-matching sequences using two different alghorithms, TargetScan and miRanda [239, 249], and identified a highly conserved miR-34a seed sequence in this region. A 3´-UTR-reporter of *SNAIL* displayed a significant repression after cotransfection of a pre-miR-34a oligonucleotide. Mutation of the seed-matching sequence in the 3´-UTR abolished the miRNA-mediated repression. These results indicate that p53 represses SNAIL indirectly via direct induction of miR-34a.

5.1.2 miR-34a regulates markers of mesenchymal-epithelial transition

To investigate whether miR-34a alone induces MET-like changes, my colleague Dr. Helge Siemens transfected the colorectal cancer cell line SW480 with a pRTR-miR-34a vector and checked for expression changes of MET-related factors after ectopic *miR-34a* expression. Indeed, western blot analysis revealed a robust down-regulation of the mesenchymal markers SNAIL, ZEB1, Vimentin and an increase of the epithelial marker E-cadherin after induction of miR-34a. Furthermore, HDAC1 and ß-catenin were both repressed on protein level. In addition, the localization of ß-catenin changed from nuclear to cytoplasmic after miR-34a expression. qPCR analyses confirmed the up-regulation of *CDH1* and the down-regulation of *Vimentin*, *SNAIL*, *ZEB1* and *SLUG*.

Furthermore, the stemness markers *CD133*, *OLFM4*, *BMI1* as well as the known miR-34a targets *CD44 [250]* and *c-MYC* [251, 252] were down-regulated upon ectopic *miR-34a* expression indicating a potential loss of stemness. The down-regulation of stem cell-like properties has already been described for miR-200c [245, 253]. Furthermore, an investigation of the 3´-UTR of the EMT-inducing factors *SLUG*, *ZEB1* and *ZEB2* for miR-34a- as well as miR-200-seed-matches revealed miR-200 binding sites in the 3´-UTRs of *SLUG*, *ZEB1* and *ZEB2* as shown previously [97, 98]. A miR-34a seed-match was only present in the 3´-UTR of *ZEB2*. However, *ZEB1*- and *ZEB2* 3´-UTR constructs were only repressed upon pre-miR-200 transfection whereas the transfection of a pre-miR-34a oligonucleotide did not have any effect. This indicates that miR-34a induces MET-like changes in the studied colorectal cancer cell line SW480 by directly down-regulating SNAIL. However, the results of Dr. Helge Siemens show that other mesenchymal markers such as *SLUG*, *ZEB1* and *ZEB2* are not direct miR-34a targets. Their repression might rather be mediated by the up-regulation of the miR-200 family, which is in part the result of down-regulated SNAIL levels.

5.1.3 miR-34a dependent regulation of MET-like changes

Next, we investigated, whether p53 inhibits EMT-associated functions, such as migration and invasion, via the induction of miR-34a. A scratch-assay revealed that wound closure was significantly decreased after DOX treatment in the SW480/pRTR-p53-VSV cells when compared to the untreated control (Fig. 11A, B). Furthermore, SW480/pRTR-p53-VSV cells showed a significant reduction in relative migration after ectopic p53 expression (Fig. 11C).

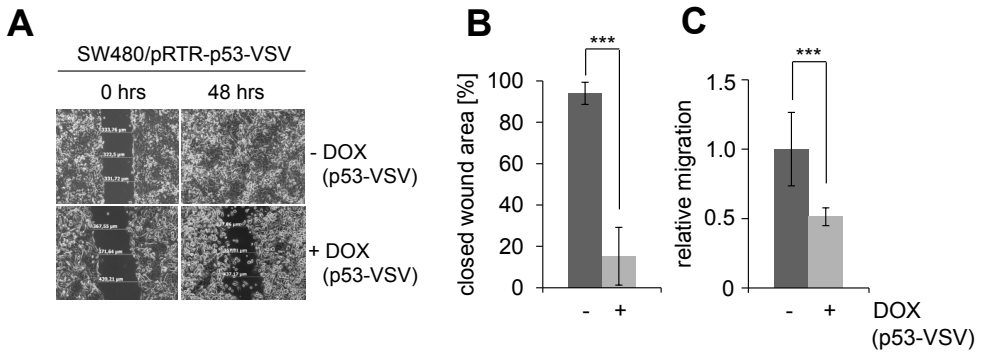

Figure 11: **p53 inhibits wound closure and migration in SW480 cells**. (A) SW480/pRTR-p53-VSV cells were treated with or without DOX for 48 hours before a scratch was generated and representative pictures were taken directly after the scratch (0 hours) and after 48 hours; 100x magnification. (B) The wound width of five scratches in two wells was measured and represented as the average of the closed wound area [%] +/- SE (n=2). (C) SW480/pRTR-p53-VSV (un-)treated with DOX for 48 hours were seeded in Boyden-chambers and were allowed to migrate for 48 hours. Represented is the mean relative migration +/- SD (n=3).

To address the question how miR-34a contributes to cellular functions mediated by p53, we transfected the SW480/pRTR-p53-VSV cells with an antagomir against *miR-34a* and treated the cells with or without DOX before subjecting them to a scratch and invasion assay (Fig. 12). Treatment with the antagomir-*miR-34a* after ectopic p53 expression reversed both, the inhibition of wound closure and the inhibition of invasion (Fig. 12A and B, respectively). Furthermore, antagomir-*miR-34a* treatment led to an increase in migration and invasion when compared to the control transfection. The data indicate that p53-induced miR-34a mediates MET-like changes including decreased wound closure, migration and invasion.

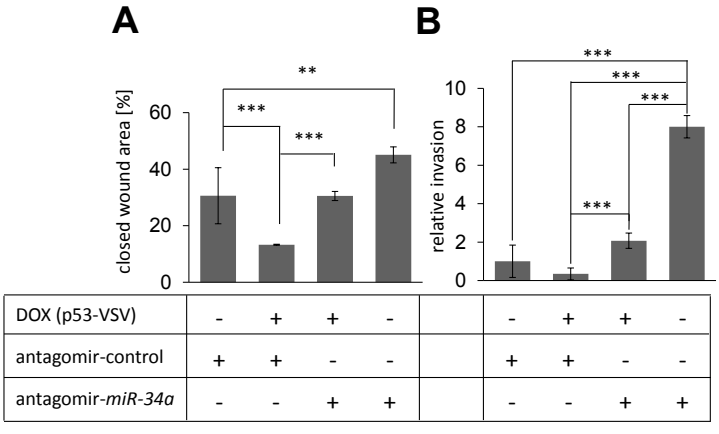

Figure 12: **p53 mediates the inhibition of wound-closure and invasion via miR-34a in SW480 cells**. SW480/pRTR-p53-VSV cells were transfected with the indicated oligonucleotides for 48 hours and treated with or without DOX for 24 hours. (A) Scratch assay: 48 hours after the scratch the wound width of five scratches in two wells was measured and represented as the average of the closed wound area [%] +/- SE (n=2). (B) Invasion assay: Cells were seeded in a Boyden-chamber and allowed to invade through the membrane for 48 hours. Represented is the mean relative invasion +/- SD (n=3).

These results were confirmed by my colleague Dr. Helge Siemens who investigated SW480/pRTR-miR-34a cells for their wound healing capacity as well as their invasion and migration ability after ectopic *miR-34a* expression. Overexpression of miR-34a inhibited wound closure as well as invasion and migration. Taken together, miR-34a is essential to mediate the inhibition of migration and invasion in colorectal cancer cells.

5.1.4 Relevance of SNAIL as a miR-34a target

Next, we determined the relevance of SNAIL repression on miR-34a-mediated MET-like changes. Dr. Helge Siemens generated all the following data. He established a colorectal cancer cell line harboring an inducible pRTR-SNAIL-VSV vector. The *SNAIL* cDNA cloned into the pRTR vector was lacking its 3´-UTR sequence and therefore the miR-34a binding site in order to check whether ectopic expression of a *miR-34*-insensitive *SNAIL* cDNA reverses the MET-like changes mediated by *miR-34a*.

Ectopic expression of SNAIL in SW480/pRTR-SNAIL-VSV cells partly prevented the inhibition of migration in a wound-healing and Boyden chamber assay. Furthermore, HCT116 *p53-/-* cells, that displayed higher levels of SNAIL than HCT116 *p53+/+* cells, showed increased migration compared to the HCT116 *p53+/+* cell line. Moreover, siRNA mediated knockdown of *SNAIL* in HCT116 *p53-/-* cells resulted in a significant decrease in their migratory capacity. Taken together, SNAIL is relevant for increased migration observed after loss of p53 and presumably also miR-34.

5.1.5 Direct repression of *miR-34* by SNAIL

Based on the negative feedback loop between the *miR-200* family genes and ZEB1/2 [254, 255], we hypothesized that miR-34a might also be a direct target of SNAIL. To test this hypothesis, Dr. Helge Siemens ectopically expressed SNAIL in DLD1/pRTR-SNAIL-VSV cells, which resulted in several EMT-like effects: down-regulation of the adherens-junction protein E-cadherin, enhanced wound closure, migration and invasion and the appearance of F-actin stress fibers. In addition, mRNA levels of the mesenchymal markers *Vimentin* and *ZEB1* were up-regulated whereas *CDH1* showed a prominent down-regulation. Interestingly, the primary transcripts of *miR-34a* and *miR-200c* were strongly repressed upon ectopic expression of SNAIL. Knocking-down *SNAIL* in the mesenchymal cell line SW480 resulted in increased expression of the *primary-miR-34a* and *–miR-34b/c* transcripts which confirms that SNAIL directly or indirectly mediates their repression.

To determine whether SNAIL is a direct repressor of the *miR-34* family genes, Dr. Markus Kaller examined the respective promoters for potential SNAIL binding sites.

Promoter-proximal E-boxes were identified for both, *miR-34a* and *miR-34b/c*. Also the promoter of the *miR-200c* gene harbored three conserved SNAIL binding sites. Indeed, a ChIP-assay in the DLD1/pRTR-SNAIL-VSV cells revealed binding of SNAIL upstream of the *miR-34a*, *-34b/c* and *-200c* promoters which confirmed that SNAIL functions as a direct repressor of the *miR-34* family and *miR-200c*. Taken together, miR-34 and SNAIL form a double-negative feedback loop that controls the transition between the epithelial and mesenchymal state.

5.2 p53-regulated networks of protein, mRNA, miRNA and lncRNA expression revealed by integrated pSILAC and NGS analyses

The following results are published in:

Hünten S, Kaller M*, Drepper F*, Oeljeklaus S, Bonfert T, Erhard F, Dueck A, Eichner N, Friedel CC, Meister G, Zimmer R, Warscheid B and Hermeking H (2015). p53-Regulated Networks of Protein, mRNA, miRNA and lncRNA Expression Revealed by Integrated Pulsed Stable Isotope Labeling With Amino Acids in Cell Culture (pSILAC) and Next Generation Sequencing (NGS) Analyses. Mol Cell Proteomics, 2015 Jul 16. pii: mcp.M115.050237. [2] *equally contributing authors

All figures shown in this section are either based exclusively on my experimental data or built on my preparatory work and experimental planning under supervision of Prof. Hermeking. Together with Prof. Hermeking I planned and developed the concept of this study including its main objectives and wrote major parts of the manuscript. I established the cell line used for the study, evaluated its functionality and prepared the cells for miRNA-, RNA- and ChIP-sequencing. Furthermore, I performed isotopic labeling of the cells for subsequent proteomic analysis. I comparatively analyzed NGS and pSILAC datasets after their raw data analysis and evaluated the results for further analysis of interesting candidate genes. I performed all cell culture related experiments, KEGG pathway and target prediction analyses and analyzed clinical relevance of the candidate genes.

To provide a comprehensive picture of the published findings the text and figures also refer to contributions of the co-authors that supported bioinformatics as well as mass spectrometric analyses. In case of contributions of the co-authors these are clearly indicated in the text and the corresponding figure legends. Sequencing of the RNA- and ChIP-samples was performed by GATC, Konstanz. miRNA-sequencing of total RNA samples was done in collaboration with A. Dueck, N. Eichner and G. Meister. Mass spectrometric analysis was performed by F. Drepper, S. Oeljeklaus and B. Warscheid. Bioinformatics analysis of the miRNA-sequencing raw data was performed by F. Erhard and R. Zimmer. T. Bonfert, C. Friedel and R. Zimmer conducted raw data analyses of RNA- and ChIP-sequencing data. A list with corresponding expression fold changes was provided by the respective contributing authors after raw data analyses of (mi-)RNA-Seq and pSILAC results. After raw data analysis of the ChIP-Seq data, T. Bonfert, C. Friedel and R. Zimmer provided the DNA-binding motifs of p53 and neighboring transcription factors, the localization and distribution of called ChIP-Seq peaks as well as a list showing all occupied p53 binding sites that were identified (including their sequence and localization). M. Kaller supported bioinformatics analyses of mRNA, miRNA and lncRNA expression results, cumulative distribution analyses and comparative analyses of p53 pSILAC data with miR-34a pSILAC results.

5.2.1 NGS and pSILAC analyses after p53 activation

We studied the effect of p53 activation on the expression of proteins, mRNAs and ncRNAs as well as genome-wide DNA-binding by p53. For this purpose, a recently described, episomal pRTR vector system that allows DOX-inducible expression of the introduced cDNA was employed (see 5.1) [1, 220]. SW480 CRC cells were transfected with pRTR-p53-VSV vectors and after selection for two weeks, stable cell pools were obtained. As a control, an SW480 cell pool harboring a pRTR vector only expressing GFP was generated. 95.7% and 85.2% of the cells in the SW480/pRTR-p53-VSV and SW480/pRTR pools, respectively, were positive for GFP-expression 48 hours after addition of DOX (Fig. 13A). SW480/pRTR-p53-VSV cells showed a prominent induction of p53 expression after addition of DOX and the p53 target p21 was up-regulated (Fig. 13B).

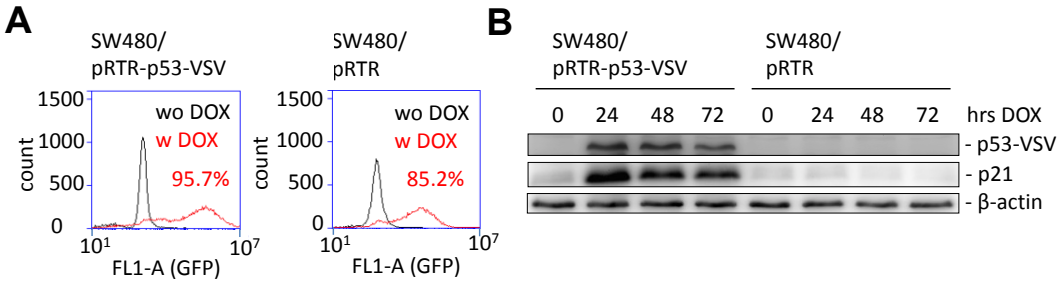

Figure 13: **Characterization of SW480 cells ectopically expressing p53.** (A) Flow cytometric determination of the percentage of GFP expressing cells in SW480 cell pools stably transfected with a pRTR-p53-VSV or a control pRTR vector 48 hours after addition of DOX. (B) The indicated proteins were detected by Western blot analysis. β-actin served as a loading control.

Moreover, p53 activation resulted in the adoption of a flat and enlarged cell shape indicating a p53-induced cell cycle arrest (Fig. 14A). In addition, we detected a 20% increase in the G_1-phase and a minor increase in the sub-G_1-phase after addition of DOX (Fig. 14B).

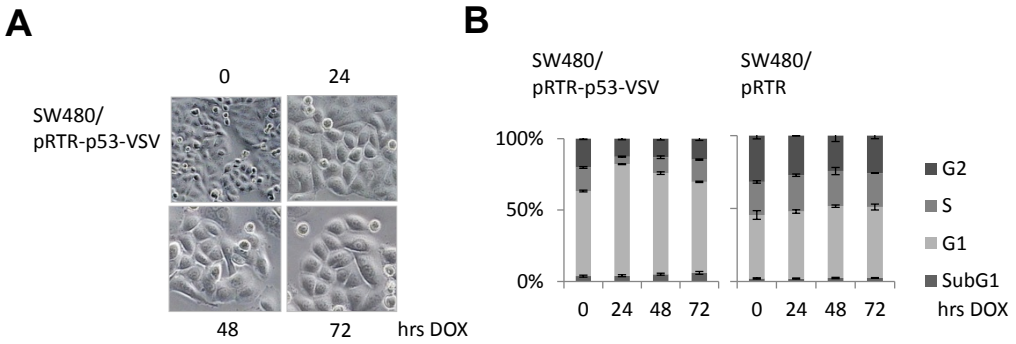

Figure 14: **Microscopic and FACS analyses of SW480/pRTR-p53-VSV cells.** (A) Representative phase-contrast pictures (200x magnification) of SW480/pRTR-p53-VSV cells after the indicated time points of DOX-treatment. (B) DNA content analysis by flow cytometry after addition of DOX for the indicated periods of time. Results represent the mean +/- SD (n=3).

Next, we performed miRNA-, RNA- and ChIP-Seq as well as pSILAC analyses (Table 1). Co-authors contributed as described on page 42. For the miR-Seq as well as for the ChIP-Seq analyses, a short period of 16 hours of p53 activation was chosen in order to preferentially identify directly regulated miRNAs. For RNA-Seq and pSILAC, late time points of 48 and 40 hours, respectively, were selected in order to allow the identification of mRNAs and proteins down-regulated by p53-induced miRNAs. The NGS analyses resulted in 13 to 42 million reads per library. The pSILAC analysis identified 67,090 peptides (60,911 unique sequences) derived from about 5,000 proteins.

Method	Reads SW480/pRTR-p53-VSV	Reads SW480/ pRTR	Addition of DOX (hrs)
miRNA-Seq	38,362,281	39,373,220	16
RNA-Seq	42,451,244	29,278,860	48
ChIP-Seq	13,245,968	21,820,442	16
pSILAC	67,090 peptides (60,911 unique sequences)		40

Table 1: **Summary of the sequencing reads obtained by ChIP-, miRNA- and RNA-Seq analysis and peptide identifications by pSILAC analysis.** The respective periods of p53 activation by addition of DOX are indicated.

5.2.2 pSILAC analysis of protein expression after p53 activation

The pSILAC analysis (contributions of the co-authors described on page 42) resulted in the identification of 5,126 proteins and the quantification of 4,692 proteins in at least two out of six replicates (including two replicates with a label swap). Only those proteins that were identified by peptide hits in at least two replicates (n = 2) with a p-value ≤ 0.05 were considered for further analysis. In order to include moderate effects by p53-induced miRNAs, which were expected due to the previously observed moderate regulation of *de novo* protein synthesis after ectopic miRNA expression [217, 256], we applied a low-stringency cutoff of ≤ -0.3 or ≥ 0.3 $\log_2$ fold changes in protein expression. Based on these criteria, we determined 542 up- und 569 down-regulated proteins (Fig. 15).

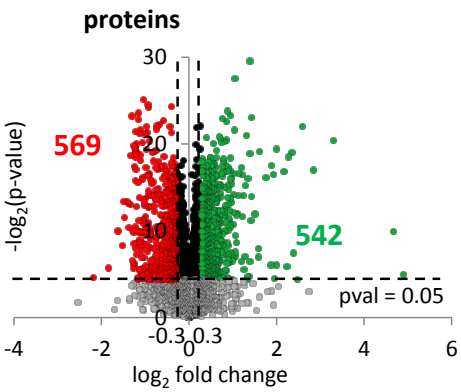

Figure 15: **Differential protein regulation by p53.** SW480/pRTR-p53-VSV were subjected to a pSILAC analysis after 40 hours DOX treatment. Volcano plot classification of quantified proteins. Log-transformed p-values ($-\log_2$) are plotted against the mean $\log_2$ of the corresponding pSILAC abundance ratios of proteins quantified in at least two out of six replicates. Significantly regulated proteins with a $\log_2$ fold change ≥ 0.3 are indicated in green, with a $\log_2$ fold change ≤ -0.3 are marked in red and with 0.3 > $\log_2$ fold change > -0.3 in black. Proteins with a p-value > 0.05 are represented by grey dots. Based on the results of the pSILAC analysis (isotopic labeling of the cells performed by myself, mass spectrometric analysis performed by F. Drepper, S. Oeljeklaus, B. Warscheid), the figure was generated.

The top 50 down- and 50 up-regulated proteins (all |log_2 fold changes| > 1) are listed in Table 2.

Top 50 down-regulated proteins (pval ≤ 0.05)

Names	log_2 fc protein	log_2 fc mRNA	Names	log_2 fc protein	log_2 fc mRNA
C6orf89	-2.19	0.21	UBE2S	-1.23	-0.73
KIF22	-1.84	-0.74	SMC4	-1.22	0.06
MDC1	-1.61	-0.81	**BAZ1B**	-1.22	-0.55
NEB	-1.51	-0.88	**CDK1**	-1.22	-0.48
TOP2A	-1.50	-0.48	KIAA1524	-1.21	0.02
SPC25	-1.46	-0.57	SHCBP1	-1.21	-0.16
HIST1H4A	-1.42	_	**NCAPD2**	-1.21	-0.40
CCNB2	-1.39	-0.66	DHRSX	-1.20	_
TTK	-1.37	-0.67	FANCI	-1.20	-0.77
INCENP	-1.33	-0.37	TMEM109*	-1.18	-0.07
TK1	-1.33	0.65	FAM111B	-1.17	0.23
PBK	-1.30	-0.60	PTTG1	-1.16	-0.45
RIF1	-1.29	-0.53	HIST1H1B	-1.16	-0.79
CISD2	-1.26	-0.06	CDC20	-1.15	-0.69
UTP20	-1.26	-0.71	NCAPG	-1.15	-0.29
UBE2T	-1.26	-0.64	RFT1*	-1.15	-0.33
SPC24	-1.26	-0.88	SPAG5	-1.14	-0.27
BIRC5	-1.25	0.06	PTDSS1*	-1.13	0.14
BUB1B	-1.25	-0.44	DLGAP5	-1.13	-0.49
DHFR	-1.24	-0.54	RRM2	-1.13	0.46
KIF2C	-1.23	-0.67	CCNB1	-1.12	-0.57
HIST2H2AA3	-1.23	_	SMPD4*	-1.12	-0.50
KIF11	-1.23	-0.75	LMO7	-1.12	-1.51
GINS3	-1.23	-0.37	UHRF1	-1.11	-0.29
RACGAP1	-1.23	-0.52	HIST2H3PS2	-1.11	_

Top 50 up-regulated proteins (pval ≤ 0.05)

Names	log_2 fc protein	log_2 fc mRNA	Names	log_2 fc protein	log_2 fc mRNA
NGFR	4.91	0.50	KLK6	1.40	1.08
CDKN1A	4.67	2.41	**TIGAR**	1.40	0.60
TP53I3	3.31	3.34	PDCD4	1.40	-0.23
ALDH1A3	2.84	-0.54	ZG16B	1.38	_
CMBL	2.60	2.29	TGM2	1.35	3.28
CST5	2.48	3.18	MT1H	1.34	_
FDXR	2.38	1.83	CDA	1.34	3.94
DDB2	2.36	1.63	ANXA4	1.32	0.80
SERPINE1	2.27	3.97	**GSN**	1.29	1.96
FBXO2	2.24	3.85	CST1	1.28	1.56
FUCA1	2.18	1.15	TIMP3	1.26	2.28
MVP	2.01	4.12	APOBEC3C	1.25	0.06
EPS8L2	2.00	2.00	NT5E	1.22	3.16
CCND2	1.95	0.96	PHPT1	1.21	0.49
ABAT	1.93	3.28	HMOX1	1.21	-0.91
CCND1	1.89	0.31	**LIMA1**	1.20	0.29
FAT1	1.88	1.35	CST7	1.13	0.56
RPS27L	1.76	2.46	DOCK9	1.13	0.00
NUCKS1	1.61	-0.86	**DCP1B**	1.10	0.65
PGPEP1	1.60	0.71	TUBA1A	1.09	0.24
RRM2B	1.59	2.07	OSBPL3	1.08	-0.03
SLC5A3	1.51	2.66	OTUB2	1.07	1.58
BAX	1.42	0.83	**MT2A**	1.06	1.65
CTSB	1.42	2.18	KIAA1609	1.06	1.43
PYCARD	1.42	2.59	FHL2	1.06	0.37

Table 2**: 100 most up- and down-regulated proteins detected by pSILAC and high-resolution mass spectrometry.** List of the (left) 50 most down- and (right) 50 most up-regulated proteins detected by pSILAC with a log_2 fold change ≤ -0.3 or ≥ 0.3, respectively, and a p-value ≤ 0.05. The corresponding mRNA log_2 fold change detected by RNA-Seq is indicated. Proteins that showed a heterogeneous distribution of fold changes in independent experiments (class II candidates, see Experimental procedures) are marked with an asterisk (*). Proteins marked in bold harbor an occupied p53 binding site in the vicinity of the respective gene promoter (+/-20 kb) according to our ChIP-Seq data. Those additionally underlined represent already described, direct p53 target genes. Based on the pSILAC, RNA-/ChIP-Seq results (contributions of the co-authors described on page 42), the data were analyzed and this table was generated.

A KEGG pathway analysis revealed that the set of proteins involved in DNA replication (p = 1.14E-28) and cell cycle regulation (p = 9.59E-14) was highly enriched among the down-regulated proteins (Fig. 16A). Almost all members of the mini-chromosome maintenance (MCM) family, catalytic subunits of different DNA polymerases (POLA, POLE, POLD) and members of the replication factor C (RFC) family, which are involved in the initiation of eukaryotic DNA replication, were significantly down-regulated. In addition, known protumorigenic factors involved in cell cycle regulation, such as TTK [257], BIRC5 [258], CDK1 [259] and CDK6, CDC20 [260], CCNB1 [261] and BUB1B, were also significantly down-regulated. Among the up-regulated proteins, factors involved in the p53 signaling pathway (p = 6.86E-03) were significantly enriched, including several proteins encoded by known p53 target genes, such as BAX, CDKN1A, DDB2, SERPINE1, TIGAR or TP53I3 [58] (Fig. 16B). Surprisingly, we detected an increase in proteins involved in glycolysis and the TCA cycle, which was however less significant than the afore mentioned enriched KEGG groups DNA replication, cell cycle or p53 signaling pathway. Since the KEGG pathway analysis does not take into account the extent of expression changes in *de novo* protein synthesis, it is possible that significantly enriched KEGG groups include proteins that are above the chosen cutoff for differential expression ($-0.3 \geq \log_2$ fold change ≥ 0.3) but only show relatively weak expression changes. Therefore it is not clear, whether the observed up- or down-regulation of enzymes associated with specific, overrepresented KEGG categories actually leads to the activation of these pathways. Indeed, a gene set enrichment analysis (GSEA) for the differentially regulated proteins detected by pSILAC revealed that those proteins assigned to the KEGG pathway categories glycolysis and TCA cycle display a relatively weak induction when compared to the $\log_2$ fold changes of those proteins in the category p53 signaling pathway (data not shown).

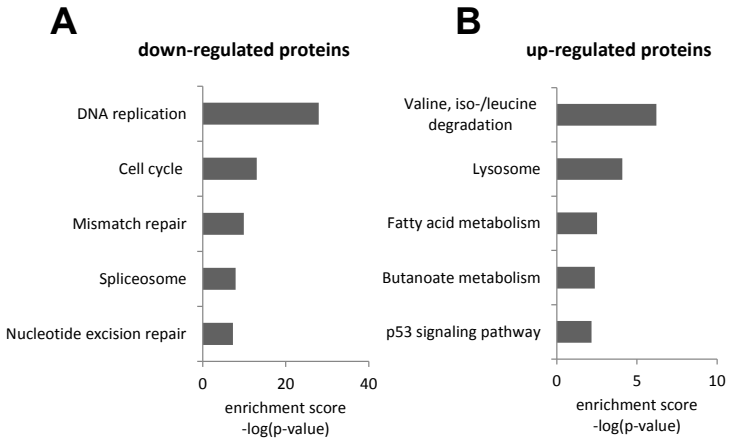

Figure 16**: KEGG pathway analysis of differentially regulated proteins detected by pSILAC.** Translationally (A) down- and (B) up-regulated proteins detected by pSILAC with a $\log_2$ fold change ≤ -0.3 or ≥ 0.3, respectively, and a p-value ≤ 0.05 were analyzed for enriched biological processes applying a KEGG pathway analysis. The different KEGG terms and their enrichment scores –log(p-value) are indicated. Based on the pSILAC results (contributions of the co-authors described on page 42), a KEGG pathway analysis was performed and this figure was generated.

5.2.3 RNA-Seq analysis of differential RNA expression after p53 activation

In total, 20,397 protein-coding mRNAs were identified by RNA-Seq (contributions of the co-authors described on page 42) (Fig. 17). 11,801 showed robust expression levels (rpkm ≥ 0.5 in at least one condition) and were considered for further analysis.

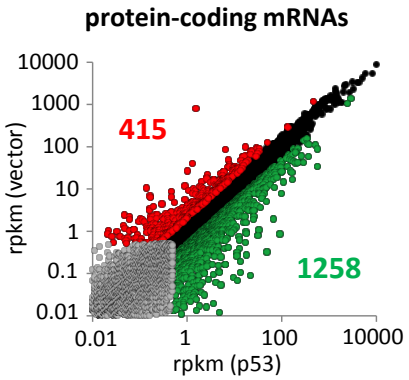

Figure 17: **Differential regulation of protein-coding mRNAs by p53.** SW480/pRTR-p53-VSV were subjected to a RNA-Seq analysis after 48 hours DOX treatment. RPKM scatter plot depicting expression changes of protein-coding mRNAs detected by RNA-Seq. Transcripts below 0.5 rpkm in both conditions are shown in grey. Transcripts with a $\log_2$ fold change ≥ 1 are shown in green, with a $\log_2$ fold change ≤ -1 in red and with 1 > $\log_2$ fold change > -1 in black. After raw data analysis by T. Bonfert, the data were further analyzed and the figure was generated with support of Dr. M. Kaller.

The top 50 down- (all $\log_2$ fold change ≤ -3.30) and 50 up-regulated (all $\log_2$ fold change ≥ 5.36) mRNAs are shown in in Table 3.

Top 50 down-regulated mRNAs

Genes	$\log_2$ fc	Genes	$\log_2$ fc
DEFA5	-12.10	*CPNE8*	-4.29
DEFA6	-10.77	*HTRA3*	-4.29
AC087071.2	-10.49	*AMBP*	-4.26
AL031003.1	-10.39	*TMEM204*	-4.26
DBH	-10.21	*C2CD4C*	-4.25
AC093859.1	-9.17	*KCNE3*	-4.20
DKK4	-9.03	*FAM129A*	-4.12
AC005544.1	-9.02	*ADAMTS19*	-4.04
CIB2	-9.00	*IL16*	-4.02
TMEM47	-6.24	*ADAMTSL2*	-3.90
PCBP3	-5.69	*CHN2*	-3.90
SPNS3	-5.53	*AFF3*	-3.89
PCSK9	-5.38	*CACNG4*	-3.81
CHSY3	-5.34	*HOXC5*	-3.79
FSTL4	-5.23	*FGF19*	-3.73
AHRR	-5.17	*CALHM3*	-3.72
RFX8	-4.92	*PRUNE2*	-3.71
KCNJ5	-4.91	*PROX1*	-3.69
GPX2	-4.89	*SARDH*	-3.62
GRM8	-4.87	*GLT25D2*	-3.58
BNC2	-4.85	*CXCL14*	-3.55
GNAI1	-4.71	*UPK3B*	-3.52
KIF21B	-4.58	*CYS1*	-3.45
CDK15	-4.39	*CAMK4*	-3.33
LRRC10B	-4.35	*ZNF501*	-3.30

Top 50 up-regulated mRNAs

Genes	$\log_2$ fc	Genes	$\log_2$ fc
KRTAP3-1	12.66	*PADI3*	6.64
LCE1B	11.62	*KIAA1755*	6.58
CD70	11.00	*C17orf72*	6.46
LCE1C	10.82	*TMC8*	6.23
NTF4	9.93	*G0S2*	6.13
IL1RL2	9.87	*HMGCS2*	6.12
SPANXN3	9.69	*WFDC2*	6.07
VAV1	9.67	*ESM1*	6.06
GNGT2	9.50	*KRT13*	6.04
INSL3	9.18	*CSF2*	5.81
LCE1D	9.11	*RNF128*	5.76
DUSP13	9.09	*RAC2*	5.74
HIST1H2AE	9.03	*C1orf233*	5.68
CAPN8	8.68	*INPP5D*	5.67
MARCH4	7.97	*ALCAM*	5.62
ICAM2	7.59	*ZC4H2*	5.53
PSG5	7.51	*TP53INP1*	5.53
SLC43A3	7.42	*PAPL*	5.48
EDA2R	7.34	*CHST3*	5.43
KRTAP2-1	7.25	***KRT17***	5.43
RHOD	7.03	*SERP2*	5.40
ROBO4	6.92	*PSG2*	5.40
LCE1F	6.90	*ZNF556*	5.39
KRT23	6.76	***RASAL1***	5.37
ANTXR1	6.74	*NHLRC1*	5.36

Table 3**: 100 most up- and down-regulated mRNAs detected by RNA-Seq.** List of the (left) 50 most down- and (right) 50 most up-regulated mRNAs detected by RNA-Seq ($\log_2$ fold change ≤ -1 or ≥ 1, respectively; rpkm ≥ 0.5 in at least one condition). mRNAs marked in bold harbor an occupied p53 binding site in the vicinity of the respective gene promoter (+/-20 kb) according to our ChIP-Seq data. Those additionally underlined represent already described, direct p53 target genes. Based on the RNA- and ChIP-Seq results (contributions of the co-authors described on page 42), the data were analyzed and this table was generated.

A KEGG pathway analysis of the down-regulated mRNAs revealed down-regulation of the Wnt signaling pathway (p = 9.26E-03) (Fig. 18). As expected, components of the p53 signaling pathway were enriched among the up-regulated mRNAs (p = 7.81E-04), including known p53 target genes, such as *CDKN1A*, *MDM2*, *TP53I3*, *SERPINEB5*, *ZMAT3* or *SERPINE1* [58].

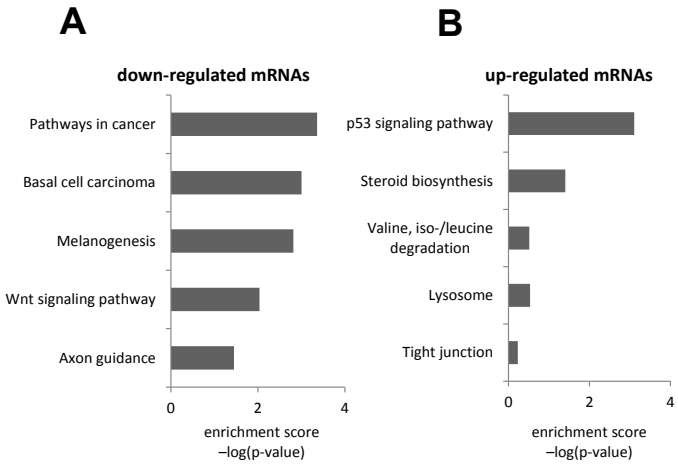

Figure 18: **KEGG pathway analysis of differentially regulated mRNAs detected by RNA-Seq.** (A) Down- and (B) up-regulated mRNAs detected by RNA-Seq with a $\log_2$ fold change ≤ -1 or ≥ 1, respectively, and rpkm ≥ 0.5 in at least one condition were analyzed for enriched biological processes applying a KEGG pathway analysis. The different KEGG terms and their enrichment scores –log(p-value) are indicated. Based on the RNA-Seq data (contributions of the co-authors described on page 42), a KEGG pathway analysis was performed and this figure was generated.

Next, my colleague Markus Kaller analyzed the expression of lncRNAs (including long intergenic noncoding (linc) RNAs, antisense RNAs and transcribed pseudogenes), which were also detected by RNA-Seq (Fig. 19). Of the 4,608 detected lncRNAs, 1,719 showed robust expression levels (rpkm ≥ 0.5 in at least one condition) and were considered for further analysis. Out of these, 270 showed induced ($\log_2$ fold change ≥ 1) and 123 repressed expression ($\log_2$ fold change ≤ -1).

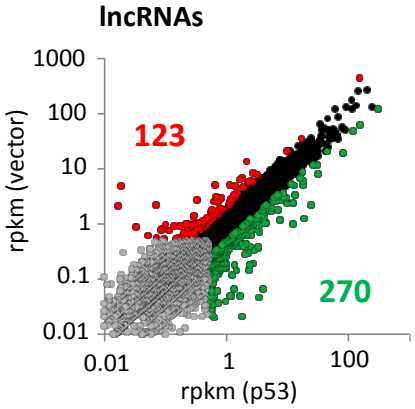

Figure 19: **Differential regulation of lncRNAs by p53.** SW480/pRTR-p53-VSV were subjected to a RNA-Seq analysis after 48 hours DOX treatment. RPKM scatter plot depicting expression changes of lncRNAs detected by RNA-Seq. Transcripts below 0.5 rpkm in both conditions are shown in grey. Transcripts with a $\log_2$ fold change ≥ 1 are shown in green, with a $\log_2$ fold change ≤ -1 in red and with 1 > $\log_2$ fold change > -1 in black. After raw data analysis by T. Bonfert, Dr. M. Kaller analyzed the lncRNA data and generated the figure.

The top 50 down- (all log_2 fold change ≤ -1.57) and 50 up-regulated (all log_2 fold change ≥ 2.95) lncRNAs are shown in Table 4.

Top 50 down-regulated lncRNAs

lncRNA	log_2 fc	lncRNA	log_2 fc
RP11-166N17.1	-10.10	*RP11-544L8__B.2*	-2.17
RP11-148K1.10	-9,45	*RP11-498B4.5*	-2.16
RP11-346A9.1	-9.34	*AC013403.9*	-2.06
AC011247.3	-9.24	*AC015712.2*	-1.99
RP11-197M22.2	-9.13	*AC104186.1*	-1.91
RP1-122O8.7	-9.07	*Z97989.1*	-1.88
NCRNA00118	-7.98	*AC007362.3*	-1.85
AC004671.1	-6.97	*RP1-118J21.5*	-1.80
AC021068.1	-4.96	*CTC-338M12.6*	-1.80
RP11-155L15.1	-4,73	*AC018730.1*	-1.79
AC005304.2	-3.57	*AC015691.13*	-1.79
AC093388.3	-3.28	*AP001992.1*	-1.79
RP11-478J18.2	-3.18	*AC007405.4*	-1.79
RP1-85F18.5	-3.17	*AC091167.5*	-1.79
AP002478.1	-2.98	*AL157687.1*	-1.78
AC004540.4	-2.96	*AC138904.1*	-1.78
RP11-478J18.1	-2.95	*CTC-564N23.2*	-1.75
RP11-714G18.1	-2.72	*AC091805.1*	-1.74
RP3-486B10.1	-2.70	*AC010883.5*	-1.69
AC007277.3	-2.65	*RP11-46A10.4*	-1.65
AC021224.1	-2.47	*RP11-359P5.1*	-1.64
RP4-583P15.10	-2.38	*AC073321.5*	-1.63
RP4-639F20.3	-2.28	*BOKAS*	-1.58
AC147651.1	-2.21	*AC007276.7*	-1.57
RP11-875H7.4	-2.17	*CLTCL1*	-1.57

Top 50 up-regulated lncRNAs

lncRNA	log_2 fc	lncRNA	log_2 fc
RP3-326I13.1	12.05	*RP11-521D12.1*	4.11
RP3-510D11.2	11.41	*RP1-14N1.2*	4.05
RP11-78C3.1	10.58	*RP13-463N16.6*	3.91
RP11-462G8.3	10.43	*C11orf76*	3.90
AC019349.5	10.12	*RP11-25G10.2*	3.83
AC128709.2	10.11	*AP005210.2*	3.83
AC112721.2	10.04	*AC159540.1*	3.77
AP001468.58	9.89	*AL583842.6*	3.75
RP11-137H2.4	9.26	*RP1-63G5.5*	3.73
SNORA71B	9.22	*RP3-467K16.7*	3.69
AC022596.6	9.02	*AC012065.6*	3.68
RP3-510D11.1	9.02	*CTC-529P8.1*	3.67
RP11-267A15.1	9.01	*RP11-217C7.1*	3.54
LINC01021	6.44	*RP3-434O14.8*	3.52
RP11-399K21.6	6.24	*RP3-389A20.4*	3.52
RP11-11N9.4	5.89	*AL356390.1*	3.48
AC006948.1	5.06	*RP11-240D10.2*	3.43
AC104135.3	4.96	*RP11-181K12.2*	3.39
MYH16	4.76	*CECR7*	3.34
BX571672.2	4.65	*RP11-554I8.2*	3.22
AC004834.1	4.65	*RP11-219G10.3*	3.19
AC003958.2	4.55	*RP11-134G8.8*	3.11
CTD-2021J15.2	4.35	*RP11-382A18.1*	3.09
AL133493.2	4.33	*BX004987.5*	2.96
RP3-395M20.8	4.30	*AC002558.2*	2.95

Table 4**: 100 most up- and down-regulated lncRNAs detected by RNA-Seq.** List of the (left) 50 most down- and (right) 50 most up-regulated lncRNAs detected by RNA-Seq (log_2 fold change ≤ -1 or ≥ 1, respectively; rpkm ≥ 0.5 in at least one condition). Based on the RNA-Seq results (contributions of the co-authors described on page 42), the data were analyzed and this table was generated.

Next, we determined the overlap between the RNA-seq and pSILAC results and found that nearly all (93%) of the quantified proteins were also detected on RNA-level (Fig. 20A). Moreover, we determined that a subset of 130 genes was differentially regulated on both, the mRNA- and *de novo* protein synthesis-level. When we applied a low-stringency cutoff (-0.3 ≥ log_2 fold change ≥ 0.3) for differential mRNA regulation the number of differentially regulated mRNAs that also display differential *de novo* protein synthesis increased from 130 to 636 (data not shown).

My colleague Markus Kaller performed a cumulative distribution analysis of differentially up- and down-regulated proteins that showed their significantly increased and decreased expression on mRNA-level ($p < 0.0001$ in both cases), respectively, substantiating a positive correlation between p53-induced changes in mRNA expression and *de novo* protein synthesis (Fig. 20B).

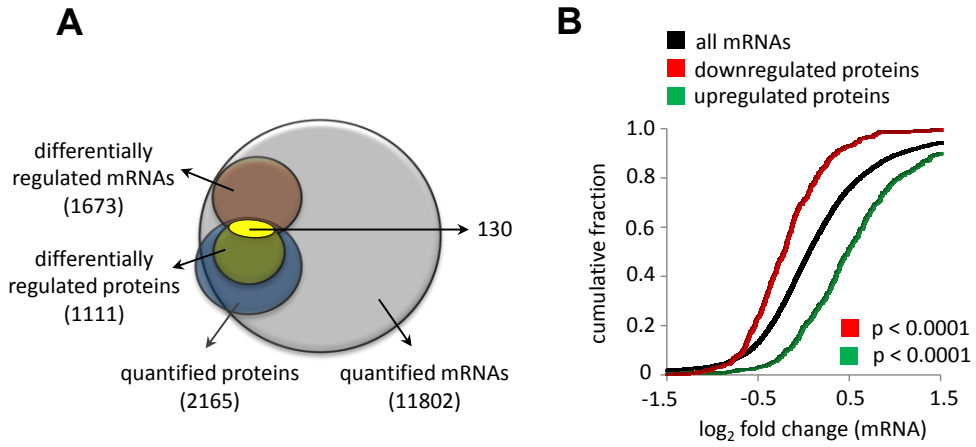

Figure 20**: Correlation of mRNA- and protein-expression fold changes.** (A) Venn diagram displaying the overlap between quantified mRNAs (with an rpkm ≥ 0.5 in at least one condition) (shown in grey) and proteins (with a p-value < 0.05) (shown in blue) and differentially regulated mRNAs (-1 ≥ $\log_2$ fold change ≥ 1) (shown in orange) and proteins (-0.3 ≥ $\log_2$ fold change ≥ 0.3) (shown in green). Genes differentially expressed on the mRNA level and the level of *de novo* protein synthesis are indicated in yellow. (B) Cumulative distribution plot displaying changes in mRNA expression of up- and down-regulated proteins compared to the normal distribution of all mRNAs detected by RNA-Seq after activation of p53. Dr. Markus Kaller analyzed the data for Fig. 20B and generated the figure.

5.2.4 miR-Seq analysis after p53 activation

Next, we used miR-Seq (contributions of the co-authors described on page 42) to determine miRNA expression after activation of p53 for 16 hours. In total, 411 different miRNAs were detected: 107 miRNAs were up-regulated ($\log_2$ fold change ≥ 1), whereas 101 were down-regulated ($\log_2$ fold change ≤ -1) by p53 (Fig. 21).

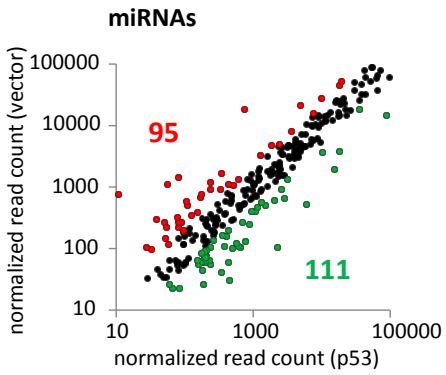

Figure 21: **Differential regulation of miRNAs by p53.** SW480/pRTR-p53-VSV were subjected to a miRNA-Seq analysis after 16 hours DOX treatment. RPKM scatter plot depicting expression changes of miRNAs detected by miRNA-Seq. Transcripts below 0.5 rpkm in both conditions are shown in grey. Transcripts with a $\log_2$ fold change ≥ 1 are shown in green, with a $\log_2$ fold change ≤ -1 in red and with 1 > $\log_2$ fold change > -1 in black. After raw data analysis by F. Erhard, the data were further analyzed and the figure was generated with support of M. Kaller.

The top 50 up- (all log_2 fold change ≥ 5.64) and 50 down-regulated (almost all log_2 fold change ≤ -4.67) miRNAs are listed in Table 5.

Top 50 up-regulated miRNAs

miRNA	log_2 fc	miRNA	log_2 fc
miR-34a	10.04	miR-23a*	6.65
miR-373	9.38	miR-629*	6.65
miR-1266	8.97	**miR-1293**	6.63
miR-205	8.94	miR-548j	6.63
miR-576-5p	8.86	miR-195*	6.59
miR-34a*	8.61	miR-1287	6.57
miR-361-3p	8.17	**miR-145**	6.57
miR-199a-5p	7.82	miR-3691	6.55
miR-362-3p	7.75	miR-491-3p	6.53
miR-141*	7.69	miR-891a	6.53
miR-194	7.68	miR-193a-3p	6.51
miR-200c*	7.65	miR-1294	6.49
miR-3663-5p	7.63	miR-877*	6.46
miR-218	7.13	miR-18a*	6.45
miR-3174	7.02	miR-3617	6.42
miR-548u	6.99	miR-371-3p	6.38
miR-2355-3p	6.85	miR-3065-3p	6.30
miR-499-3p	6.85	miR-570	6.30
miR-1468	6.82	miR-1914	6.20
miR-3162	6.82	miR-449a	6.15
miR-592	6.82	miR-199a-3p	5.95
miR-34c-3p	6.80	miR-3937	5.91
miR-3661	6.78	miR-29c*	5.67
miR-130a	6.77	miR-3938	5.67
miR-1229	6.73	miR-22*	5.64

Top 50 down-regulated miRNAs

miRNA	log_2 fc	miRNA	log_2 fc
miR-200a*	-9.78	miR-627	-6.04
miR-1908	-9.62	miR-2116*	-6.04
miR-191*	-9.12	miR-20a*	-6.04
miR-200a	-8.81	let-7g*	-6.04
miR-767-5p	-8.52	miR-935	-6.00
miR-23b*	-8.38	miR-502-3p	-6.00
miR-374b*	-8.34	miR-142-3p	-6.00
miR-3131	-8.11	miR-196b*	-5.95
miR-200b*	-7.96	miR-3194	-5.86
miR-1262	-7.57	miR-1227	-5.86
miR-184	-7.32	miR-3159	-5.78
miR-3192	-7.27	miR-1	-5.73
miR-125b	-7.11	miR-365*	-5.70
miR-939	-6.89	miR-1226	-5.64
miR-636	-6.77	miR-664*	-5.61
miR-181a*	-6.59	miR-3181	-5.55
miR-3188	-6.57	miR-3928	-5.43
miR-3200-5p	-6.49	miR-508-3p	-5.33
miR-3909	-6.21	miR-3613-5p	-5.32
miR-551a	-6.17	miR-3191	-5.28
miR-1305	-6.13	miR-381	-5.21
miR-429	-6.11	miR-3124	-5.21
miR-3939	-6.11	miR-2277-5p	-5.04
miR-501-5p	-6.07	miR-1254	-5.03
miR-32*	-6.07	miR-200b	-4.73

Table 5**: 100 most up- and down-regulated miRNAs detected by miRNA-Seq.** List of the (left) 50 most up- and (right) 50 most down-regulated miRNAs detected by miRNA-Seq with a log_2 fold change ≤ -1 or ≥ 1, respectively. The mature miRNA is referred to as miR-x, whereas the strand that is usually degraded is indicated as miR-x*. Starting with mirBase v18, miRNA strands from one precursor are referred to as miR-x-5p and miR-x-3p depending on the arm from which they are processed since it is not clear which sequence serves as the predominant one under varying conditions. Marked in bold: miRNAs that harbor an occupied p53 binding site in the vicinity of the respective gene promoter (+/- 20 kb) according to our ChIP-Seq data. Those additionally underlined represent already described, direct p53 target genes. Based on the miRNA- and ChIP-Seq results (contributions of the co-authors described on page 42), the data were analyzed and this table was generated.

As expected, we detected the induction of several, tumor-suppressive miRNAs known to be encoded by direct p53 target genes, such as miR-34a [89, 90, 92-94], miR-205 [262], members of the miR-200 family (miR-141/-141* and miR-200c/200c*) [98], as well as the miR-192 family (miR-192, -194 and -215) [101, 102] and miR-145 [106]. Interestingly, several, putatively tumor-supressive miRNAs not previously linked to p53 were induced after p53 activation: e.g. miR-486-5p [263], miR-1266 [264] or miR-218 [265]. Furthermore, we identified oncogenic factors among the down-regulated miRNAs, such as miR-25 and miR-92a [266] and the miRNA family miR-221/222, which is known to promote EMT [267].

5.2.5 Genome-wide mapping of p53 DNA-binding

Next, DNA was isolated 16 hours after addition of DOX by VSV-antibody mediated ChIP from SW480/pRTR-p53-VSV and, as a control, SW480/pRTR cells and subjected to NGS (contributions of the co-authors described on page 42). In total, bioinformatics analysis of the NGS data by Thomas Bonfert led to the identification of 1,827 ChIP-signals in the p53-inducible SW480 cell line of which 97% (1,771 signals) colocalized with a predicted p53 binding sequence (data not shown). 22% of the ChIP-signals with p53 binding sites were located in a region < 10 kbp from a transcription start site (TSS) and 27% were located > 10 kbp upstream of a TSS (Fig. 22A). 39% of the ChIP-signals with p53 binding site were found in intragenic regions and 12% were located downstream of genes. The ChIP signals that localized in a region within 100 kbp up- and downstream from a TSS were centered around the TSS (Fig. 22B).

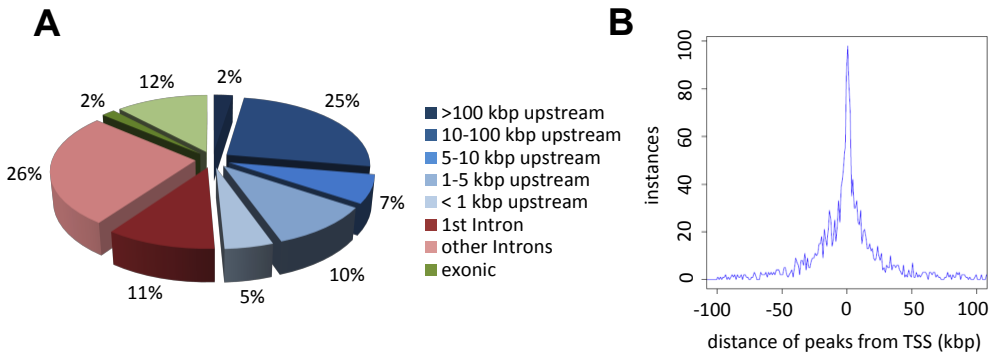

Figure 22: **Genome-wide analysis of p53 occupancy.** ChIP-Seq analysis was performed with a VSV-specific antibody 16 hours after addition of DOX to SW480/pRTR-p53-VSV and SW480/pRTR cells. (A) Localization of called ChIP-peaks obtained after p53-ChIP in SW480/pRTR-p53-VSV. (B) Distribution of p53-derived ChIP-Seq peaks 100 kbp up- and downstream of the TSS. Thomas Bonfert analyzed the ChIP-Seq raw data and generated the figures.

When p53-derived ChIP signals 20 kbp up- and downstream of transcriptional start sites were analyzed by Thomas Bonfert for enriched binding motifs using MEME [234], the identified motif was identical to the previously described p53 consensus site [56, 57] and only minor differences between the motifs associated with p53-induced and -repressed genes were observed (Fig. 23A), which is in accordance with previous findings [65, 268]. The motif associated with repressed genes showed a preference for A (instead of G) at position 1, 11 and 12, and a preference for C (instead of T) at position 18. However, the changes were restricted to the flanking sequences. A search for neighboring binding motifs of other transcription factors in the vicinity of the detected p53 ChIP-signals (+/- 250 bp) revealed an enrichment for the consensus motif WGATAR (W = A/T, R = A/G) of the GATA1 transcription factor which was present in 29% of the up-regulated genes harboring a p53 binding site (Fig. 23B). Therefore, it is possible that GATA factors and p53 cooperate in gene regulation.

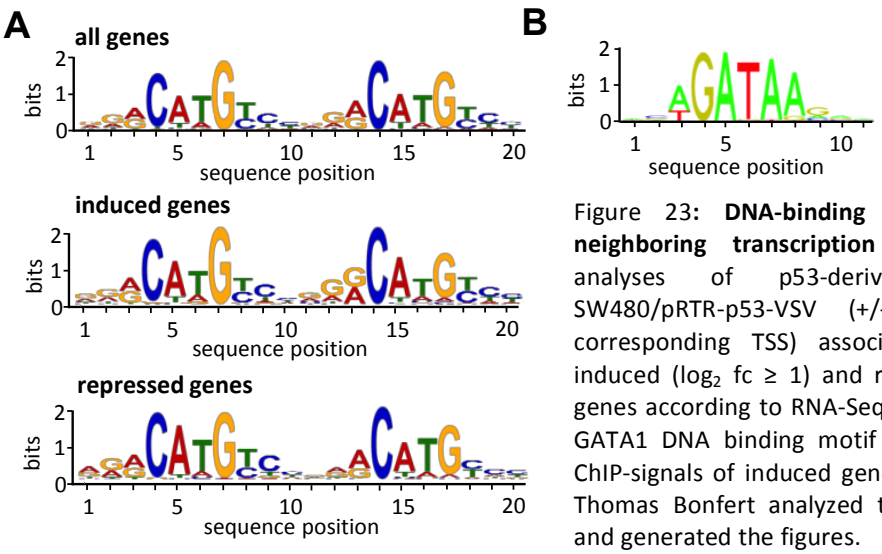

Figure 23: **DNA-binding motifs of p53 and neighboring transcription factors.** (A) MEME analyses of p53-derived ChIP-peaks in SW480/pRTR-p53-VSV (+/- 20 kbp of the corresponding TSS) associated with all genes, induced (log_2 fc ≥ 1) and repressed (log_2 fc ≤ -1) genes according to RNA-Seq. (B) Enrichment of the GATA1 DNA binding motif in the vicinity of p53 ChIP-signals of induced genes detected by SpaMo. Thomas Bonfert analyzed the ChIP-Seq raw data and generated the figures.

By using the presence of a ChIP-Seq signal located in a region +/- 20 kbp from the corresponding gene promoter as a criterion, we determined that changes in *de novo* protein synthesis of proteins showing promoter-proximal p53 binding near the respective gene promoter positively correlated with the respective changes in mRNA abundance ($p < 0.0001$) (Fig. 24A). Compared to the correlation of changes in *de novo* protein synthesis of all differentially regulated proteins to the respective mRNA fold changes ($r = 0.50$), the Pearson correlation coefficient was higher for direct p53 targets ($r = 0.54$), including several known p53-regulated target genes, such as *CDKN1A*, *TIGAR* or *BAX*. Among the differentially regulated candidates, we identified 43 putative direct targets via analysis of *de novo* protein synthesis (32 induced, 11 repressed) and 61 via differential mRNA expression (52 induced, 9 repressed) (Fig. 24B). Among the putative direct targets, 14 genes were co-regulated on the level of mRNA expression and *de novo* protein synthesis. These results indicate that only 2.4% (1.9%) of the down-regulated mRNAs (proteins) showed a p53 ChIP-signal in a region of +/- 20 kbp from the corresponding gene promoter, whereas 4.3% (5.8%) of the up-regulated mRNAs (proteins) displayed p53 binding near their corresponding gene TSS. A cumulative distribution analysis of those proteins/mRNAs showing a p53 peak in a region of +/- 20 kbp from their corresponding gene promoter plotted against all detected proteins/mRNAs which was performed by Markus Kaller confirmed that genes bound by p53 are preferentially up-regulated ($p < 0.0001$) (Fig. 24C). These results indicate that a large number of the genes repressed by p53 are not regulated by direct p53 binding, but rather indirectly, e.g. by miRNA-mediated repression or due to secondary consequences of p53 activation. In addition, we found 18 differentially expressed lncRNAs showing p53 binding near their corresponding gene TSS (Fig. 24B). 17 induced lncRNAs (6.3% of all induced lncRNAs) displayed p53 chromatin occupancy in a +/- 20 kbp region surrounding the corresponding gene TSS, whereas only one repressed lncRNA (0.8% of all down-regulated lncRNAs) showed p53 binding near the respective gene promoter.

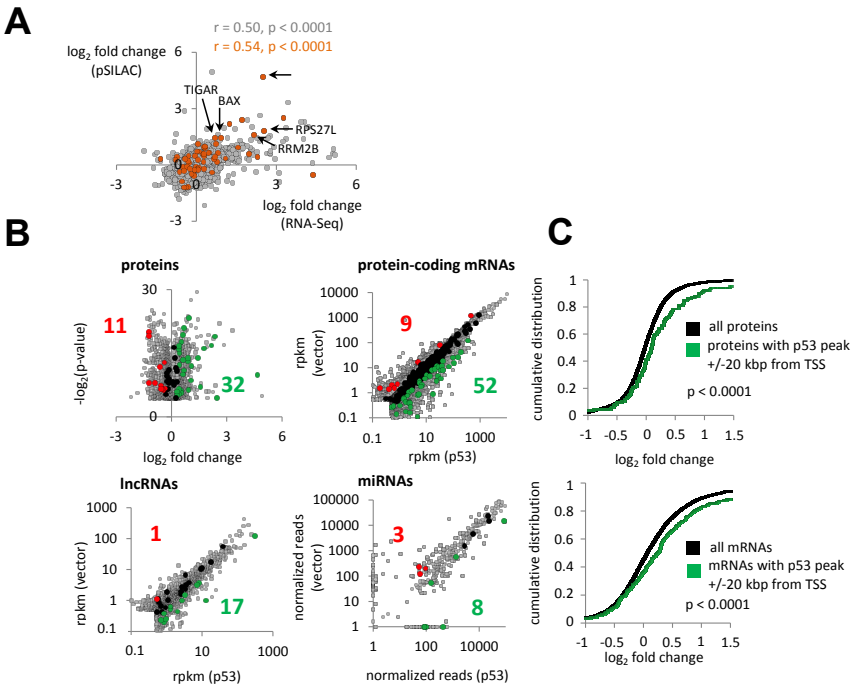

Figure 24: **ChIP-Seq results combined with the results obtained from pSILAC, RNA- and miRNA-Seq.** (A) Scatter plot correlating changes in *de novo* protein synthesis of all differentially regulated proteins with the corresponding mRNA fold changes after induction of p53 (marked in grey). Molecules showing p53 occupancy near the respective gene promoter are indicated in orange. The respective Pearson correlation coefficient and statistical significance are indicated. (B) Proteins, protein-coding mRNAs, lncRNAs and miRNAs that have an occupied p53 binding site within +/- 20 kbp of the TSS of their host gene are shown in colors or black as described under Fig. 10. Molecules without promoter-proximal p53 binding are shown in grey. M. Kaller analyzed the lncRNA data and generated the respective figure. (C) Cumulative distribution plot displaying expression changes of (upper panel) p53-occupied, protein-coding genes compared to the normal distribution of all detected proteins as detected by pSILAC, (lower panel) p53-occupied, mRNA-coding genes compared to the normal distribution of all detected mRNAs as detected by RNA-Seq. (C) was analyzed and generated by M. Kaller, based on the RNA-, miRNA-, ChIP-Seq and pSILAC-data (contributions of the co-authors described on page 42).

The previously described p53-induced lncRNA *TP53TG1* [269, 270], but none of the other described lncRNAs regulated by p53, was among the p53-induced lncRNAs. Notably, we detected the lncRNA *RP3-510D11.2* that is transcribed in the opposite direction from the previously described promoter of the p53 target gene *miR-34a* [94] to be induced and bound by p53 at the respective gene promoter (Fig. 25).

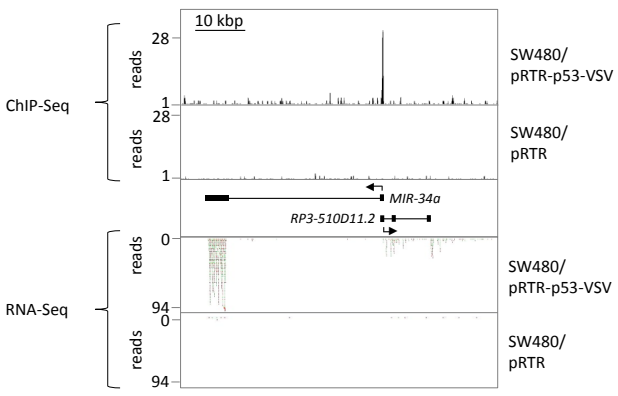

Figure 25: **ChIP- and RNA-Seq results of the *RP3-510D11.2* locus.** ChIP- and RNA-Seq results of SW480/pRTR-p53-VSV and SW480/pRTR for the genes encoding miR-34a and lncRNA RP3-510D11.2 are displayed using the UCSC genome browser and the CLC Genomics Workbench 8.0, respectively. Based on the RNA- and ChIP-Seq results (contributions of the co-authors described on page 42), the data were analyzed and this figure was generated.

Next, we determined whether p53 binds in the vicinity of TSSs of genes encoding miRNAs (according to miRStart [271]) (Fig. 24B). Among the up-regulated miRNAs, miR-34a, miR-205, miR-34-3p, miR-1293, miR-145, miR-486-5p, miR-143 and miR-641 showed p53 binding near their corresponding gene promoter (7.2% of all differentially up-regulated miRNAs). In addition, genes encoding the down-regulated miRNAs miR-3191, miR-3928 and miR-1908 displayed p53 binding (3.2% of all differentially down-regulated miRNAs). Therefore, only a minor fraction of the detected differential miRNA regulations may be directly mediated by p53.

5.2.6 Identification and confirmation of novel putative p53 target genes

Next, we compared the differentially regulated mRNAs and proteins with a p53 binding site in a region +/- 20 kbp from the TSS of the corresponding gene with recent genome-wide studies of p53-mediated gene regulation [65, 268, 272, 273]. Thereby, we confirmed that 52 putative direct p53 targets, with 31 targets being identified by RNA-Seq and 21 by pSILAC, have not been characterized as p53 targets previously (Table 6). Interestingly, three of these novel p53 targets were identified by both approaches: *ETV3*, *ST14* and *TGFBI*. In addition, we identified 17 differentially regulated lncRNAs and 6 differentially regulated miRNAs with p53 binding near their TSS that were not previously described as directly regulated by p53 (Table 6). Subsequently, we used independent methods to confirm novel direct p53 targets. We demonstrated the up-regulation of *MDFI*, *ST14* and *LINC01021 (RP11-46C20.1)* after ectopic p53-expression in the DOX-inducible cell line SW480/pRTR-p53-VSV (Fig. 26A). Moreover, p53 occupancy was confirmed by qChIP analysis for *MDFI*, *ST14 and LINC01021,* which was in line with the ChIP-Seq results (Fig. 26B, C).

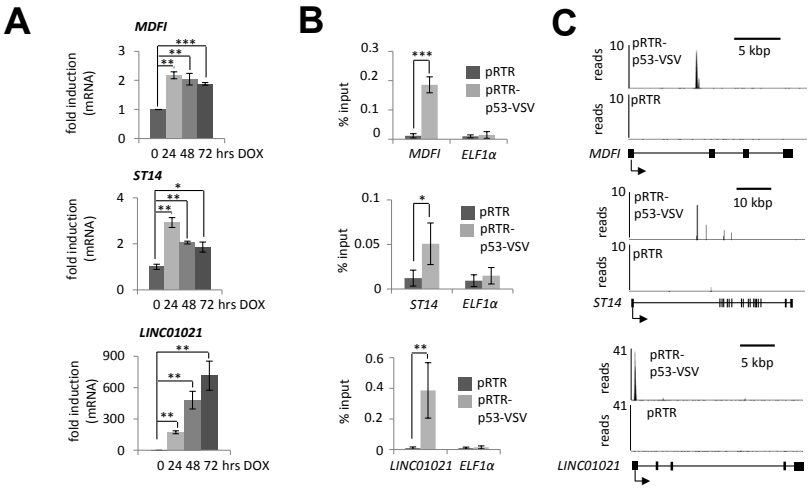

Figure 26: **Exemplary validation of the newly identified p53 target genes *MDFI*, *ST14* and *LINC01021*.** (A) qPCR analyses of *MDFI*, *ST14 and LINC01021* expression in SW480/pRTR-p53-VSV cells after addition of DOX for the indicated periods. (B) qChIP validation of p53 occupancy at the *MDFI, ST14 and LINC01021* promoters in SW480/pRTR-p53-VSV after 16 hours of DOX treatment and subsequent VSV-ChIP. (C) p53-VSV-derived ChIP-Seq results are displayed using the UCSC genome browser. Results in (A) and (B) represent the mean +/- SD (n = 3). Raw data analysis of ChIP-Seq results was performed by T. Bonfert.

proteins							
protein name	**log2 fc**	**p53_motif**	**TSS (bp)**	**protein name**	**log2 fc**	**p53_motif**	**TSS (bp)**
OSBPL3	1.08	AGGCAAGCCCGGGCACAGCT	9861	TKT	0.41	AGACATGACCCTGCTTGTCC	13810
ACTN1	0.96	AGACATGTACCAACATGCCC	8606	FAM162A	0.31	AGACATGCCCCAACATGCAC	9965
TGFBI	0.9	ATGCATGTGCGAACATGTCT	4770	PNN	-0.4	AAACTTGTAAAAACTTGTTT	12847
S100A4	0.89	GAACGTGCCCACACATGCCC	17237	URB1	-0.4	CTGCAAGCCAGGACGTGCCC	6312
PRDX5	0.7	TTGCCTGTCCTAGCATGCCC	6609	GRPEL2	-0.5	AGGCATGTCTGGACAAGAAA	19941
ALDH7A1	0.63	TGGCATGCTTTTACTAGTCC	4321	ST14	-0.6	TTTCATGACCAGACAAGTCC	19290
STAT6	0.55	CTGCAGGTGCAGGCATGTTG	14903	MTA2	-0.6	ATACCTGCAGGGACATGCCC	1475
FAH	0.55	GGGCATGTGTGGACATGCGC	15684	ZWILCH	-0.9	AGACATGTTTTCACATGTCT	18854
ETV3	0.55	AGACTAGTCTCAAACATGCCC	19095	CDK1	-1.2	TGATATGCTTGGGCATGTAC	17178
NPEPPS	0.44	CAACAAGCAGTGACATGTTT	2351	BAZ1B	-1.2	AGGCATGCACCAACATGCCC	11343
USP48	0.43	AAGCATGCCAGGGCAAATAT	4412				
protein-coding mRNAs							
gene symbol	**log2 fc**	**p53_motif**	**TSS (bp)**	**gene symbol**	**log2 fc**	**p53_motif**	**TSS (bp)**
CD70	11	GGGCTTGTCTGGGCTTGCCC	13243	*TGFBI*	1.58	ATGCATGTGCGAACATGTCT	4770
LCE1D	9.11	GGGCAAGTCCTCTCATGCCC	10422	*LOXL4*	1.53	AGGCATGCGCCAACATGCCC	2506
LCE1F	6.9	GGGCAAGTCCTCTCATGCCC	9458	*SLC25A42*	1.44	GCTCATGCTAAGACATGTCC	12896
RASAL1	5.37	AGACAAGTGTGGACAGGTAT	19376	*PPP4R1L*	1.39	AGGCATGTGCCAGCATGCCC	10077
APOD	5.32	GGACGTGTTGCAACATGTTT	156	*GAS7*	1.13	GGACTTGCCCAGACATGCCC	6959
ST14	4.39	TTTCATGACCAGACAAGTCC	19290	*IFNGR2*	1.11	TGACATGCCCAGACATGTTC	17245
MDFI	4.02	GGGCAGGTGAGAGCATGCCT	7276	*LRIG3*	1.09	GTACATGCCCAGGCATCTTC	13121
DHRS2	2.89	AGGCAAGTTCAGACAAGCAG	1662	*NELL2*	-1.2	AGGCATGTAACAACATGCCC	1188
ELFN2	2.71	TGACAGGTCAGGGCATGCAA	4585	*FTH1*	-1.3	AGGCATGTAACAACATGCCC	1188
CDC42BPG	2.66	GGACAAGTAGAGACAAGCAG	1178	*FAM183A*	-1.3	AGACATGCCTGGGCTTGAAC	8442
PRDM1	2.6	GTGCAAGTCTGGACATGTTT	11869	*NRP2*	-1.6	ATGCTTGTCC13bpGGAAGAGCAT	2684
DENND2D	2.58	GGGCATGTCTTAGGCAAGCCC	9820	*OTOP1*	-1.7	AGACATGTTATGACAAGTTA	7271
RNF182	2.05	CCACAAGTCAGGACAAGCCT	10981	*HSPG2*	-1.7	AGACTTGCCCAAGCTTGCCC	18529
ETV3	1.98	AGACTAGTCTCAAACATGCCC	19095	*FGF9*	-3	GGAGACGTTCAGACACGTCC	16485
SCAMP5	1.83	GAACATGTTTTCACATGATT	4790	*PCBP3*	-5.7	AGACATGTCCTGGCATGCCC	10611
PARD6B	1.78	TTACAGGCCCTGACATGCAC	1582				
lncRNAs							
lncRNA gene name	**log2 fc**	**p53_motif**	**TSS (bp)**	**lncRNA gene name**	**log2 fc**	**p53_motif**	**TSS (bp)**
RP3-326I13.1	12.1	GCCCTTGTCTGGACATGCCC	54	*RP11-34A14.3*	1.47	AGGCATGCGCCAACATGCCC	13222
RP3-510D11.2	11.4	GAACAAGCCCAGGCAAGCCC	184	*AP000944.1 (NEAT1)*	1.36	GAGCAAGCCTGGGCTTGCCA	1183
RP11-462G8.3 (TCERG1L-AS1)	10.4	AGACTTGCCTGGGCTTGTTC	165	*BX470102.3*	1.29	GCACATGTTTAGGCAAGCCC	7120
LINC01021 (RP11-46C20.1)	6.44	GGGCTTGTCTGGGCATGCCC	51	*RPL39P5*	1.21	GGGCTTGCCTGTGACTTGCTT	14805
BX571672.2	4.65	TGTCTTGCCTGGACATGCCC	8650	*AP000525.8 (DUXAP8)*	1.21	AGACATGCCTGTGCAAGCCT	11881
AC012065.6 (HS1BP3-IT1)	3.68	GGACATGCACACCACATGTCT	7567	*AC078883.4*	1.2	GAGCATGTGTGAGCTTGTTT	14043
RP11-432J9.5	2.12	TGGCTTGACGACTCTTGTGA	288	*AC008759.1 (ZNF256-AS1)*	1.19	ATACATGTTCAAAATGCTTGTTC	314
RP11-553A21.3	1.94	TAGCATGCCCCTGCAAGCCT	8009	*AC008937.2*	-1.1	AGGCAAGTCTCAACATGCAG	76
RP11-611D20.2 (MIR4674HG)	1.61	GGGCAAGTCC	4220				
miRNAs							
miRNA gene name	**log2 fc**	**p53_motif**	**TSS (bp)**	**miRNA gene name**	**log2 fc**	**p53_motif**	**TSS (bp)**
miR-1293	6.5	AGACAAGTCTGCAGGCATGTTA	23563	*miR-3191*	-5.9	GGACATGCCTGGGCAGACCC	158
miR-486-5p	2.7	TAACTTGCCCAGACATGCCG	20047	*miR-3928*	-6.1	AGACAGGCTCAGGCATGCCA	17299
miR-641	1.3	AGGCATGAACCAACATGCCT	10361	*miR-1908*	-9.3	GGTCATGCCTAGTCATGTCT	3811

Table 6: **Novel p53 target genes identified by RNA-Seq, pSILAC and ChIP-Seq.** The table indicates 21 new direct p53 targets identified by pSILAC, 31 targets identified by RNA-Seq, 17 new p53-regulated lncRNAs identified by RNA-Seq (if available, the ENSEMBL gene name for the corresponding ENSEMBL gene ID is indicated) and 6 new p53-regulated miRNAs identified by miRNA-Seq in combination with ChIP-Seq. The log_2 fold change of the respective target, the sequence of the p53 binding motif and its distance from the TSS (bp) are indicated. Based on the pSILAC, RNA-/miRNA-/ChIP-Seq results (contributions of the co-authors described on page 42), the data were analyzed and this table was generated.

Furthermore, *MDFI*, *ST14* and *LINC01021* showed an up-regulation after Nutlin-treatment in HCT116 *p53+/+* but not in HCT116 *p53-/-* cells (Fig. 27).

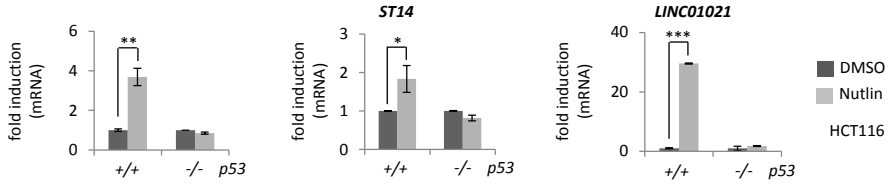

Figure 27: **p53-dependent regulation of the newly identified p53 target genes *MDFI*, *ST14* and *LINC01021* after Nutlin treatment.** qPCR analyses of *MDFI*, *ST14* and *LINC01021* expression after addition of Nutlin or DMSO for 48 hours in HCT116 *p53+/+* and HCT116 *p53-/-*. Results were normalized to β-actin expression and represent the mean +/- SD (n = 3).

In addition, we confirmed induced levels of primary and mature miR-486 after ectopic p53-expression in the DOX-inducible cell line SW480/pRTR-p53-VSV (Fig. 28A). Moreover, we confirmed p53 occupancy by qChIP analysis for *miR-486*, which is line with the ChIP-Seq results (Fig. 28B, C). A reporter assay showed that the isolated p53 binding site upstream of the *miR-486* host gene *ANK1* is indeed responsive to p53, providing further evidence for the direct regulation of miR-486-5p by p53 (Fig. 28D).

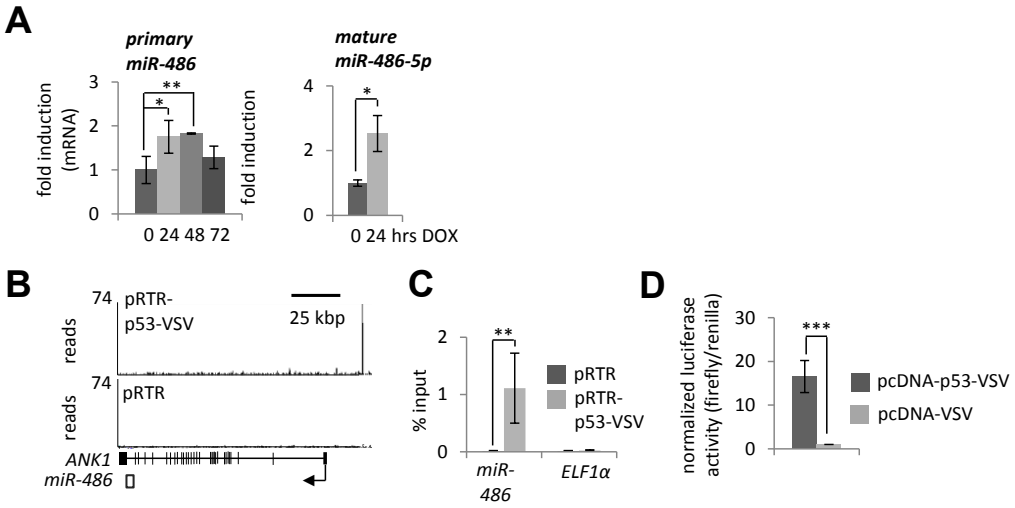

Figure 28: **Validation of the new p53 target miRNA miR-486-5p.** (A) qPCR analyses of primary and mature miR-486-5p expression in SW480/pRTR-p53-VSV cells after addition of DOX for the indicated periods. (B) p53-VSV-derived ChIP-Seq result displayed using the UCSC genome browser. (C) qChIP validation of p53 occupancy at the *miR-486* promoter in SW480/pRTR-p53-VSV after 16 hours of DOX treatment and subsequent VSV-ChIP. Raw data analysis of ChIP-Seq results was performed by T. Bonfert. (D) Luciferase-reporter assay after transfection of a pcDNA-p53-VSV or pcDNA-VSV vector together with a pBV-Luc vector harboring the p53 binding site of the gene encoding miR-486-5p. Results in (A), (C) and (D) represent the mean +/- SD (n = 3).

Moreover, the induction of primary and mature miR-34a and miR-205 by p53 was confirmed by qPCR (Fig. 29A). In contrast to a previously identified p53 RE 1 kbp upstream of the gene encoding miR-205 [262], we validated a p53 binding site approximately 17 kbp upstream of the *miR-205* TSS (Fig. 29B).

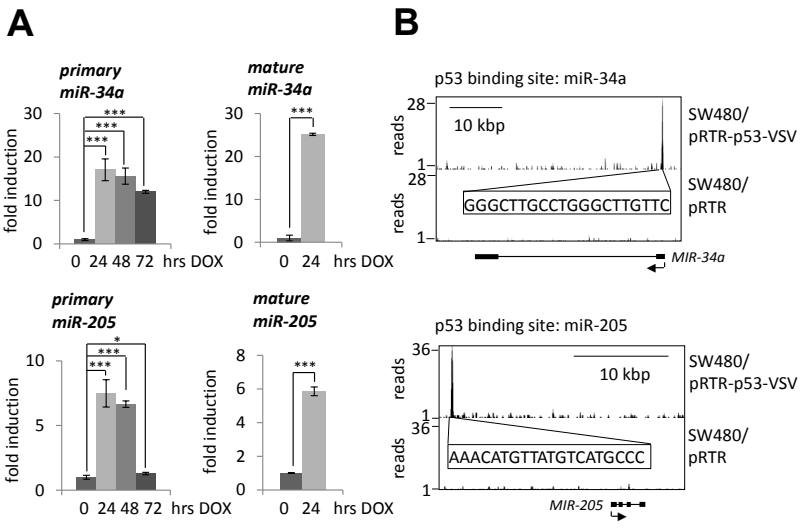

Figure 29: **Validation of the p53-regulated miR-34a and miR-205.**
(A) qPCR analyses of (left) primary and (right) mature miRNA-levels of miR-34a and miR-205 in SW480/pRTR-p53-VSV cells after addition of DOX for the indicated periods. Results re-present the mean +/- SD (n = 3). (B) p53-VSV-derived ChIP-Seq results are displayed using the UCSC genome browser. Raw data analysis of ChIP-Seq results was performed by T. Bonfert.

Because of its exceptionally pronounced induction after p53-activation, we further analyzed *LINC01021*. According to the ENSEMBL genome browser, the *LINC01021* locus encodes six alternatively spliced transcripts (Fig. 30A). We introduced the longest transcript, *LINC01021_A*, into the DOX-inducible pRTR-vector and subsequently confirmed its prominent induction after treatment with DOX in SW480/pRTR-LINC01021_A cells (Fig. 30B).

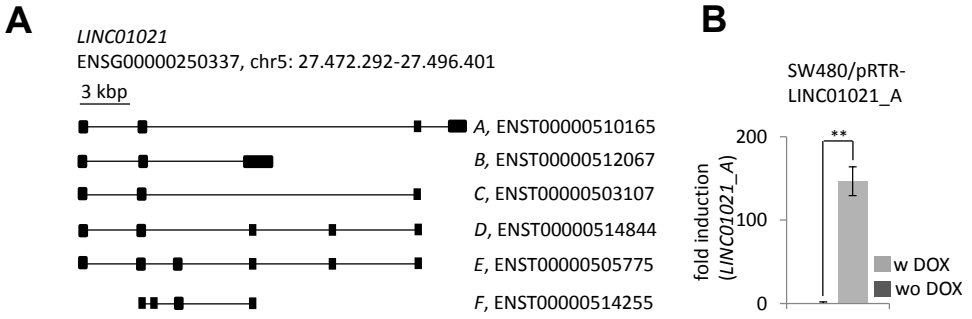

Figure 30**: Ectopic expression of LINC01021.** (A) Scheme showing the different splice variants of LINC01021. The longest *LINC01021* transcripts, *LINC01021_A*, has 945 nt and was inserted into the pRTR vector. (B) qPCR analysis of *LINC01021* expression in SW480/pRTR-LINC01021_A cells after 48 hours of DOX treatment. Results were normalized to β-actin expression and represent the mean +/- SD (n = 3).

Notably, ectopic *LINC01021_A* expression after addition of DOX resulted in decreased proliferation as determined by realtime impedance measurement and cell counting (Fig. 31A), whereas addition of DOX had no effect on SW480/pRTR cells (Fig. 31B).

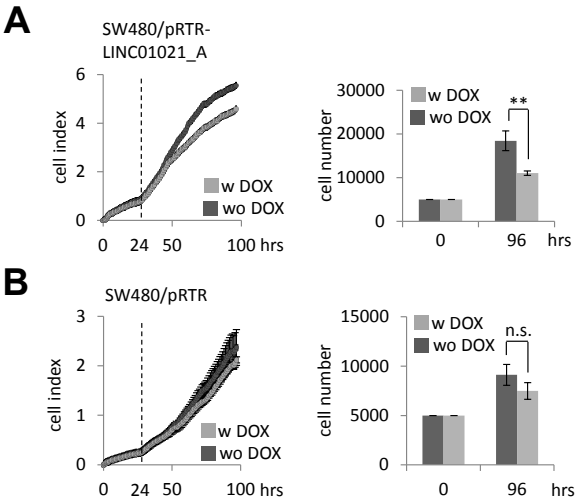

Figure 31**: Effect of LINC01021 expression on proliferation.** (A) SW480/pRTR-LINC01021_A and (B) SW480/pRTR cell pools were subjected to (left) impedance measurements and (right) cell counting using trypan blue exclusion. 24 hours after seeding, DOX was added as indicated by the dotted line in the left panel. Results represent the mean +/- SD (n=3).

5.2.7 Comparison of p53 and miR-34a effects on *de novo* protein synthesis

Recently, my colleague Markus Kaller performed a proteome-wide analysis of miR-34a targets in the colorectal cancer cell line SW480 using the pSILAC method [217]. When we compared the sets of down-regulated proteins from both analyses, a significant overlap was detected (Fig. 32): Almost 35% of the proteins down-regulated in the miR-34a pSILAC analysis were also down-regulated after ectopic expression of p53.

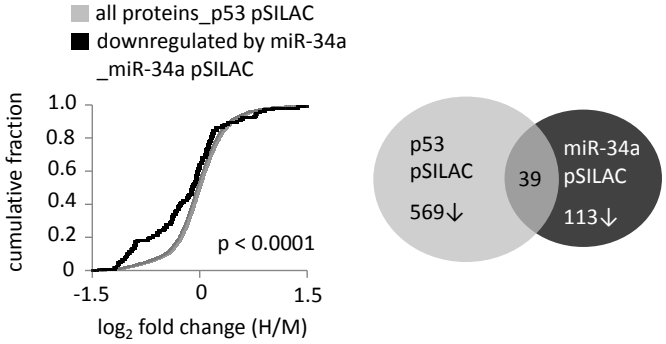

Figure 32: **Overlap between changes in *de novo* protein synthesis after p53- or miR-34a-induction**. (Left) Cumulative distribution plot displaying p53-induced changes in *de novo* protein synthesis of 113 proteins down-regulated after induction of miR-34a [217] compared to the normal distribution of all detected proteins. (Right) Venn diagram displaying the overlap between proteins down-regulated (log_2 fold change $\leq$ -0.3) after ectopic p53 and miR-34a expression. Based on the p53 pSILAC results (contributions of the co-authors described on page 42), the data were analyzed and the figures generated with support of M. Kaller.

Moreover, the log_2 fold changes of those co-regulated proteins showed a significant, positive correlation (Fig. 33).

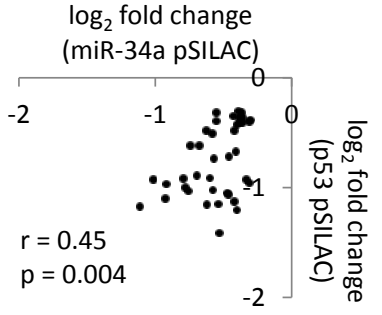

Figure 33: **Changes in *de novo* protein synthesis after p53-induction positively correlate with miR-34a-induced changes in *de novo* protein synthesis**. Scatter plot displaying the correlation of changes in *de novo* protein synthesis between proteins down-regulated by p53 and miR-34a. The Pearson correlation coefficient and statistical significance are indicated. Based on the p53 pSILAC results (contributions of the co-authors described on page 42), the data were analyzed and this figure was generated with support of M. Kaller.

Interestingly, almost all members of the MCM protein family, which mediate initiation of DNA replication, were among the co-regulated proteins. Among these were only four direct miR-34a targets: MTA2, SURF4, TMEM109 and UCK2. Therefore, Markus Kaller determined whether the proteins down-regulated after p53 and miR-34a expression harbor common transcription factor binding motifs in a region +/-2 kbp from the corresponding gene promoter using the Molecular signatures database (MSigDB) [274, 275] (Fig. 34). Interestingly, we found that the binding motif for the transcription factor E2F1 was significantly enriched among down-regulated proteins in both pSILAC-datasets (Fig. 34A), but not among the up-regulated proteins (data not shown). A cumulative distribution analysis of proteins with an E2F1 binding motif near their corresponding TSS (+/-2 kbp) revealed significantly decreased protein expression ($p < 0.0001$) when compared to the normal distribution of all proteins detected in the p53 pSILAC analysis (Fig. 34B). Using a dataset of experimentally validated E2F1 regulated genes further supported this finding (Fig. 34B). It is known that E2F transcription factors are targeted by miR-34a [95, 218, 276, 277]. Indeed, a cumulative distribution analysis of proteins with an E2F1 binding motif near their corresponding gene TSS (+/-2 kbp) revealed significantly decreased *de novo* protein synthesis ($p < 0.0001$) when compared to the normal distribution of all proteins detected in the miR-34a pSILAC approach (Fig. 34C). Interestingly, almost all members of the MCM protein family, that are known E2F target genes [120, 278-280], were among the proteins co-regulated by miR-34a and p53 (data not shown). Therefore, it is possible that miR-34a indirectly contributes to a p53-induced cell cycle arrest by targeting E2F and thereby E2F target genes.

A

TF binding motifs +/- 2 kbp from TSS of downregulated proteins

p53_pSILAC		miR-34a_pSILAC	
TF	p-value	TF	p-value
E2F1	1.80E-40	E2F1DP2	3.23E-16
E2F1DP1	3.32E-40	E2F1	2.15E-14
E2F1DP2	3.32E-40	E2F1DP1	2.54E-14

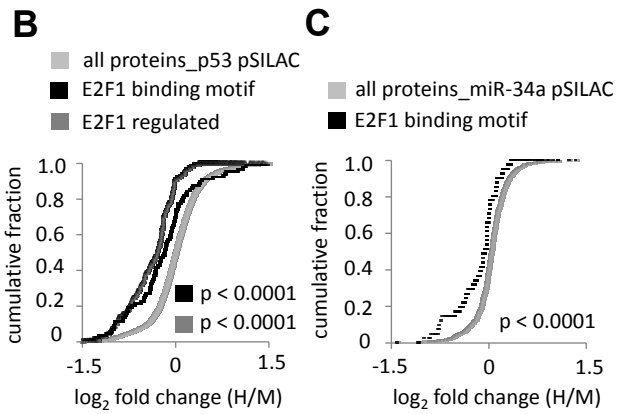

Figure 34**: Common transcription factor binding motifs among proteins down-regulated after miR-34a or p53.** (A) Enrichment of E2F1, E2F1DP1 and E2FDP2 binding motifs in the promoters of genes encoding proteins down-regulated by p53 and miR-34a. pSILAC datasets were analyzed with the Molecular Signature database (MSigDB) at http://www.broadinstitute.org/gsea/msigdb/index.jsp. TF = transcription factor. (B) Cumulative distribution plot displaying in black the p53-induced changes in *de novo* protein synthesis of proteins with E2F1 binding motifs in their gene promoters (in black) compared with the normal distribution of all detected proteins. p53-induced changes in *de novo* protein synthesis of proteins (in light grey) positively regulated by E2F1 are displayed in dark grey. (C) Cumulative distribution plot displaying miR-34a-induced changes in *de novo* protein synthesis of proteins with E2F1 binding motifs in their gene promoters compared to the normal distribution of all detected proteins.The E2F1 datasets V$E2F_Q6 [281] and E2F1_UP.V1_UP [282] for (B) and V$E2F1_Q3_01 for (C) were obtained at MSigDB. Based on the p53 pSILAC results (contributions of the co-authors described on page 42), the data were analyzed and figures were generated by M. Kaller.

5.2.8 miRNA-mediated repression by p53

To assess the effect of miRNA-mediated repression after activation of p53, we performed a scan for targets of the p53-induced miRNAs (log_2 fold change ≥ 1) among the differentially down-regulated proteins and mRNAs identified in this study by using a combination of the TargetScan and Pictar [239, 240] target prediction algorithms. Thereby, 284 predicted targets of the p53-induced microRNAs were identified among the down-regulated proteins (log_2 fold change ≤ -0.3; pval ≤ 0.05) (data not shown). 37% (105) of these targets were also down-regulated on the mRNA level. In addition, we detected 203 putative targets that were regulated on mRNA level only. A KEGG pathway analysis of the 284 predicted targets using DAVID [241, 242] revealed a significant over-representation of miRNA targets involved in DNA replication (p = 9.40E-07) and cell cycle progression (p = 6.80E-04), indicating that induction of miRNAs may contribute to inhibition of these processes by p53 (data not shown). Subsequently, we focused on the targets of the miRNAs miR-34a, -34c-3p, -145, -205 and -486-5p, which are directly induced by p53. Out of 77 putative miRNA targets with reduced *de novo* protein synthesis, 33 were repressed on both, the protein- and mRNA-level and 44 only on the level of *de novo* protein synthesis (Fig. 35A and B, respectively).

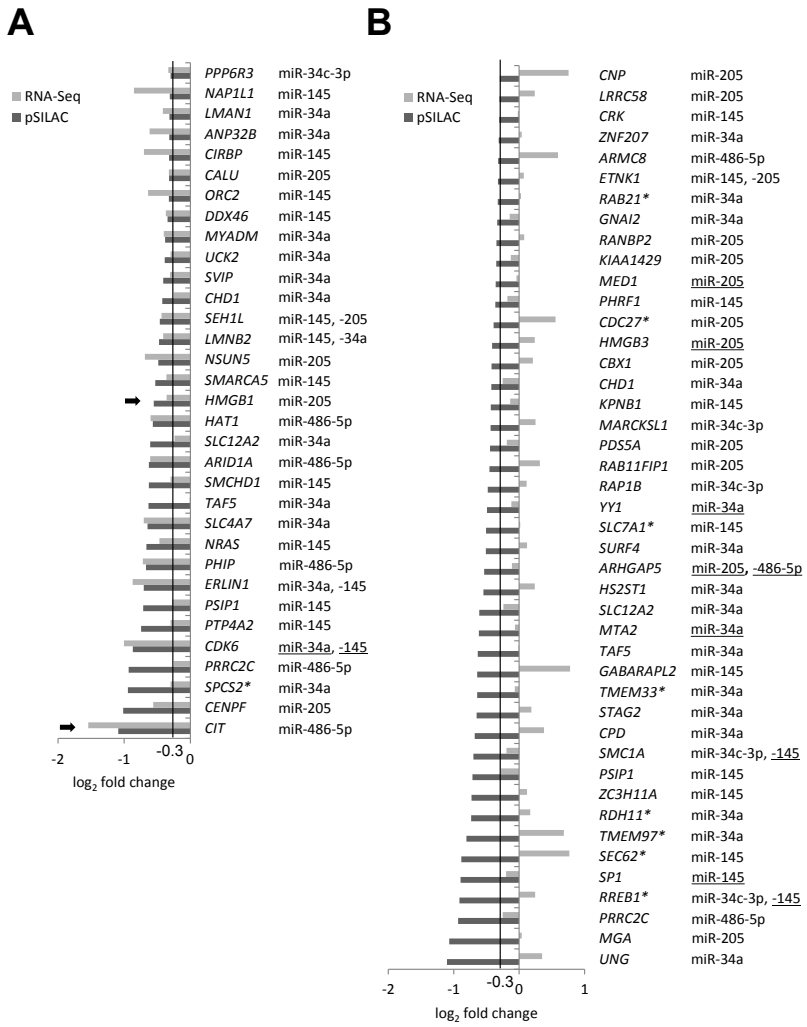

Figure 35: **Putative targets of miRNAs directly induced by p53 with down-regulated mRNA- and *de novo* protein synthesis or reduced *de novo* protein synthesis only.** Predicted miRNA targets with (A) down-regulated mRNA- and *de novo* protein synthesis, (B) reduced *de novo* protein synthesis only are displayed. Proteins that showed a heterogeneous distribution of fold changes in independent experiments (class II candidates, see Experimental procedures) are marked with an asterisk (*). Known miRNA targets are underlined and targets experimentally validated in this study are marked with a black arrow. The mature miRNA is referred to as miR-x, whereas the strand that is usually degraded is indicated as miR-x*. Starting with mirBase v18, miRNA strands from one precursor are referred to as miR-x-5p and miR-x-3p depending on the arm from which they are processed since it is not clear which sequence serves as the predominant one under varying conditions. Based on the pSILAC, RNA- and miRNA-Seq results (contributions of the co-authors described on page 42), the data were analyzed and this figure was generated.

In addition, we identified 51 repressed putative miRNA target mRNAs for which the corresponding protein was not detected by pSILAC (Fig. 36). Among the identified targets, several were already shown to be regulated by one or several of the studied miRNAs, such as the miR-34a targets *CDK6*, *MTA2* and *YY1* [217] (underlined in Fig. 35, 36). None of the predicted conserved targets showed p53 enrichment in the ChIP-Seq analysis in the vicinity (+/- 20 kbp) of the respective gene promoter except for *MTA2*. Since *MTA2* is a known target of miR-34a [217], this indicates that additional direct transcriptional repression by p53 may augment the

miRNA-mediated down-regulation of this gene by a coherent feed forward regulation [283].

These results indicate that p53 indirectly down-regulates many genes on mRNA- and/or protein-level by inducing miRNAs on a genome-wide scale. Part of the miRNA-mediated repression is presumably mediated by enhanced mRNA degradation. However, approximately 60% of the conserved miRNA targets are presumably not repressed on the mRNA level, but only on the level of *de novo* protein synthesis, indicating that miRNA-mediated translational repression may represent an important regulatory mechanism employed by p53.

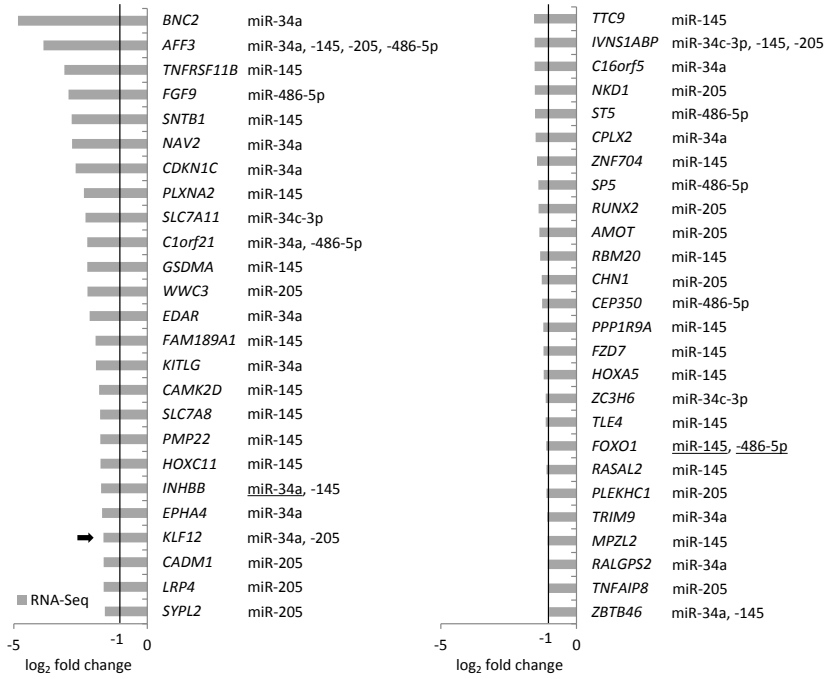

Figure 36: **Putative targets of miRNAs directly induced by p53 with down-regulation of mRNA expression.** Predicted miRNA targets down-regulated only on the mRNA level. Known miRNA targets are underlined and targets experimentally validated in this study are marked with a black arrow. Based on the RNA- and miRNA-Seq results (contributions of the co-authors described on page 42), the data were analyzed and this figure was generated.

5.2.9 p53-induced miRNAs regulate putative prognostic markers

Next, we focussed on three factors that displayed down-regulation by p53, were putative targets of p53-induced miRNAs and had previously reported cancer-relevant functions. HMGB1, which was down-regulated on the mRNA level and showed reduced *de novo* protein synthesis after p53 induction (Fig. 35A), has a predicted conserved seed-match (SM) for miR-205 in its 3´-UTR (Fig. 37A) and a published SM for miR-34c-3p and miR-34a [284]. *KLF12* also showed a prominent down-regulation on mRNA-level (Fig. 36) and has predicted conserved seed-matches for miR-34a and miR-205 (Fig. 37B). The citron rho-interacting serine/threonine kinase (CIT), which was also down-regulated on the mRNA level and showed reduced *de novo* protein

synthesis (Fig. 35A), is a predicted target of the newly identified p53-regulated miRNA miR-486-5p (Fig. 37C).

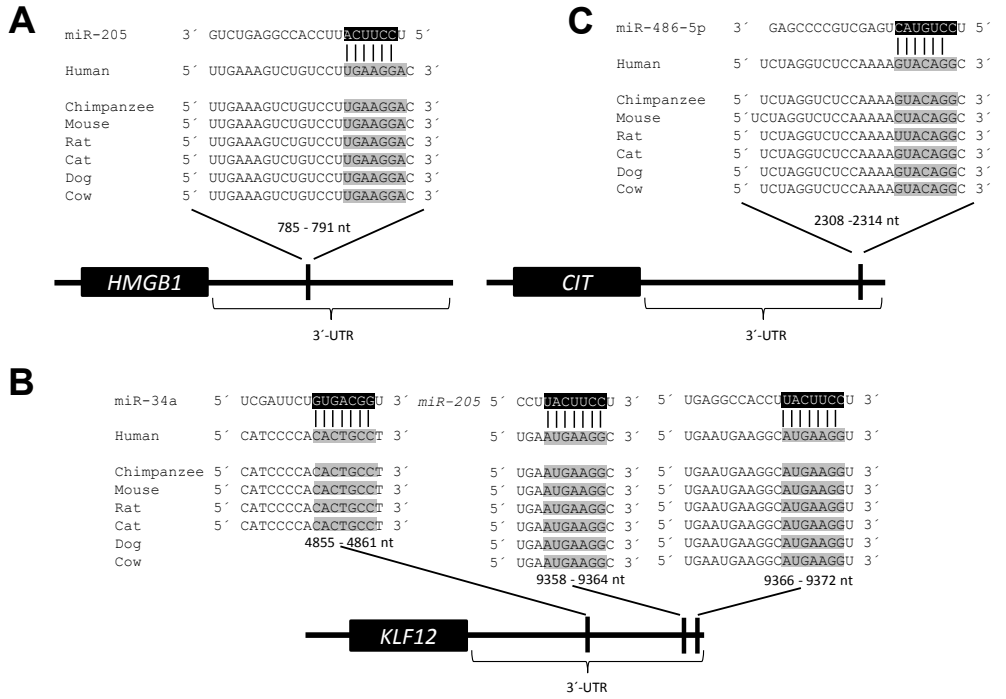

Figure 37: **Detection of conserved seed-matching sites of p53-regulated miRNAs in the 3´-UTRs of *HMGB1*, *KLF12* and *CIT*.** The indicated 3´-UTRs were analyzed with TargetScan (http://www.targetscan.org) and Pictar (http://pictar.mdc-berlin.de).

Down-regulation of *HMGB1, KLF12 and CIT* expression by p53 was confirmed on the mRNA level in SW480/pRTR-p53-VSV cells (Fig. 38A). Furthermore, all three genes were down-regulated after treatment with Nutlin or Etoposide in HCT116 *p53+/+* but not in HCT116 *p53-/-* cells (Fig. 38B). Therefore, their repression by DNA-damage is p53-dependent.

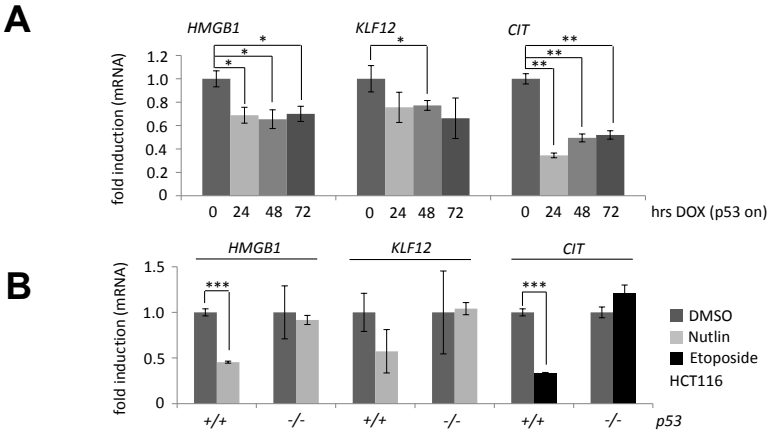

Figure 38: **Validation of p53-mediated down-regulation on mRNA level.** qPCR analyses of the indicated mRNAs after (A) addition of DOX to SW480/pRTR-p53-VSV cells for the indicated periods, (B) treatment of HCT116 *p53+/+* and *p53-/-* cells with Nutlin or Etoposide for 48 hours. Results in (A) and (B) represent the mean +/- SD (n = 3).

To confirm direct miRNA-mediated down-regulation of *KLF12*, *HMGB1* and *CIT*, dual reporter assays were performed (Fig. 39A). 3'-UTR-reporters of *KLF12*, *HMGB1* and *CIT* displayed a significant repression after cotransfection with the matching miRNA. Mutation of the seed-matching sequences in the 3´-UTRs abolished the miRNA-mediated repression in all cases (Fig. 39A, 39B). Therefore, the three selected miRNA targets represent direct targets of p53-induced miRNAs.

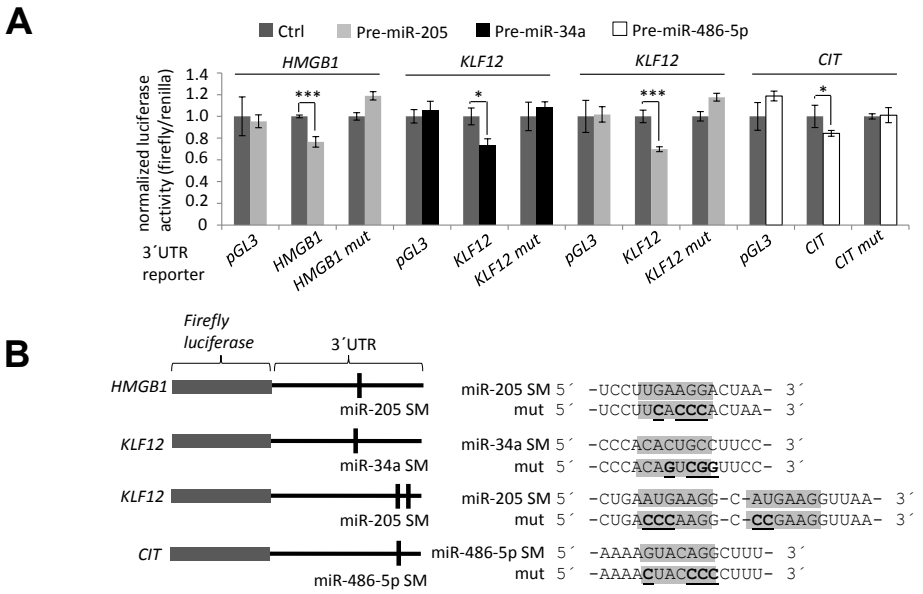

Figure 39: **Validation of p53- and miRNA-mediated down-regulation.** (A) Dual reporter assays of H1299 cells co-transfected with the indicated miRNA mimics or controls and the indicated 3´-UTR constructs. Results represent the mean +/- SD (n = 3). (B) Details of the mutant 3´-UTR reporter constructs. SM = seed-match.

We then asked whether up-regulation of any of the three miRNA targets occurs during tumor progression using expression data from collections of patient-derived tumor samples in the databases Oncomine [237], TCGA (The Cancer Genome Atlas) [244] and PROGgene [238]. Analysis of the Oncomine database [237] showed a significant up-regulation of *HMGB1* in tumor versus normal tissue in 15 out of 20 different tumor entities, such as colon, pancreatic, prostate and invasive breast carcinoma (Fig. 40).

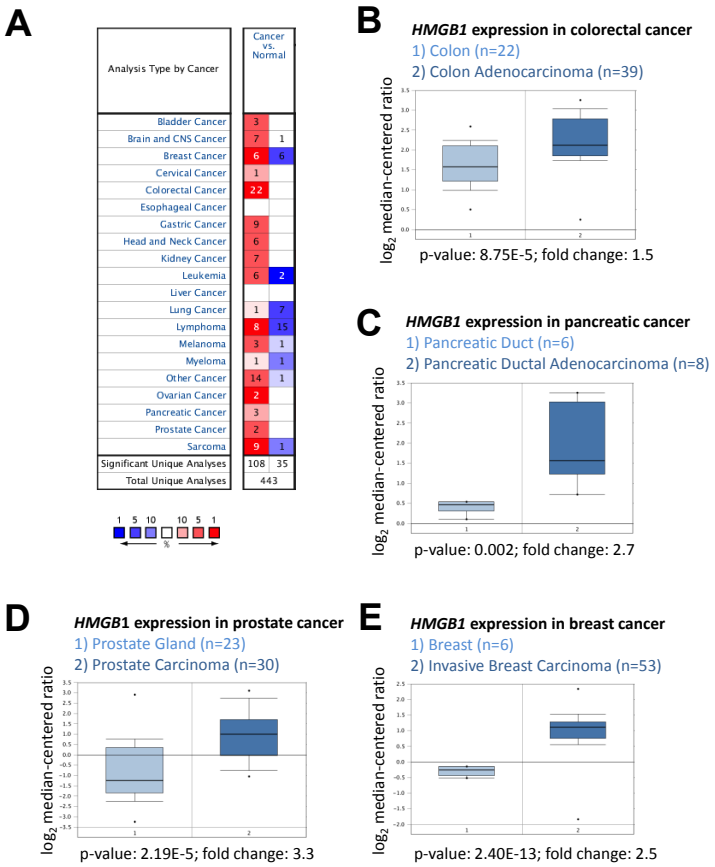

Figure 40: **Analysis of the *HMGB1* mRNA level in different tumor entities.** Analysis of *HMGB1* mRNA expression in the human Oncomine dataset (p-value < 0.05; fold change > 1.5). (A) Summary of *HMGB1* expression in different types of human cancer; red: up-regulated, blue: down-regulated. Comparison of *HMGB1* mRNA expression in corresponding normal tissue and (B) colon adenocarcinoma in the Alon colon dataset [285], (C) pancreatic ductal adenocarcinoma in the Buchholz pancreas dataset [286], (D) prostate carcinoma in the Tomlins prostate dataset [287], (E) invasive breast carcinoma in the Finak breast dataset [288].

Similarly, *KLF12* was up-regulated in different tumor types, such as pancreatic ductal adenocarcinoma, invasive breast carcinoma, gastrointestinal stromal tumor, melanoma, T-cell acute lymphoblastic leukemia and teratoma (Fig. 41A-D). When expression data of 424 colorectal tumors from TCGA were analyzed, a significant increase in *KLF12* mRNA expression in those cases showing metastasis to distant organs (M1) compared to those without distant metastasis (M0) was detected (Fig.

41E). *KLF12* mRNA expression was also significantly elevated in tumors with nodal status N2 compared to N0 and in advanced tumor stage IV versus tumor stage I.

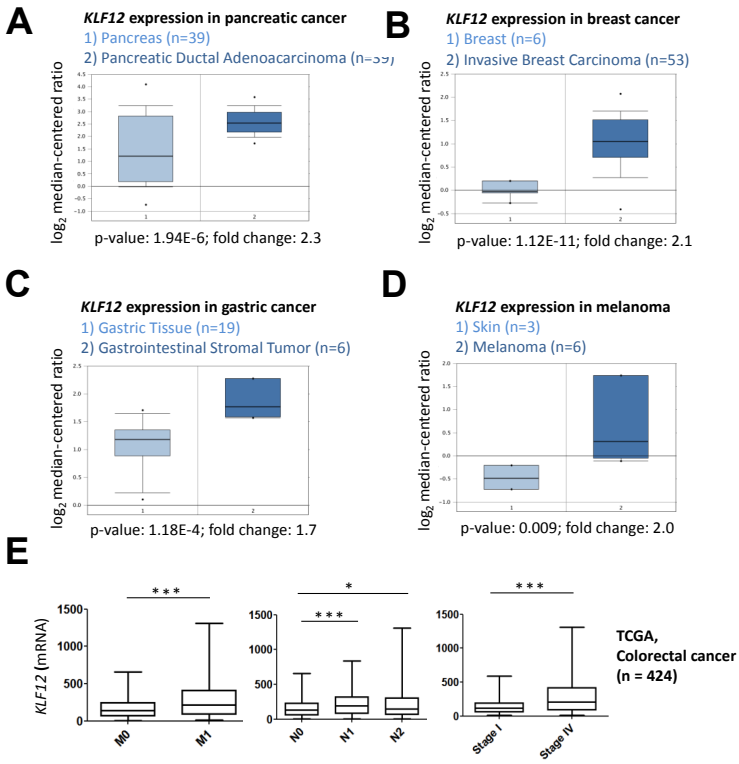

Figure 41: **Analysis of the *KLF12* mRNA level in different tumor entities and advanced tumor stages.** Analysis of *KLF12* mRNA expression in (A-D) the human Oncomine dataset (p-value < 0.05; fold change > 1.5) and (E) the public database TCGA. Comparison of *KLF12* mRNA expression in the corresponding normal tissue and (A) pancreatic ductal adenocarcinoma in the Badea pancreas dataset [289], (B) invasive breast carcinoma in the Finak breast dataset [288], (C) gastrointestinal stromal tumor in the Cho gastric dataset [290], (D) melanoma in the Haqq melanoma dataset. (E) *KLF12* mRNA expression data derived from primary CRC samples (n = 424) from the public database TCGA.

Furthermore, *CIT* mRNA expression was elevated in several tumor entities, such as colon, lung, breast, pancreas and gastric cancer (Fig. 42).

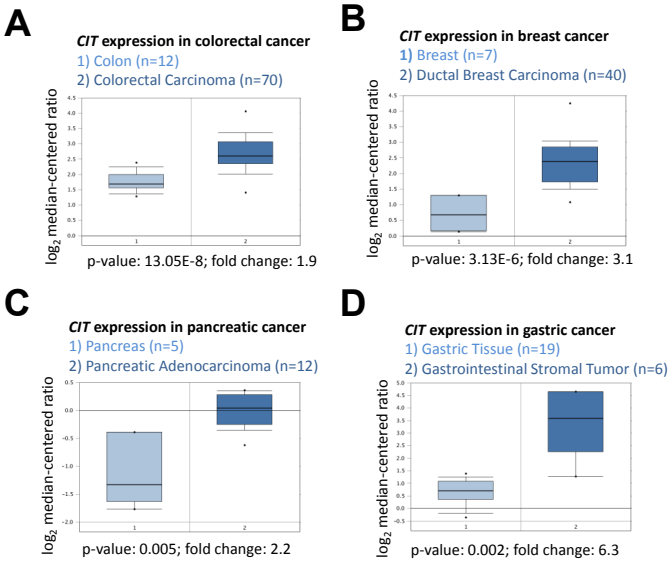

Figure 42**: Analysis of the *CIT* mRNA level in different tumor entities.** Analysis of *CIT* mRNA expression in the human Oncomine dataset (p-value < 0.05; fold change > 1.5). Comparison of *CIT* mRNA expression in corresponding normal tissue and (A) colorectal carcinoma in the Hong colon dataset [291], (B) ductal breast carcinoma in the Richardson breast 2 dataset [292], (C) pancreatic adenocarcinoma in the Iacobuzio-Donahue pancreas 2 dataset [293], (D) gastrointestinal stromal tumor in the Cho gastric dataset [290].

Interestingly, patients showing decreased expression of *HMGB1*, *KLF12* and *CIT* had an increased overall and metastasis-free survival in two different colorectal cancer patient cohorts (Fig. 43). In summary, these results suggest that *HMGB1*, *KLF12* and *CIT* may represent clinically relevant prognostic markers. Moreover, the serine/threonine kinase *CIT* represents an interesting candidate for tumor therapeutic approaches, since its activity may be inhibited by small molecules.

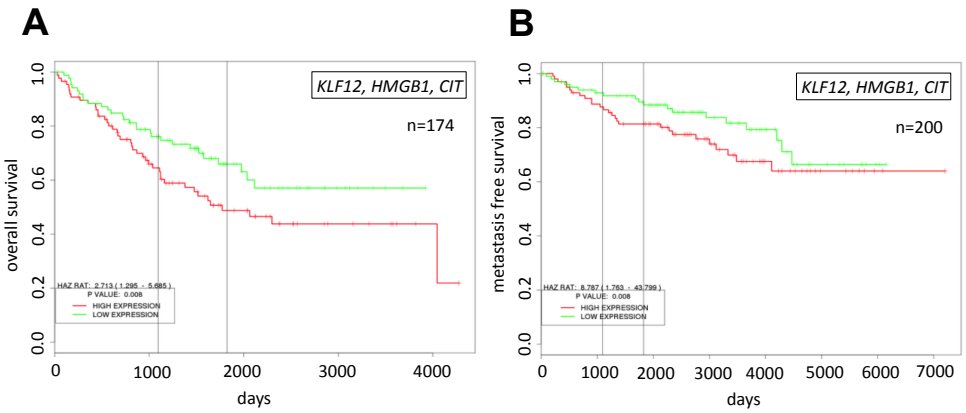

Figure 43: **Correlation of *HMGB1*, *KLF12* and *CIT* mRNA expression with increased overall and metastasis free survival.** Association analysis of (A) overall and (B) metastasis free survival of colorectal cancer patients and *HMGB1*, *KLF12* and *CIT* expression in the primary tumor using the datasets GSE15736 and GSE11121, respectively, from the PROGgene database (www.compbio.iupui.edu/proggene).

5.3 p53 directly activates *CST5* to mediate mesenchymal-epithelial transition

The following results are published in:

Hünten, S. and H. Hermeking, p53 directly activates cystatin D/CST5 to mediate mesenchymal-epithelial transition: a possible link to tumor suppression by vitamin D3. Oncotarget, 2015. **6**(18): p. 15842-56. [3]

All figures shown in this section are exclusively based on my experimental work under supervision of Prof. Hermeking.

5.3.1 p53 induces *CST5* expression

In the screen for p53-regulated factors described in the previous chapter (5.2) we had detected an ~6-fold increase of CST5 protein by pulsed SILAC and a ~9-fold induction of *CST5* mRNA expression by RNA-Seq analysis after addition of doxycycline (DOX) to activate expression of ectopic p53 in the colorectal cancer cell line SW480 harboring a pRTR-p53-VSV vector for 48 and 40 hours, respectively. Here, we confirmed the up-regulation of the CST5 protein by p53 by Western blot analysis (Fig. 44A). As expected, p53 expression also resulted in the induction of the known p53 target p21. The kinetics of induction by p53 were similar for p21 and CST5: at 24 hours an induction was detectable and by 72 hours both proteins were still elevated. After p53 activation, *CST5* mRNA expression displayed a similar induction as *p21* (Fig. 44B).

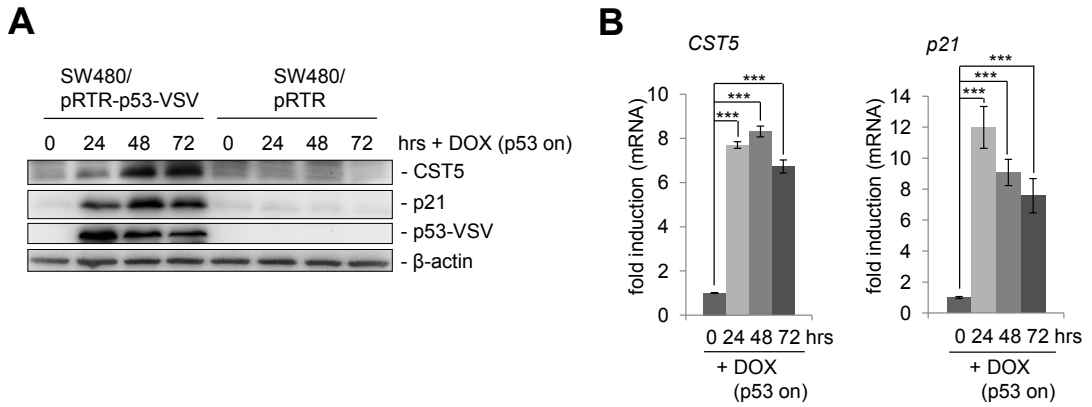

Figure 44: **CST5 is up-regulated after ectopic p53 expression in SW480/pRTR-p53-VSV**. SW480/pRTR-p53-VSV or SW480/pRTR cells were treated with DOX for the indicated timepoints. (A) Western blot analysis of the indicated proteins. β-actin served as a loading control. (B) The indicated mRNAs were measured by qPCR-analysis. *β-actin* served as a normalization control. Fold changes represent mean values of triplicate analyses of DOX-treated versus untreated cells and error bars represent standard deviations.

An immunofluorescence analysis confirmed increased CST5 protein levels after ectopic p53 expression and showed its predominant cytoplasmic localization after DOX treatment in SW480/pRTR-p53-VSV cells (Fig. 45).

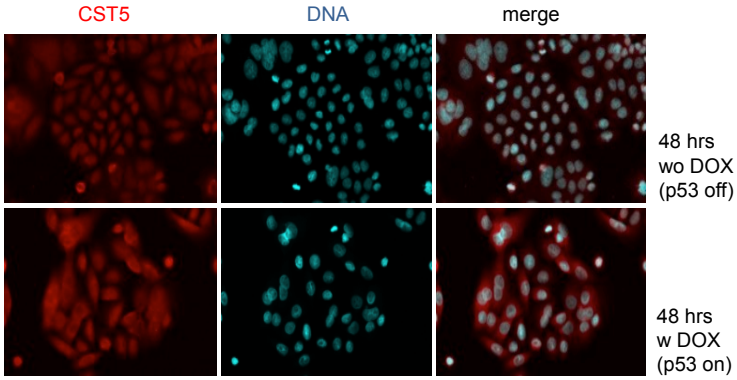

Figure 45: **Localization of the CST5 protein after ectopic p53-expression in SW480/ pRTR-p53-VSV.** Analysis of CST5 expression and localization in SW480/pRTR-p53-VSV cells by confocal immunofluorescence microscopy after 48 hours with and without DOX treatment. Nuclear DNA was visualized by DAPI staining. 200x magnification.

Recently, *CST5* was shown to be induced by vitamin D3 via direct binding of the vitamin D receptor (VDR) to its promoter in human colon cancer cell lines [200]. In addition, the *VDR* gene is a known p53 target [294]. To determine whether p53 induces *CST5* in a VDR-independent manner, VDR-deficient HEK293T cells were transfected with a DOX-inducible pRTR-p53-VSV vector (Fig. 46). Activation of p53 expression by treatment with DOX resulted in a significant induction of *CST5* and, as a control, *p21* mRNA. These results show that p53 induces *CST5* expression in a VDR-independent manner.

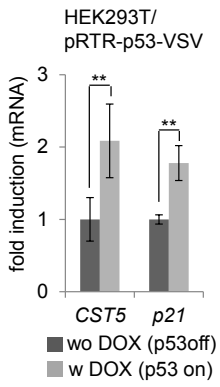

Figure 46: **CST5 up-regulation after p53 is independent of VDR**. qPCR-analysis of *CST5*- and *p21*-mRNA levels in HEK293T/pRTR-p53-VSV cells after 24 hour DOX-treatment. *β*-actin served as a normalization control. Fold changes represent mean values of triplicate analyses of DOX-treated versus untreated cells and error bars represent standard deviations.

To further interrogate the p53-dependency of the *CST5* expression, the colorectal cancer cell lines HCT116 and RKO and their isogenic p53-deficient variants, which were generated by homologous recombination [246], were treated with either Nutlin-3a, a small-molecule inhibitor of MDM2 [247], or the DNA-damaging agent Etoposide (Fig. 47). Both treatments resulted in a time-dependent up-regulation of *CST5* in HCT116 *p53+/+* cells (Fig. 47A). Since *CST5* expression was not induced in HCT116 *p53-/-* cells, the activation of *CST5* transcription was mediated by p53. Also

RKO cells showed p53-dependent induction of *CST5* after induction of DNA damage by Etoposide (Fig. 47B). The p53-dependent induction of *p21* mRNA was more pronounced than the induction of *CST5* expression in RKO and HCT116 cells (Fig. 47C, D). Taken together, these results show that p53 mediates the induction of CST5 by DNA damage.

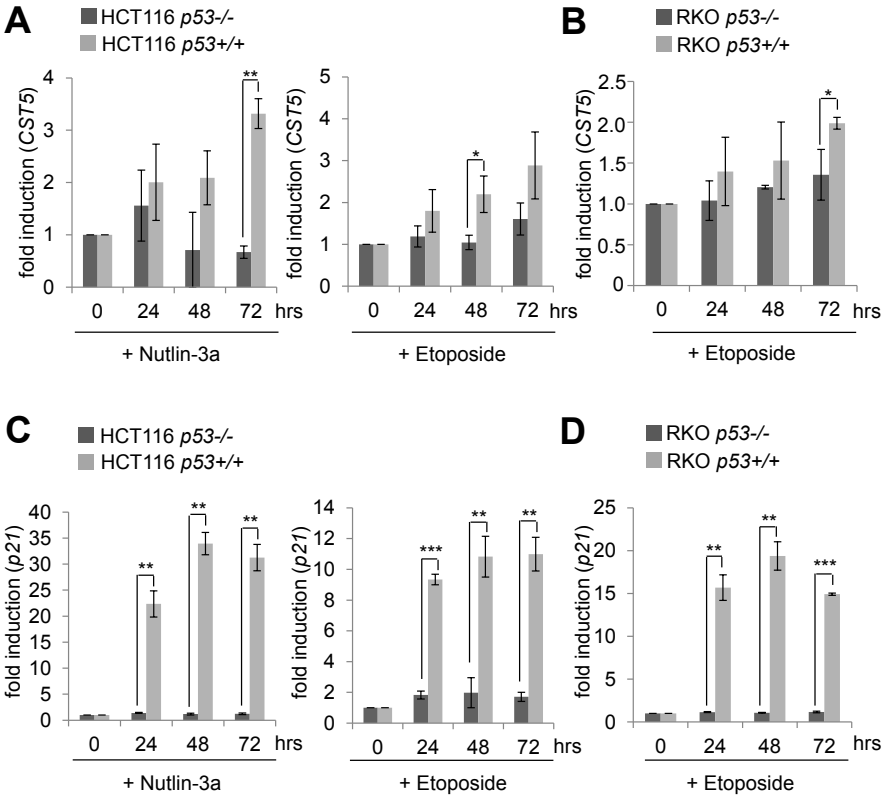

Figure 47: **p53-dependent regulation of CST5 in HCT116 and RKO cells**. (A, B) *CST5*- and (C, D) *p21*-mRNA levels were measured by qPCR analysis after the indicated time points. (A, C) HCT116 *p53-/-* and *p53 +/+* and (B, D) RKO *p53+/+* and *p53-/-* were treated with Nutlin-3a or Etoposide and the vehicle DMSO. Fold changes represent mean values of triplicate analyses of Nutlin-3a/Etoposide versus DMSO treated cells normalized to *β-actin* expression. Error bars represent standard deviations.

5.3.2 *CST5* is a direct p53 target

In a genome-wide p53/ChIP-Seq analysis we had previously detected ChIP-signals in the vicinity of the *CST5* promoter indicating direct p53 binding (Fig. 48A; see 5.2). A sequence that fits well to the p53 binding consensus sequence [56, 57] was identified 1106 base-pairs upstream of the transcriptional start site (TSS) of *CST5* underneath a ChIP-signal with ~10 reads (Fig. 48A). This p53 binding element was conserved between human and rat (Fig. 48B).

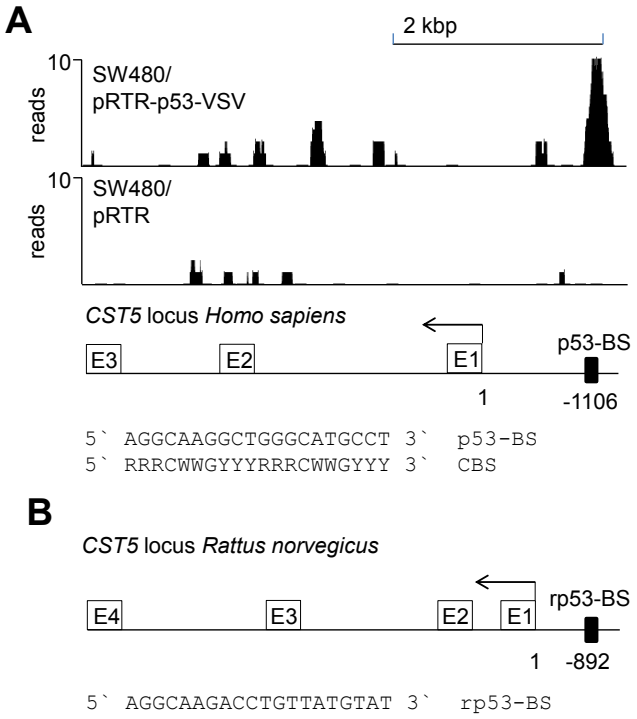

Figure 48: **Direct binding of p53 upstream of the *CST5* promoter**. (A) ChIP-Seq analysis was performed with a VSV-specific antibody 16 hours after addition of DOX to SW480/pRTR-p53-VSV and SW480/pRTR cells. The ChIP-Seq results are represented in the UCSC browser showing p53 binding to the indicated p53 binding site in a region 1106 bp upstream of the *CST5* promoter. (B) p53 binding site upstream of the *CST5* locus of *Rattus norvegicus*. BS = binding site, CBS = consensus binding site.

p53 binding at this site was confirmed by qChIP analysis in SW480/pRTR-p53-VSV cells treated with DOX for 16 hours, whereas no enrichment was detected in the control cell line SW480/pRTR (Fig. 49A). After DNA damage induced by addition of Etoposide, HCT116 *p53+/+*, but not HCT116 *p53-/-* cells, displayed increased p53 occupancy at this site (Fig. 49B). Therefore, also endogenous p53 occupied these binding sites. Together with the results presented above, these findings establish *CST5* as a direct transcriptional target of p53.

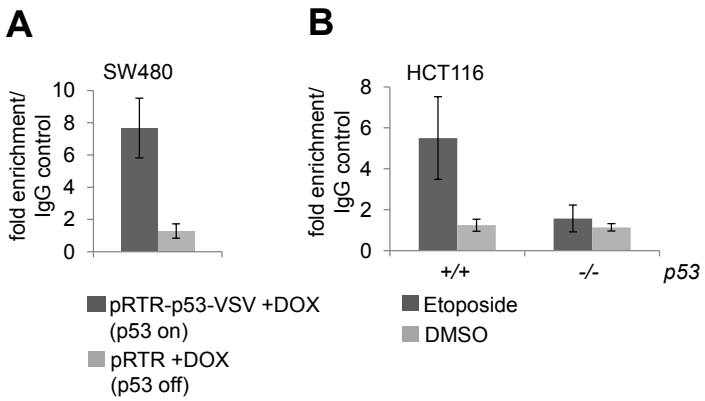

Figure 49: **Experimental validation of p53 binding upstream of the *CST5* promoter**. (A) qChIP analysis of SW480/pRTR-p53-VSV cells 16 hours after activation of p53-VSV expression versus SW480/pRTR cells using anti-VSV and anti-rabbit IgG for ChIP. Experiments were performed in triplicates. Error bars represent +/- SD (n = 3). (B) qChIP analysis of HCT116 *p53+/+* versus HCT116 *p53-/-* after 16 hours Etoposide treatment using anti-p53 and anti-mouse IgG for ChIP; this ChIP analysis was performed in unicates and measured in triplicates.

5.3.3 Role of CST5 in p53-mediated MET

In order to determine the requirement of CST5 for p53-mediated mesenchymal-epithelial transition (MET) and related processes, such as cellular migration, we silenced *CST5* expression in the colorectal cancer cell line SW480/pRTR-p53-VSV using siRNAs (Fig. 50). After treatment with a *CST5*-directed siRNA CST5 protein was undetectable after induction of ectopic p53 expression (Fig. 50A). In the presence of *CST5* silencing the p53-mediated repression of SNAIL protein was less pronounced than in cells transfected with control siRNAs. The same effect was observed on the level of mRNA expression (Fig. 50B).

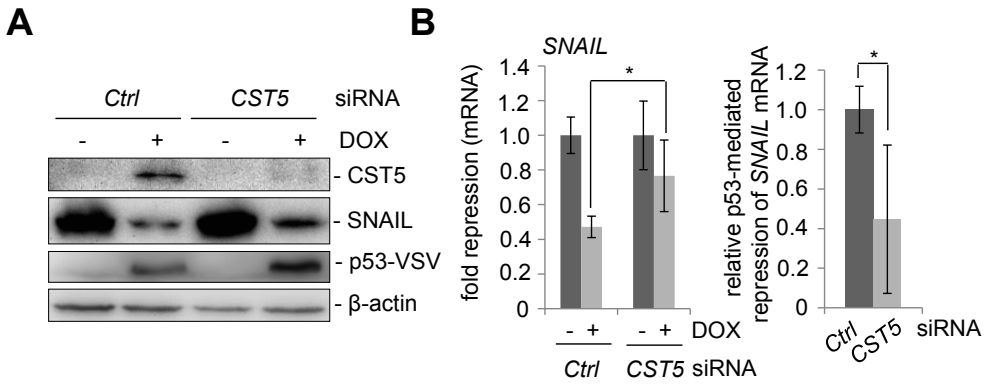

Figure 50: **Knock-down of *CST5* leads to reduced repression of SNAIL after ectopic p53 expression in SW480/pRTR-p53-VSV cells.** SW480/pRTR-p53-VSV cells were transfected with a *CST5*-specific siRNA or a control oligonucleotide for 72 hours and treated with DOX for the last 48 hours. (A) Western blot analysis of the indicated proteins. ß-actin served as a loading control. (B) The indicated mRNAs were measured by qPCR-analysis. *ß-actin* served as a normalization control. Fold changes represent mean values of triplicate analyses and error bars represent standard deviations. The relative p53-mediated repression of *SNAIL* is indicated. Error bars represent +/- SD (n = 3).

Subsequently, we determined whether down-regulation of *CST5* influences p53-mediated inhibition of cellular migration in a scratch/ wound-closure assay and in a Boyden-chamber assay (Fig. 51). When *CST5* was silenced by siRNAs, wound closure of SW480/pRTR-p53-VSV cells was generally less suppressed by p53 than in control cells (Fig. 51A, B). Also in a Boyden-chamber assay a reduction in the inhibition of migration by p53 after treatment with si*CST5* was observed (Fig. 51C). Taken together, these results show that the induction of CST5 by p53 contributes to the inhibition of migration by p53.

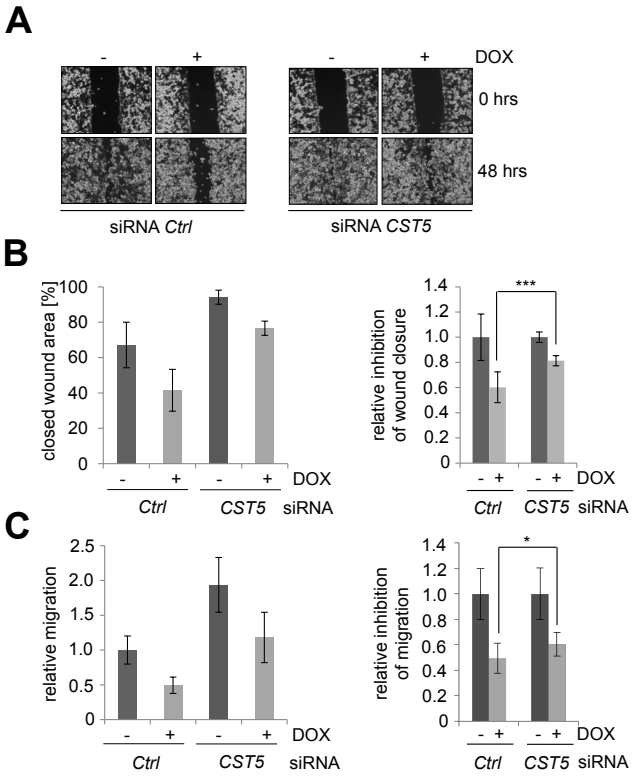

Figure 51: ***CST5* knock-down results in reduced repression of migration after ectopic expression of p53 in SW480/pRTR-p53-VSV cells.** Wound-healing assay using Ibidi-Inlets. (A) Representative pictures of the wound area obtained 48 hours after scratching. 100 x magnification. (B) Left: Average [%] of the closed wound area determined by the final width of the scratch in three independent wells. Right: The relative p53-mediated inhibition of wound-closure. (C) Boyden chamber-assay of cellular migration. Left: The relative migration through the filter with the untreated control set as one. Right: The relative p53-mediated inhibition of migration. (B, C): Error bars represent +/- SD (n = 3).

5.3.4 Combined treatment with calcitriol and DOX enhances *CST5* induction

Recently, the active metabolite of vitamin D3, calcitriol ($1,25(OH)_2D_3$), was shown to induce *CST5* expression in colorectal cancer cells [200]. To examine whether a combination of p53 activation and treatment with calcitriol leads to an enhanced *CST5* induction, we treated the colorectal cancer cell line SW480/pRTR-p53-VSV with DOX, calcitriol or both agents (Fig. 52).

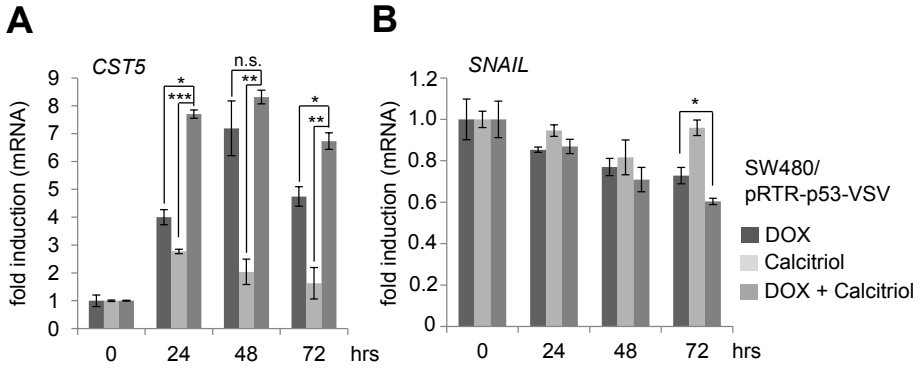

Figure 52: **p53 activation in combination with calcitriol treatment enhances CST5 induction on mRNA level.** SW480/pRTR-p53-VSV cells were treated with DOX, calcitriol or both agents for the indicated timepoints. (A) The indicated mRNAs were measured by qPCR-analysis. *β-actin* served as a normalization control. Fold changes represent mean values of triplicate analyses of DOX / calcitriol / DOX + calcitriol treatment versus vehicle treated cells normalized to β-*actin* expression. Error bars represent standard deviations (n = 3).

As shown before, induction of ectopic p53 expression led to a robust increase in *CST5* expression on mRNA level (Fig. 52). Calcitriol treatment alone resulted in a comparatively minor induction in *CST5* expression, whereas the combination of DOX and calcitriol led to significantly higher *CST5* mRNA levels when compared to single DOX or calcitriol treatments. Furthermore, CST5 protein induction was more pronounced after combined activation of p53 and the VDR when compared to addition of DOX or calcitriol alone (Fig. 53). In addition, the EMT transcription factor SNAIL displayed a stronger decrease on the mRNA and protein level after a combined treatment with DOX and calcitriol when compared to each stimulus alone (Fig. 52, 53).

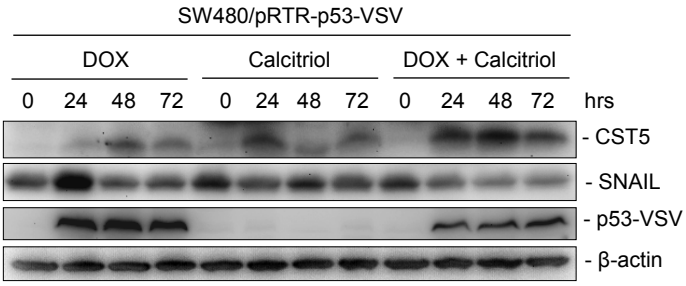

Figure 53: **p53 activation in combination with calcitriol treatment enhances CST5 induction on protein level.** SW480/pRTR-p53-VSV were treated with DOX, calcitriol or both agents for the indicated timepoints. Western blot analysis of the indicated proteins. β-actin served as a loading control.

5.3.5 Opposing regulation of *CST5* by SNAIL and VDR activation

Since we had observed that VDR activation via calcitriol results in the repression of SNAIL, we asked whether conversely SNAIL may directly or indirectly lead to repression of CST5 as part of a SNAIL-induced EMT program. Indeed, *CST5* mRNA levels decreased by up to 80% after induction of *SNAIL* by DOX treatment in SW480/pRTR-SNAIL-VSV cells (Fig. 54). Expectedly, *SNAIL* mRNA levels were up-regulated.

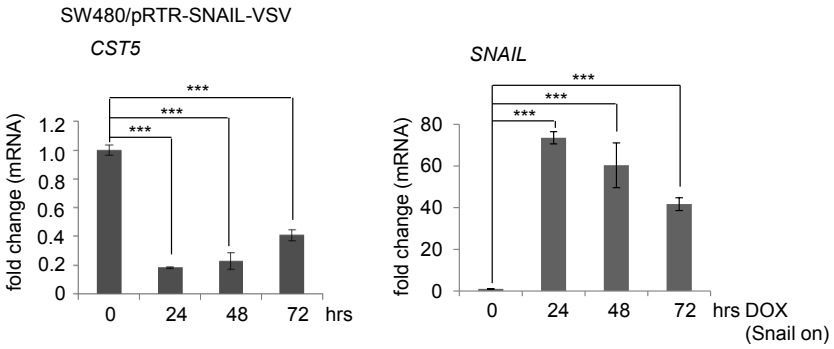

Figure 54: ***CST5* expression after SNAIL induction**. *CST5* and *SNAIL* mRNA levels were measured by qPCR analysis after treatment with DOX at the indicated time points in SW480/pRTR-SNAIL-VSV cells. Fold changes represent mean values of triplicate analyses after DOX treatment versus vehicle treated cells normalized to *β-actin* expression. Error bars represent standard deviations (n = 3). SW480/pRTR-SNAIL-VSV cells were generated by Dr. Helge Siemens.

To determine whether this repression is mediated directly by SNAIL occupancy at the *CST5* promoter, we inspected this region for E-boxes, which may mediate SNAIL binding. We identified several E-boxes upstream of the *CST5* promoter and confirmed the direct binding of SNAIL to an E-box, which is located 50 bp upstream of the *CST5* promoter, using qChIP analysis (Fig. 55A, B). The SNAIL binding site in the *E-cadherin/CDH1* promoter served as a positive control (Fig. 55B).

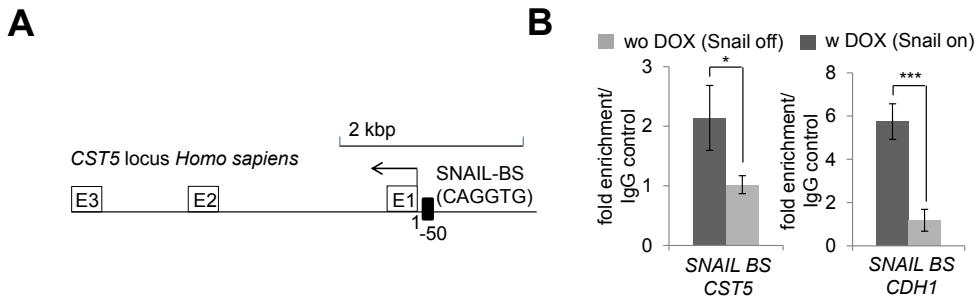

Figure 55: **SNAIL directly targets *CST5***. (A) Schematic SNAIL binding site 50 bp upstream of the *CST5* transcriptional start site. (B) qChIP analysis of DLD1/pRTR-SNAIL-VSV cells 24 hours after activation of SNAIL-VSV expression by addition of DOX using anti-VSV and anti-rabbit IgG for ChIP; this ChIP analysis was performed in unicates and measured in triplicates.

Next, we assessed the combined effect of SNAIL activation with calcitriol treatment in SW480/pRTR-SNAIL-VSV cells (Fig. 56). When ectopic SNAIL expression was combined with calcitriol treatment, *CST5* was no longer repressed by SNAIL but showed a five-fold induction. Treatment with calcitriol alone led to a robust induction of *CST5,* whereas *SNAIL* mRNA levels were not affected. Therefore, induction of *CST5* expression by VDR activation is dominant over its repression by SNAIL. This may at least partially explain the effect of vitamin D3 in the treatment of cancer.

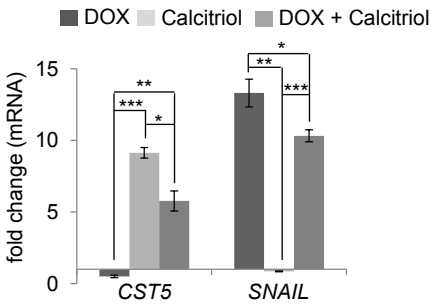

Figure 56: **Calcitriol treatment prevents SNAIL-mediated repression of *CST5***. *CST5* and *SNAIL* mRNA levels were measured by qPCR analysis after treatment with DOX, calcitriol or both agents at the indicated time points in SW480/pRTR-SNAIL-VSV cells. Fold changes represent mean values of triplicate analyses of DOX / calcitriol / DOX+calcitriol treatment versus vehicle treated cells normalized to *β-actin* expression. Error bars represent standard deviations (n = 3). SW480/ pRTR-SNAIL-VSV cells were generated by Dr. Helge Siemens.

6. DISCUSSION

6.1 p53-induced *miR-34* targets SNAIL to repress EMT and stemness

The miR-34 family, including *miR-34a/b/c*, were the first miRNA encoding genes that were shown to be directly induced by p53 [89, 90, 92-94]. Since then, a lot of different targets of miR-34a have been identified and validated [86, 96, 217]. As part of this thesis, we investigated the importance of miR-34 as a downstream effector of p53´s tumor suppressive functions and showed that the induction of MET by p53 is mediated by miR-34a. Additionally, we demonstrated that SNAIL is a direct miR-34a target and identified a double-negative feedback loop between miR-34 and SNAIL. The down-regulation of SNAIL shifted the cells towards an epithelial state and led to reduced expression of stemness factors. Furthermore, invasion and migration were down-regulated in a miR-34 dependent manner and the expression of stemness markers such as *BMI1*, *CD44*, *c-Myc*, *OLFM4* or *CD133* was decreased after ectopic miR-34 expression. Our findings are illustrated in Figure 57.

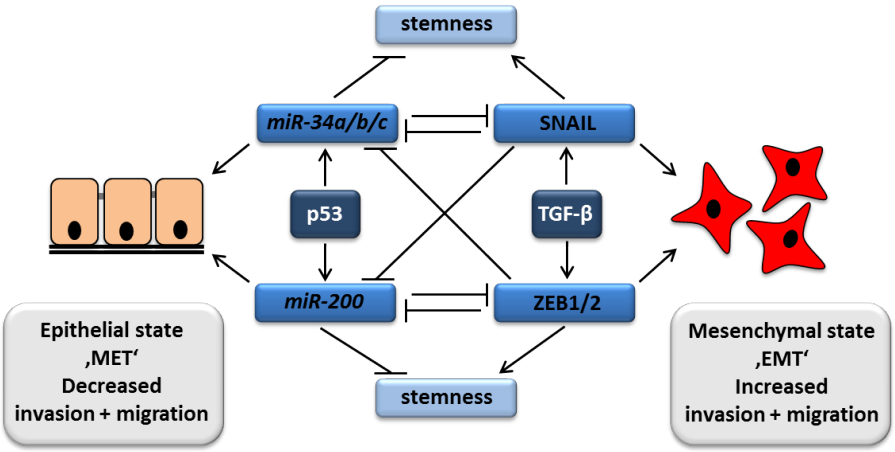

Figure 57: **Two double-negative feedback loops that control cellular plasticity.** Model of the findings published in [1] combined with previous results concerning the p53/miR-200/ZEB1/2 axis [97, 98, 245]. The p53-induced miRNAs miR-34a/b/c and miR-200 and the TGF-β induced transcription factors SNAIL and ZEB1/2 form a double-negative feedback loop to control EMT/MET and stemness.

The EMT-transcription factor SNAIL has been shown to be overexpressed in colorectal cancer and to be responsible for the enhanced invasive potential and self-renewal capacity of tumor initiating cells [295, 296]. It has been demonstrated in several studies that increased expression of SNAIL correlates with stemness features in different types of cancer [71, 180, 297-301]. Mani and colleagues demonstrated that high *SNAIL*-expression generates cells with stem cell-like properties by showing that the number of mammospheres increases along with *SNAIL* expression in

immortalized mammary epithelial cells [180]. Furthermore, colonospheres that were derived from a colorectal tumor, showed high expression of the EMT-transcription factor *SNAIL* and increased formation of colonospheres was seen in human colorectal carcinoma cell lines when SNAIL was ectopically expressed indicating that SNAIL regulates stem cell-like activites of cancer cells [302]. In addition, high nuclear SNAIL expression was observed in the stem cell niche of the murine small intestine [303]. By showing that miR-34 directly regulates *SNAIL* expression we unravelled a new mechanism that explains how miR-34 expression leads to reduced stemness properties in colorectal cancer cells.

Apart from SNAIL, multiple miR-34 targets were shown to be involved in stemness regulation. It has been demonstrated that miR-34a directly targets *Notch1* in colorectal cancer stem cells [304]. The authors report that a bimodal switch between miR-34a and Notch1 decides between a symmetric or asymmetric cell division and therefore leads the cells towards self-renewal or differentiation. Differentiated cells are characterized by increased miR-34a- and low Notch1-expression levels whereas colorectal cancer stem cells show the opposite pattern, i.e. low miR-34a- and high Notch1-levels. Furthermore, it has been reported that miR-34a represses the receptor tyrosine kinase *c-Kit* which leads to reduced stemness and migration in colorectal cancer cells [305]. Additionally, miR-34a was shown to repress *ZNF281,* which was demonstrated to promote EMT in colorectal cancer cells [5]. Moreover, the stemness marker *CD44* was shown to be directly targeted by miR-34a [250].

Apart from the direct repression, there are several indirect ways as to how miR-34 might negatively affect *SNAIL* expression. *miR-200c* was shown to be repressed by SNAIL and to directly target the polycomb repressor *BMI1* [181]. Consequently, miR-34a-mediated down-regulation of *SNAIL* might lead to increased miR-200c levels and reduced expression of *BMI1*. Moreover, SNAIL functions might be affected by HDAC1 that was recently described as a miR-34a target and as a cofactor of SNAIL in E-cadherin repression [217, 306, 307].

Besides down-regulating stemness factors and inhibiting EMT, miR-34 controls numerous other cancer-relevant pathways and processes. It has been demonstrated that miR-34 negatively affects cell cycle progression, enhances apoptosis and regulates the metabolic switch to aerobic glycolysis also known as the Warburg effect (reviewed in [96]). SNAIL-mediated repression of miR-34, may therefore not only lead to enhanced invasion, migration and stemness features but also to a loss of cell cycle control, enhanced aerobic glycolysis and decreased apoptosis.

Apart from miR-34, p53 controls EMT and stemness via multiple miRNA-mediated regulations including miR-145, the miR-200 family and miR-15a/16-1 [97, 110, 308]. Furthermore, mutant p53 was shown to gain oncogenic functions by inducing miR-130b, a repressor of ZEB1, to promote mesenchymal traits [309].

Besides miRNA-mediated regulations, p53 has been shown to regulate invasion via the MDM2-mediated degradation of SLUG in non-small cell lung cancer [248]. The authors showed that mutant p53 represses MDM2 expression which results in increased SLUG levels. Similar to this finding, p53 decreases SNAIL protein levels via MDM2-mediated proteasomal degradation [310]. Moreover, CXCR4, a chemokine receptor that is involved in metastasis of breast cancer cells, was shown to be repressed by p53 [311].

Similar to our results, a double-negative feedback loop between the p53-controlled miR-200 family and the EMT transcription factors ZEB1 and ZEB2 was already described [97, 98, 245]. Based on a bioinformatically derived hypothetical model, Lu and colleagues suggested that the determination of a mesenchymal, epithelial or a mixed phenotype mainly depends on these two highly interconnected circuits, the miR-34/SNAIL and the miR-200/ZEB1/2 double-negative feedback loops [312]. They proposed that the miR-200/ZEB1/2 circuit acts as a ternary switch between the three phenotypes and that the miR-34/SNAIL loop functions as a module integrating internal and external signals. In addition, another double-negative feedback loop between SNAIL and the tumor suppressive miR-203, which is post-transcriptionally induced by p53 through p53´s interaction with the Drosha complex [126], was shown to regulate EMT [313]. Moreover, the p53-target miRNAs miR-15a/16-1 have recently been demonstrated to directly suppress the c-MYC induced EMT-transcription factor AP4, that was shown to directly induce the expression of SNAIL and to repress miR-15a/16-1 expression [109, 110, 220]. The present results add another p53-controlled and miRNA-mediated negative feedback loop to the complex network of p53´s transcriptional control and suggest that a loop-like regulation of gene expression is a mechanism widely applied by miRNAs and their respective targets.

The described double-negative feedback loops demonstrate the importance of epithelial-mesenchymal plasticity. First, tumor cells need to undergo EMT in order to disseminate from the tumor, intravasate into the lymph or bloodstream and extravasate at a distant site. However, once settled down in a distant organ, cancer cells regain epithelial traits during mesenchymal-epithelial transition, a process necessary to proliferate and build micro- and macrometastases [174, 182, 295, 314]. It has been reported that the same epithelial-like pattern was found in primary colorectal carcinomas and the corresponding metastases which further confirms that MET is implicated in metastasis formation [315]. Additionally, cells that have undergone EMT and express high levels of the EMT transcription factor SNAIL, show decreased proliferative potential with a partial G1/S cell cycle arrest [316, 317].

Among the important EMT transciption factors ZEB1/2, TWIST, SLUG and SNAIL, the latter is so far the only EMT regulator that is directly targeted by miR-34. However, miR-34 may indirectly influence the expression of the described miR-200 targets *ZEB1/2* and *SLUG* via the repression of *SNAIL*: miR-34 targets *SNAIL* which

results in a derepression of miR-200. Subsequently, increased miR-200 levels might lead to the repression of *ZEB1/2* and *SLUG*.

Due to its diverse tumor suppressive functions it is not surprising that the miR-34 family is permanently inactivated by epigenetic silencing in different tumor types [318-320]. In colorectal cancer, CpG methylation leads to silencing of *miR-34b/c* in 99% and of *miR-34a* in 74% of the studied 114 cases [320]. The authors report a significant correlation between *miR-34a* methylation and the absence of p53 mutations in colorectal cancer. Recently, epigenetic inactivation of *miR-34a* in combination with elevated SNAIL, c-Met and β-catenin expression has been shown to be strongly associated with liver metastasis in colon cancer [321]. In addition to epigenetic silencing, *miR-34a* resides on a chromosomal locus that is frequently deleted in neuroblastoma and other tumor types [322]. This frequent loss or constriction of miR-34´s function as a tumor suppressor further substantiates the need and importance for establishing a miRNA replacement as a potential therapeutic approach in the clinic. Indeed, treatment with miR-34a mimics was successful in several preclinical studies [323-325]. Recently, treatment with a liposome based miR-34 mimic, MRX34 (developed by Mirna Therapeutics), led to decreased tumor burden in two orthotopic mouse models of liver cancer after tail-vein injection and subsequently entered clinical phase I studies in patients with advanced hepatocellular carcinoma [326, 327].

6.2 Genome-wide analysis of the p53-induced transcriptome and proteome

The genome-wide screen performed here led to the identification of a number of p53-regulated targets including miRNAs, lncRNAs, mRNAs and proteins (summarized in Figure 58).

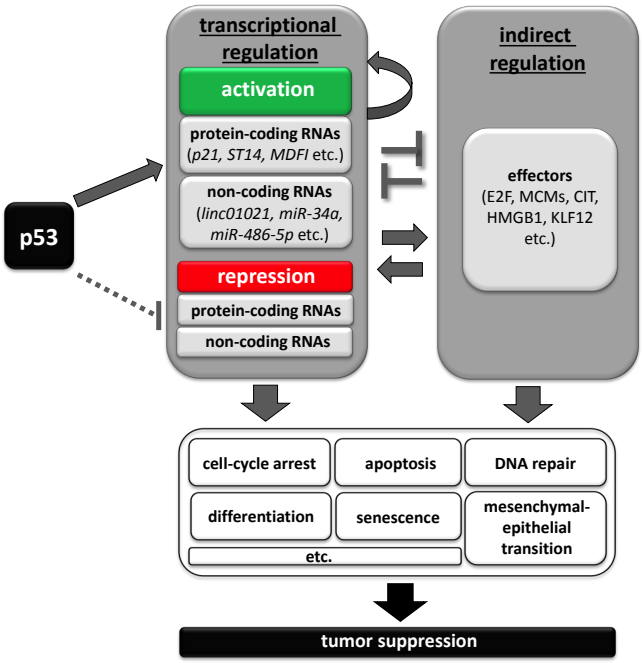

Figure 58: **Schematic model of effector pathways that mediate tumor suppression by p53.** Upon activation, regulates the transcription of mRNAs that encode proteins and/or non-coding RNAs, such as miRNAs and lncRNAs. p53 mainly acts as a transcriptional activator and to a minor extent as a transcriptional repressor. In addition, p53 indirectly regulates numerous effectors, for example E2F or MCM complex components via its direct target genes, such as *p21* and *miR-34a*. Moreover, there is extensive crosstalk between direct and indirect p53 targets. The differential expression of direct and indirect p53 targets leads to the induction of specific cellular processes, such as cell-cycle arrest, apoptosis or mesenchymal-epithelial transition, which supress tumor progression. Figure from [2].

We found that the majority of the down-regulated genes show no promoter-proximal p53 binding, which indicates that they must be regulated via indirect, for example miRNA-mediated mechanisms. This result is similar to the findings of a previous study, which reported that only ~15% of the known and validated p53 binding sites are linked to transcriptional repression [60]. Several genome-wide screens have been conducted in the past to identify p53-regulated gene expression [65, 268, 272, 273, 328, 329]. Similar to our results, more induced than repressed genes displayed promoter-proximal p53 binding [65, 204, 268, 273]. Similar to our results, Nikulenkov and colleagues showed that the p53 binding motif associated with up- and down-regulated target genes only showed minor differences [65]. A recent computational meta-analysis based on the results of several genome-wide studies even reported that p53 binding to its consensus elements only results in transcriptional activation and that transcriptional repression by p53 solely occurs via indirect mechanisms [204]. The authors re-analyzed different p53 targets that were

reported to be repressed via direct p53-binding but could not confirm these results. Furthermore, they showed that indirect p53-mediated repression mainly occurs via p21-DREAM and E2F/RB complex formation at promoters.

Our results demonstrate that the consensus binding motif of the GATA1 transcription factor is present in a significant number of p53-bound and up-regulated genes. Transcription factors of the GATA family activate and repress transcription of their targets and are known to have both, oncogenic and tumor-suppressive functions (reviewed in [330]). GATA1, for example, is known to control erythroid-specific genes but has also been observed to control cellular proliferation by silencing the proto-oncogenes *Kit*, *Myc* and *Myb* during erythroid maturation [331-333]. However, GATA1 may interact with the transactivation domain of p53 to inhibit p53´s function [334] and activate the expression of the anti-apoptotic gene Bcl-xL in erythroid cells [335]. Furthermore, the GATA1 motif is enriched near p53 REs in response to genotoxic stress [272]. In addition, GATA3 has opposing functions that seem to be highly context-dependent. It partly reverses EMT in a breast cancer cell line by inducing E-cadherin and inhibiting N-cadherin and vimentin [336], but may indirectly increase the expression of *Myc* [337]. How GATA1 binding in the vicinity of p53 binding sites of induced genes influences their expression needs to be further investigated. Another study showed that distal enhancer-activity might be important for p53-mediated repression in mouse embryonic stem cells [338]. This shows that in addition to direct binding of p53 to p53 response elements, many other indirect mechanisms are relevant for p53-mediated gene repression (reviewed in [60]).

The results presented here indicate that besides p53-mediated repression via direct binding to p53 response elements, many other indirect e.g. miRNA-mediated mechanisms are relevant for p53-mediated gene repression (reviewed in [60]). In fact, different examples of miRNA-mediated gene repression by p53 are known [339]. By directly inducing miR-34a, p53 down-regulates genes with oncogenic functions like *SNAIL* [1, 98] or *ZNF281* [5], thereby inducing MET (mesenchymal-epithelial transition). Moreover, our data indicate that the p53-mediated transcriptional repression may involve a combination of different mechanisms as shown in this study for the known miR-34a target *MTA2* [217]. Apart from the miRNA-mediated repression by miR-34a, *MTA2* also shows p53 occupancy in the vicinity of its transcriptional start site that may additionally mediate its repression. This indicates that the different mechanisms for p53-mediated repression are not mutually exclusive. This is also in accordance with previous studies showing that *c-Myc* is repressed by direct transcriptional repression by p53 as well as by miRNA-mediated mechanisms of the p53-induced miRNA miR-145 [68, 106].

In our study we confirmed several p53 target genes that were already described to be directly regulated by p53, such as *CDKN1A*, *BAX*, *DDB2*, *RPS27L*, *RRM2B* or *SERPINE1.* However, some known p53 target genes were not detected in our study. Since p53 target genes have different expression kinetics [340, 341], some direct

targets might not have been detected at the specific time point selected in this study. Moreover, pSILAC might not detect all cellular proteins since insufficient labelling with Arg and Lys misses certain proteins.

Moreover, we detected several new p53-regulated miRNA-, lncRNA and protein-encoding genes. We identified *miR-486* as a direct p53-induced target gene. This potentially tumor-suppressive miRNA has been shown to target the stem cell marker *OLFM4* in gastric cancer [342] and *ARHGAP5*, a protumorigenic member of the RhoGAP family, in lung cancer [263], thereby negatively regulating tumor progression. In addition, miR-486-5p was shown to target *PIM-1* in breast and lung cancer cells suppressing cell proliferation [343, 344]. Moreover, miR-486-5p is down-regulated in hepatocellular carcinoma where it suppresses tumor growth by down-regulating p85α [345]. In addition, we detected miR-205 to be directly induced by p53. Recently, miR-205 was described as a p53-induced miRNA in a breast cancer cell line and a p53 RE 1 kbp upstream of the pre-miR genomic sequence was suggested [262]. Additionally, miR-205 was shown to inhibit EMT by targeting *ZEB1* and *ZEB2*/*SIP1* [97]. Here we identifed a p53 binding sequence 17 kbp upstream of the *miR-205* host gene in the colorectal cancer cell line SW480 and validated p53 occupancy at this motif.

Furthermore, we identified several putatively p53-regulated lncRNAs and determined an anti-proliferative effect of the newly identified p53 target *LINC01021*. In addition, the lncRNA *lnc-H6PD-1* (*RP3-510D11.2*), which is transcribed from the *miR-34a* promoter but in the opposite direction than *MIR-34a*, was induced and directly bound by p53 at its promoter after p53 activation. This type of regulation is similar to the recently identified *lincRNA-p21*, which is located upstream of the p53 target gene *p21*/*CDKN1A* [153].

A recent genome-wide analysis unveiled a p53-specific lncRNA tumor suppressor signature in a colorectal cancer cell line [346]. The authors show that 18 different lncRNAs are transcriptionally controlled by p53 and demonstrate that two out of those lncRNAs contribute to p53´s ability to bind to some of its target genes. However, there is no overlap with our results, presumably due to different approaches and cell lines that were used. Several studies revealed that lncRNAs have important functions during tumorigenesis [347]. Moreover, lncRNAs offer an important advantage over protein-coding genes: they show a highly tissue- and tumor type-specific expression pattern suggesting that they may represent superior biomarkers. For example, the lncRNAs *PCA3* and *HULC* are used for the detection of prostate and hepatocellular carcinoma, respectively [348-350]. lncRNA-based therapies are only in the early steps of development and far from a clinical use. RNAi-based therapies targeting protein-coding mRNAs are currently tested in clinical trials and could potentially be applied for non-coding RNAs as well [351, 352]. Additionally, antisense oligonucleotides or (deoxy-) ribozymes might be applied for targeting lncRNAs in case a siRNA-targeted approach is not applicable due to an

intensive secondary structure or an unfavourable nucleotide sequence of the lncRNA [353].

In addition to non-protein coding genes, we identified numerous protein-coding direct p53 target genes. Several of the detected genes have known tumor suppressive functions: RASAL1 for example, a transcriptional target of the tumor suppressor PITX1, suppresses RAS activity in colon cancer cells [354]. In addition, decreased RASAL1 protein levels are associated with colorectal cancer progression [355]. Moreover, *RASAL1* is hypermethylated in gastric and thyroid cancer and its overexpression inhibits the proliferation and transformation ability of gastric cancer cells [356-360]. Recently it was shown that RASAL1 inhibits gastric carcinogenesis in nude mice by blocking RAS/ERK signaling [361]. Moreover, we identified and confirmed *ST14* as new p53 target gene. ST14 was shown to exert tumor-suppressive functions in inflammation-associated colon carcinogenesis [362]. In addition, ST14 exerts an inhibitory effect on cell growth in human breast cancer cells [363]. *MDFI,* which was also experimentally confirmed as a new p53-regulated target gene in this study, is a candidate tumor suppressor gene that is highly methylated in colorectal cancer and pancreatic adenocarcinoma [364, 365]. Furthermore, we identified *DHRS2*, which encodes a mitochondrial protein that – similar to p14ARF – inhibits MDM2 which leads to the stabilization of p53 [366]. Another new p53 target, *DENND2D*, inhibits proliferation and tumorigenicity of non-small cell lung cancer and is hypermethylated in hepatocellular and squamous cell carcinoma [367-369]. The identified p53-regulated gene *TGFBI* seems to have opposing functions in different tumor types. In mesothelioma and breast cancer it is associated with tumor suppression [370, 371]. In addition, it decreases the metastatic potential of lung and breast cancer cells [372] and its expression positively correlates with a better response to chemotherapy in non-small cell lung cancer [373]. Moreover, *TGFBI* was shown to function as a tumor suppressor in mice [374]. However, *TGFBI* expression promotes metastasis and is associated with poor prognosis in colorectal cancer patients [375, 376] and induces invasion in melanoma cells [377]. *LOXL4*, which was up-regulated and directly bound by p53, is hypermethylated in human bladder cancer [378] but has tumor-promoting functions in gastric, breast and head and neck cancer [379-382]. Furthermore, *LRIG3* inhibits growth and invasion in bladder cancer cells but promotes cell cycle arrest and apoptosis in glioma cells [383-385].

We also detected a small number of directly regulated p53 target genes that showed decreased expression on the level of *de novo* protein synthesis after p53 activation. One of these genes was *NELL2.* Interestingly, *NELL2* has cancer-promoting functions in human breast cancer cells and is transcriptionally regulated by E2F1 [386]. Moreover, *NELL2* is a target of miR-22, which is induced by vitamin D3 and inhibits proliferation and migration [387]. Another down-regulated direct target identified in this study, Neuropilin-2 (*NRP2*), is up-regulated in lung cancer cells [388], promotes EMT in colorectal cancer cells [389] and was also shown to

contribute to tumorigenicity *in vivo* [390]. *FGF9,* which was down-regulated and showed promoter-proximal p53-binding in our study, is overexpressed in colon cancer cells and is associated with EMT in prostate cancer cells [391, 392]. Moreover, *FGF9* expression positively correlates with poor prognosis in non-small cell lung cancer patients [393].

In addition to direct targets, we identified many indirect target genes that are predicted to be regulated by one or several of the miRNAs directly induced by p53. We confirmed that *HMGB1* is down-regulated by the p53-inducible miR-205. *HMGB1* promotes invasion, metastasis and angiogenesis in different cancer types, inhibits antitumor immunity and represents a possible cancer therapeutic target [394-396]. Furthermore, p53 interacts with the transcription factor CTF2 and thereby indirectly down-regulates *HMGB1* expression [397]. Furthermore, it has been shown that direct molecular interactions between *HMGB1* and p53 regulates the balance between apoptosis and autophagy in colorectal cancer cells [398]. In *p53-/-* cells, *HMGB1* is required for autophagy and knockdown of *HMGB1* results in increased apoptosis and decreased autophagy. Because autophagy is important for resistance to chemo- and radiation therapy, HMGB1 might represent an attractive therapeutic target in p53-deficient cells [399]. In addition, *HMGB1* is targeted by the p53-inducible miR-200c and miR-34a in breast cancer [400] and retinoblastoma cells [284], respectively. Here we provide an additional mechanism as to how *HMGB1* expression may be down-regulated by p53 via miRNA-mediated mechanisms.

In addition, the miRNA-34a/205 target *KLF12* emerged as an interesting candidate for a use as a prognostic marker. Interestingly, ectopic expression of *KLF12* promotes invasion, whereas its knockdown results in a growth arrest in human gastric cancer cells. Therefore, KLF12 may have oncogenic functions in gastric cancer progression [401].

Furthermore, we confirmed that CIT is down-regulated by the p53-inducible miR-486-5p. It was shown before that knock-down of CIT in hepatocellular carcinoma cells significantly inhibits proliferation [402]. In addition, *CIT* induces cell growth in prostate cancer cells [403] and is highly expressed in ovarian carcinoma [404]. In a recent study, CIT was shown to phosphorylate the GLI2 transcription factor, thereby activating a non-canonical hedgehog/GLI2 transcriptional program to promote breast cancer metastasis [405]. Therefore, loss of p53-mediated suppression of CIT may promote tumor formation. Moreover, the serine/threonine kinase CIT is an attractive candidate for therapeutic inhibition by small molecules as previously shown for other serine/threonine kinases [406].

Because p53 is inactivated late during colorectal cancer progression [407], increased expression of *HMGB1*, *KLF12* and *CIT* in advanced tumor stages and/or in different tumor types in the TCGA and Oncomine databases is in accordance with our findings. It also suggests that miRNA replacement may be used as therapeutic approach to treat advanced cancer in the future (as discussed for miR-34 in 6.1).

This thesis shows that p53 controls diverse tumor suppressive targets in colorectal cancer cells. Therefore, the pharmacological reactivation of p53 function in tumor cells, where p53 is mostly mutated or inactivated, might be an attractive strategy for cancer therapy [11-14, 17]. There are several approaches trying to find specific and efficient ways to reactivate either wild-type or mutant p53. Activators of wild-type p53, such as the small molecules Nutlin or RITA (Reactivation of p53 and Induction of Tumor cell Apoptosis), antagonize the function of MDM2 to prevent p53 ubiquitination and degradation [247, 408, 409]. Moreover, APR-246 and PRIMA-1 restore the wild-type conformation of mutant p53 and APR-246 has been tested recently in a phase I/II clinical trial in patients with refractory hematologic malignancies and prostate cancer [410, 411].

Several quantitative mass spectrometry-based proteomic studies after p53-mediated regulations have been conducted previously [412-414]. An amino acid-coded mass tagging (AACT)-assisted mass spectrometry approach identified 417 different proteins and revealed several pathways involved in p53-induced apoptosis in DLD-1 cells transfected with an inducible p53 construct [412]. In addition, an ICAT (isotope-coded affinity tag) quantitative mass spectrometry analysis identified 46 proteins that show differential expression after infrared radiation [413]. A recent iTRAQ (isobaric tag for relative and absolute quantitation) proteomics screen identified 78 unique proteins that showed expression changes upon Nutlin treatment in MCF7 cells [414]. However, pSILAC with its advantages to study *de novo* protein synthesis and to detect modest changes in protein expression typical for miRNA-mediated effects was never applied before to study differential protein expression after p53 activation. The current p53 pSILAC study allowed us to identify more than 1,000 significantly and differentially regulated proteins after ectopic p53 expression. We have recently applied pSILAC after ectopic expression of miR-34a in colorectal cancer cells to comprehensively identify miR-34a-targets [217]. As observed after miR-34a activation, changes in mRNA expression correlated with those in protein expression after p53 activation. Surprisingly, only four out of 36 putative miR-34a targets that were down-regulated in the miR-34a pSILAC screen were also identified as down-regulated proteins after p53 activation. This indicates that activation of p53 has numerous other effects on protein expression in addition to the activation of miR-34a. Known miR-34a targets might be targeted by other p53-regulated genes which results in a gene expression pattern different to the one observed after miR-34a activation alone. Furthermore, p53 might induce competitive endogenous RNAs (ceRNAs) functioning as miRNA sponges, which may attenuate target repression by miR-34a [415].

However, we found that a large number of the proteins down-regulated in the miR-34a pSILAC analysis were also down-regulated after ectopic expression of p53, including almost all members of the MCM protein family, which are important for the initiation of DNA replication. Interestingly, the E2F1 transcription factor binding

motif was overrepresented in the promoters of genes encoding the proteins down-regulated by both, miR-34a and p53. MCM proteins are induced by the E2F transcription factors, which are known targets of miR-34a [95, 218, 276, 277, 279]. Taken together, this suggests that, in addition to p21-mediated suppression of E2F [416], miR-34a-mediated inhibition of the E2F pathway contributes to the cell cycle arrest induced by p53 via down-regulation of MCM proteins.

E2F transcription factors are downstream targets of the retinoblastoma protein. Since mutations in the RB pathway occur in nearly all human cancers, E2Fs might play a significant role in oncogenesis [417]. However, E2Fs are known to act as both, tumor suppressors and oncogenes in a probably context-specific manner [418]. Nikulenkov and colleagues found that the E2F response element is enriched in the vicinity of p53-binding sites of repressed genes [65]. They stated that the transcription factors E2F and IRF cooperate with p53 to mediate gene repression and that p53 interferes with STAT3-mediated activation of genes by occupying overlapping binding sites at several promoters. Another study also confirmed that genes repressed by p53 are enriched for E2F binding sites [204].

In conclusion, our results indicate that p53 indirectly down-regulates a large number of genes via the activation of miRNAs. The results add new insights into the p53-regulated network of gene expression. Furthermore, our results will promote further studies by providing numerous p53-regulated molecules and pathways that represent attractive candidates for biomarkers and/or therapeutic targets.

6.3 The p53 target gene *CST5* mediates in part p53´s tumor suppressive functions

The third part of this thesis describes the characterization of cystatin D (*CST5*), an inhibitor of cysteine cathepsins, as a new p53 target gene that was identified in the genome-wide screen described in 5.2. Our findings combined with previous results are summarized in Figure 59.

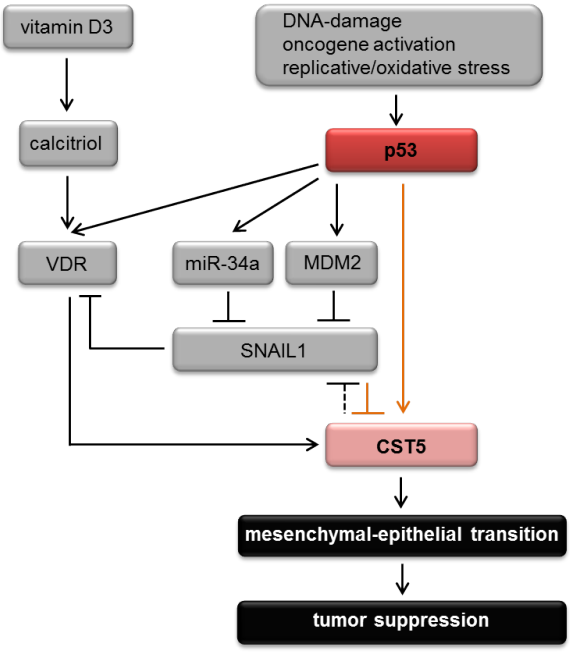

Figure 59: **The p53 - vitamin D3 - CST5 regulatory network.** Schematic model of *CST5* regulation integrating the results of this study (marked with orange arrows) with previous findings (marked with black arrows Vitamin D3, that is converted to its active metabolite calcitriol, induces *CST5* via the vitamin D receptor (VDR) [200]. In addition, p53 positively influences *CST5* expression via different pathways. p53 directly binds to a p53 binding site upstream of the *CST5* promoter. Furthermore, p53 directly induces VDR which might lead to the induction of *CST5* [294]. And third, p53 indirectly represses SNAIL expression which results in the induction of *CST5* [1, 178, 310]. Moreover, *CST5* expression indirectly leads to the repression of SNAIL by inhibiting the transcriptional activity of β-catenin/TCF complexes [200]. Upon induction, CST5 promotes mesenchymal-epithelial transition to suppress tumor progression and metastasis. Figure from [3].

Individual cysteine cathepsins were shown to have diverse cancer promoting roles during tumorigenesis [419, 420]. Especially cathepsin B plays an oncogenic role and is overexpressed in a variety of human tumors [421]. Cathepsins are up-regulated in various tumors due to different mechanisms including gene amplification, posttranscriptional- and epigenetic-regulation, as well as transcript variants that arise from alternative promoters and alternative splicing (reviewed in [422]). Several studies show a positive correlation between increased cathepsin expression and poor outcome for cancer patients [423, 424]. Cathepsins often change their subcellular localization during cancer progression. In normal cells they are located in lysosomes. During tumorigenesis they are relocated to the cellular surface and secreted into the extracellular milileu [422]. A multistep process

chronologically integrating different members of the cysteine cathepsin family was characterized in a cancer mouse model of pancreatic islet cell tumors [419, 425]: In the beginning, cathepsins B and S contribute to the release of pro-angiogenic factors and the degradation of the basement membrane, followed by the expression of cathepsins C and Z that are in part responsible for the exponential tumor growth. In later tumor stages, cathepsins H and L contribute to invasive tumor growth by the degradation of the basement membrane, extracellular matrix and the directed proteolysis of specific targets on the cell-surface, such as E-cadherin. Recently, this proposed model was tested using cathepsin B, S, L and C knockout mice [426]. This study revealed that cathepsin B/S knockout mice show reduced tumor formation and angiogenesis, while cathepsin B/L knockout mice display decreased cell proliferation and tumor growth. However, knockout of cathepsin C did not affect tumor formation and progression.

Different members of the cystatin family of protease inhibitors are known to inhibit the protumorigenic actions of cathepsins. Cystatin M exerts tumor-suppressive effects by inhibiting cell proliferation, migration and invasion in breast cancer cells and is epigenetically silenced in breast cancer [427-429]. In addition, silencing of cystatin M leads to increased cell proliferation and invasion in an oral cancer cell line [430]. Overexpression of cystatin C results in decreased invasion and metastasis and leads to increased apoptosis in melanoma and squamous carcinoma cells [431-434]. Cystatin D (*CST5*), an endogenous inhibitor of cathepsins S, H and L, was recently demonstrated to exert tumor-suppressive functions in colon cancer cells and to be directly induced by calcitriol [183, 187, 200]. The underlying mechanisms as to how cystatin D exerts its functions are unclear. The use of cystatin D proteins with a mutated proteolytic site revealed that the inhibition of proliferation and down-regulation of c-MYC were independent of cathepsin-suppression and rather mediated by the repression of the Wnt/β-catenin pathway by cystatin D. However, the induction and repression of mesenchymal and epithelial markers, respectively, and the decrease in migration were supposed to be cathepsin-dependent. This is in accordance with the finding that cathepsin L, one of the targets of cystatin D, cleaves E-cadherin [426]. Furthermore, it was demonstrated that *CST5* expression negatively correlated with human colon cancer progression in tumor tissue [200]. By showing that p53 directly induces the expression of *CST5* we uncovered a new mechanism as to how p53 indirectly inhibits tumor development and growth.

During the last years there has been increasing evidence that vitamin D3 deficiency is protumorigenic, especially since it enhances colorectal cancer incidence and mortality. In addition to convincing effects of vitamin D3 in *in vivo* and *in vitro* studies, data from several preclinical and clinical trials provide evidence for the anti-tumoral effects of vitamin D3 supplementation (reviewed in [187]).

Vitamin D3 deficiency is a worldwide problem [435]. It is caused by reduced sunlight exposure due to the fear of developing skin cancer, increased skin pigmentation, the use of sunscreen or the living in northern latitudes [436-438]. Moreover, vitamin D3 deficiency increases along with aging and obesity [439, 440]. Given that there is strong evidence that vitamin D3 decreases the risk for colorectal cancer, it would be an easy and economical way to reduce colorectal cancer incidence and risk by supplementation of vitamin D3 [435].

Our results suggest that p53 activation might even enhance the oncosuppressive effect of vitamin D3. A combination of small molecules reactivating p53 such as PRIMA or RITA [441] together with calcitriol - or an analog like EB1089 to avoid hypercalcemia - might potentially lead to an enhanced inhibition of cancer progression in the clinic. The VDR is highly expressed in early stages but shows decreased expression in advanced stages of colorectal tumorigenesis [192, 195, 442-444]. Also the occurrence of p53 mutations is a late event in colorectal cancer development which is mostly observed during the transition from adenoma to carcinoma [407]. Therefore, a combination of p53 activation and calcitriol treatment might be more important to prevent tumor initiation or early progression. At later stages, reactivation of the wild-type p53 conformation may inhibit tumor progression via preventing the interaction of mutant p53 with VDR [445].

Similar approaches combining calcitriol with different known anti-cancer agents to achieve an enhanced anti-tumorigenic effect have been conducted in several *in vitro* and *in vivo* analyses, and provide an opportunity for successful anticancer treatment when chemotherapy alone is not effective [186]. Combined treatment with calcitriol and the chemotherapeutic docetaxel significantly enhanced overall survival and time to progression in prostate cancer [446]. In addition, the combination of calcitriol and docetaxel reestablished the sensitivity to chemotherapy in prostate cancer patients that showed no inhibition of tumor growth after first line chemotherapy [447].

Cystatin D is not the only cystatin that is induced by calcitriol: cystatin E/M was identifed as a target of the VDR in squamous carcinoma cells and shows decreased expression in breast cancer [428, 429, 448, 449]. Furthermore, cystatin A is induced by calcitriol addition in normal keratinocytes [450]. Besides cystatins, VDR regulates a large set of target genes upon calcitriol binding [451, 452]. The intracellular modulator of EGFR, SPROUTY-2, is negatively regulated by calcitriol-bound VDR [451]. In xenografted colorectal cancer tumors, SPROUTY-2 is overexpressed and shows an inverse expression to CDH1 [453]. In addition, several proteins implicated in the epigenetic control of gene expression are regulated by calcitriol-bound VDR. The histone demethylase JMJD3, that exerts anti-proliferative, pro-differentiative and MET-like effects in colon cancer cells, is induced by VDR after calcitriol treatment [454-456]. In addition, miRNAs have been shown to be under the control of the VDR in calcitriol-treated colon cancer cells [387]. Especially miR-22 was demonstrated to

be important for mediating calcitriol´s anti-proliferative and anti-migratory effects in those cells. This shows that VDR acts via various targets to effectively function as a tumor-suppressive transcription factor.

Our study showed that SNAIL directly suppresses *CST5* expression and that calcitriol treatment counteracts this effect. It has been shown that SNAIL directly represses *VDR* which might contribute to the inhibition of *CST5* [457], but direct binding of SNAIL to the *CST5* promoter, as shown here, has not been demonstrated before. The abrogation of SNAIL-mediated repression of *CST5* by calcitriol treatment may explain how calcitriol inhibits tumor progression even in cells that show high SNAIL-expression and therefore have a high metastatic potential. It was previously demonstrated that p53 inhibits the EMT-TF SNAIL via the induction of MDM2, which mediates ubiquitylation and proteasomal degradation of SNAIL [310]. Moreover, others and we have shown that p53 mediates the inhibition of SNAIL via the induction of miR-34a [1, 178]. Based on our findings, p53 therefore not only directly induces CST5 expression but also enhances *CST5* expression by the indirect repression of SNAIL.

Taken together, we identified *CST5* as a new direct p53 target gene, which is relevant for the tumor suppressive function of p53. Due to its diverse anti-cancer functions and decreased expression during colorectal cancer tumorigenesis [200], which is reversible by p53 and/or VDR activation, CST5 might be an important therapeutic target in the treatment of colorectal cancer.

7. SUMMARY

p53 is one of the most important tumor suppressors and was found to be mutated or inactivated in more than half of all human tumors. As a transcription factor p53 controls the expression of target genes that are involved in processes such as the regulation of cell cycle arrest, DNA repair or apoptosis and thereby prevents the development and the spreading of cancer. Though extensive research led to the identification of a lot of p53-regulated target genes, the list of p53 targets still continues to grow and seems to be far from complete.

Here, we showed that p53 controls the EMT transcription factor SNAIL via the induction of miR-34 in colorectal cancer cells. This regulation shifted the cells towards an epithelial phenotype and inhibited migration, invasion and stemness features. In addition, we demonstrated a double-negative feedback loop between miR-34 and SNAIL that controls the transition between epithelial and mesenchymal states.

In a further study we determined p53-regulated mRNAs, lncRNAs, miRNAs and proteins on a genome-wide scale. In combination with a p53 DNA binding analysis, this led to the identification of genes that are directly or indirectly regulated by p53. We found that the majority of differentially expressed genes, which were directly bound by p53 near their TSS, were up-regulated and experimentally confirmed several induced target genes that showed promoter proximal p53 binding. Moreover, we determined that transcriptional repression by p53 mainly occurs via indirect mechanisms and studied the impact of miRNA-mediated mechanisms on p53-controlled gene repression. Almost half of the down-regulated proteins displayed seed-matching sequences of p53-induced miRNAs in the corresponding 3'-UTRs. Exemplarily, the clinically relevant miRNA targets *HMGB1*, *CIT* and *KLF12* were confirmed to be directly repressed by the p53-regulated miRNAs miR-34a, miR-486-5p and miR-205, respectively.

Subsequently, we characterized cystatin D (*CST5*), a vitamin D3-inducible inhibitor of cysteine proteases, as a new direct p53 target gene that resulted from the genome-wide analysis mentioned above. *CST5* inactivation decreased p53-induced MET, as evidenced by decreased inhibition of SNAIL and of migration by p53. In addition, simultaneous activation of p53 and treatment with calcitriol enhanced *CST5* induction. Furthermore, we provided evidence that SNAIL directly represses *CST5* expression which could be diminished by calcitriol treatment.

Taken together, our results illustrate the complex network of protein-coding and non-coding genes that is directly or indirectly controlled by the tumor suppressor p53. The data obtained in these studies might pave the way for new diagnostic and therapeutic approaches in the treatment of cancer.

8. ZUSAMMENFASSUNG

p53 ist einer der wichtigsten Tumorsuppressoren und ist in etwa der Hälfte aller menschlichen Krebsarten mutiert oder inaktiviert. Als Transkriptionsfaktor kontrolliert p53 die Expression von Zielgenen, die an der Regulierung des Zellzyklus, der DNA-Reparatur oder Apoptose beteiligt sind, und verhindert dadurch die Entstehung und Ausbreitung von Krebs. Trotz umfangreicher Forschungsarbeiten ist die Gesamtheit der durch p53-regulierten Gene noch nicht vollständig erfasst.

In dieser Arbeit konnten wir zeigen, dass p53 den EMT Transkriptionsfaktor SNAIL indirekt über die Induktion von miR-34 reprimiert. Diese Regulation überführte die untersuchten Zellen in einen epithelialen Zustand und inhibierte Migration, Invasion und Stammzelligkeit. Des Weiteren wiesen wir eine doppelt-negative Rückkopplungsschleife zwischen SNAIL und miR-34 nach, die den Übergang zwischen den epithelialen und mesenchymalen Zuständen kontrolliert.

Zudem bestimmten wir in einer genomweiten Studie die p53-regulierte Expression von mRNAs, lncRNAs, miRNAs und Proteinen. In Kombination mit einer genomweiten Analyse der p53 DNA-Bindung konnten wir direkt oder indirekt regulierte p53-Zielgene identifizieren. Wir stellten fest, dass die Mehrheit der differentiell regulierten Gene, die in der Nähe ihres Transkriptionsstarts von p53 gebunden sind, induziert wird und bestätigten experimentell die Induktion von einigen neuen p53-regulierten Zielgenen. Außerdem konnten wir zeigen, dass die transkriptionelle Repression durch p53 zum Großteil über indirekte Mechanismen erfolgen muss und untersuchten, welchen Einfluss miRNA-vermittelte Effekte auf die p53-kontrollierte Genrepression haben. Wir stellten fest, dass etwa die Hälfte der reprimierten Proteine Bindestellen für p53-induzierte miRNAs in den entsprechenden 3´-UTRs aufzeigen. Exemplarisch wurde die direkte Repression der klinisch relevanten Gene *HMGB1*, *CIT* und *KLF12* durch die p53-regulierten miRNAs miR-34a, miR-486-5p beziehungsweise miR-205 bestätigt.

Nachfolgend wurde das zuvor identifizierte p53-Zielgen Cystatin D (*CST5*), ein durch Vitamin D3 induzierbarer Inhibitor von Cystein Proteasen, genauer charakterisiert. *CST5*-Inaktivierung führte zu einer abgeschwächten p53-induzierten MET. Dies konnte anhand einer verminderten Inhibition von SNAIL und von Migration nach p53-Aktivierung gezeigt werden. Zudem verstärkte eine zeitgleiche p53-Aktivierung und Calcitriol-Behandlung die Induktion von *CST5*. Außerdem wurde nachgewiesen, dass *CST5* direkt von SNAIL reprimiert wird und diese Repression durch die Behandlung mit Calcitriol vermindert werden kann.

Zusammenfassend verdeutlichen die Ergebnisse das komplexe Netzwerk aus Protein-kodierenden und nicht-kodierenden Genen, das direkt oder indirekt durch den Tumorsuppressor p53 kontrolliert wird. In Zukunft könnten diese Daten als Grundlage für neue diagnostische und therapeutische Ansätze in der Behandlung von Krebserkrankungen dienen.

9. ABBREVIATIONS

AGO	argonaute protein
ANRIL	antisense noncoding RNA in the INK4 locus
APS	ammonium peroxodisulfate
AP4	activating enhancer binding protein 4
ARHGAP5	Rho GTPase-activating protein 5
ATM	ataxia telangiectasia mutated
ATR	ataxia telangiectasia and Rad3-related protein
bp	base pair(s)
BRN3A	brain-specific homeobox/POU-domain protein 3A
CDK	cyclin-dependent kinase
CDKN1A	cyclin-dependent kinase inhibitor 1A
cDNA	complementary DNA
ceRNA	competitive endogenous RNA
(q)ChIP	(quantitative) chromatin immunoprecipitation
CHK	checkpoint kinase
CIT	citron rho-interacting serine/threonine kinase
c-MYC	v-MYC avian myelocytomatosis viral oncogene homologue
CpG	cytidine-phosphate-guanidin
CRC	colorectal cancer
CSC	cancer stem cell
CST5	cystatin D
CYP24A1	1,25-dihydroxyvitamin D_3 24-hydroxylase
Cy3	cyanine 3
DAPI	2-(4-Amidinophenyl)-6-indolecarbamidine dihydrochloride
DGCR8	diGeorge syndrome critical region gene 8
DMEM	Dulbecco`s modified Eagles medium
DMSO	dimethyl-sulfoxide
DNA	deoxyribonucleic acid
DOX	doxycycline
DUSP4	dual specificity phosphatase 4
E.coli	*Escherichia coli*
E-box	enhancer box
eGFP	enhanced green fluorescent proteine
ELISA	enzyme-linked immunosorbent assay
EMT	epithelial-mesenchymal transition
eRNA	enhancer RNA
FACS	fluorescence-activated cell sorting
FCS	fetal calf serum
HBSS	Hank’s balanced salt solution
HDAC	histone deacetylase
HMGB1	high mobility group box 1
HOTAIR	HOX transcript antisense RNA

HRP	horseradish peroxidase
hTERT	human telomerase reverse transcriptase
IF	immunofluorescence
IgG	immunoglobulin
IP	immunoprecipitation
kbp	kilo base pairs
KLF	Krüppel-like factor
KRAS	kirsten rat sarcoma
LB	lysogeny broth
lincRNA	large intergenic non-coding RNA
lncRNA	large non-coding RNA
MALAT1	metastasis associated lung adenocarcinoma transcript 1
MDM	mouse double-minute
MEG3	maternally expressed 3
MET	mesenchymal-epithelial transition
miRNA	microRNA
mRNA	messenger RNA
MTA2	metastasis-associated 1 family, member 2
ncRNA	non-coding RNA
NFκB	nuclear factor 'kappa-light-chain-enhancer' of activated B-cells
NGS	next generation sequencing
OCT4	octamer binding transcription factor 4
OLFM4	olfactomedin 4
ORF	open reading frame
PAGE	polyacrylamide gel electrophoresis
PANDA	p21 associated ncRNA DNA damage activated
PAPPA	pregnancy-associated plasma protein A
P/C	phase constrast
PBS	phosphate buffered saline
(q)PCR	(quantitative) polymerase chain reaction
PI	propidium iodide
PI3K	phosphoinositid-3-kinase
PRC	polycomb-repressive complex
pri-miRNA	primary microRNA
pSILAC	pulsed stable isotope labeling by amino acids in cell culture
RBM38	RNA-binding protein 38
RISC	RNA induced silencing complex
RNA	ribonucleic acid
RoR	regulator of reprogramming
rpkm	reads per kilobase per million reads
RT	room temperature
SD	standard deviation
SDS	sodium dodecyl sulfate
SGK	serum/glucocorticoid regulated kinase
siRNA	small interfering RNA
SIRT1	sirtuin-1

SOX2	sex determining region Y-box 2
TCGA	the cancer genome atlas
temed	tetramethylethylenediamine
TF	transcription factor
TRIS	tris(hydroxymethyl)-aminomethan
TSS	transcription start site
UTR	untranslated region
VDR	vitamin D receptor
VSV	vesicular stomatitis virus (tag)
WB	Western blot
WNT	wingless-related integration site
WRAP53	WD repeat containing, antisense to TP53
ZEB	zinc finger E-box-binding homeobox protein
ZNF281	zinc finger protein 281

10. REFERENCES

1. Siemens, H., et al., *miR-34 and SNAIL form a double-negative feedback loop to regulate epithelial-mesenchymal transitions.* Cell Cycle, 2011. **10**(24): p. 4256-71.
2. Hunten, S., et al., *p53-regulated networks of protein, mRNA, miRNA and lncRNA expression revealed by integrated pSILAC and NGS analyses.* Mol Cell Proteomics, 2015 Jul 16. pii: mcp.M115.050237.
3. Hunten, S. and H. Hermeking, *p53 directly activates cystatin D/CST5 to mediate mesenchymal-epithelial transition: a possible link to tumor suppression by vitamin D3.* Oncotarget, 2015. **6**(18): p. 15842-56.
4. Hunten, S., et al., *The p53/microRNA network in cancer: experimental and bioinformatics approaches.* Adv Exp Med Biol, 2013. **774**: p. 77-101.
5. Hahn, S., et al., *SNAIL and miR-34a feed-forward regulation of ZNF281/ZBP99 promotes epithelial-mesenchymal transition.* EMBO J, 2013. **32**(23): p. 3079-95.
6. Hanahan, D. and R.A. Weinberg, *The hallmarks of cancer.* Cell, 2000. **100**(1): p. 57-70.
7. Hanahan, D. and R.A. Weinberg, *Hallmarks of cancer: the next generation.* Cell, 2011. **144**(5): p. 646-74.
8. Lane, D.P., *Cancer. p53, guardian of the genome.* Nature, 1992. **358**(6381): p. 15-6.
9. Vousden, K.H. and C. Prives, *Blinded by the Light: The Growing Complexity of p53.* Cell, 2009. **137**(3): p. 413-31.
10. Vogelstein, B., D. Lane, and A.J. Levine, *Surfing the p53 network.* Nature, 2000. **408**(6810): p. 307-10.
11. Blons, H. and P. Laurent-Puig, *TP53 and head and neck neoplasms.* Hum Mutat, 2003. **21**(3): p. 252-7.
12. Iacopetta, B., *TP53 mutation in colorectal cancer.* Hum Mutat, 2003. **21**(3): p. 271-6.
13. Schuijer, M. and E.M. Berns, *TP53 and ovarian cancer.* Hum Mutat, 2003. **21**(3): p. 285-91.
14. Olivier, M., et al., *The IARC TP53 database: new online mutation analysis and recommendations to users.* Hum Mutat, 2002. **19**(6): p. 607-14.
15. Campo, E., et al., *Loss of heterozygosity of p53 gene and p53 protein expression in human colorectal carcinomas.* Cancer Res, 1991. **51**(16): p. 4436-42.
16. Brosh, R. and V. Rotter, *When mutants gain new powers: news from the mutant p53 field.* Nat Rev Cancer, 2009. **9**(10): p. 701-13.
17. Zhang, Y. and Y. Xiong, *Mutations in human ARF exon 2 disrupt its nucleolar localization and impair its ability to block nuclear export of MDM2 and p53.* Mol Cell, 1999. **3**(5): p. 579-91.
18. Marine, J.C. and G. Lozano, *Mdm2-mediated ubiquitylation: p53 and beyond.* Cell Death Differ, 2010. **17**(1): p. 93-102.
19. Haupt, Y., et al., *Mdm2 promotes the rapid degradation of p53.* Nature, 1997. **387**(6630): p. 296-9.

20. Kubbutat, M.H., S.N. Jones, and K.H. Vousden, *Regulation of p53 stability by Mdm2.* Nature, 1997. **387**(6630): p. 299-303.
21. Danovi, D., et al., *Amplification of Mdmx (or Mdm4) directly contributes to tumor formation by inhibiting p53 tumor suppressor activity.* Mol Cell Biol, 2004. **24**(13): p. 5835-43.
22. Momand, J., et al., *The mdm-2 oncogene product forms a complex with the p53 protein and inhibits p53-mediated transactivation.* Cell, 1992. **69**(7): p. 1237-45.
23. Oliner, J.D., et al., *Oncoprotein MDM2 conceals the activation domain of tumour suppressor p53.* Nature, 1993. **362**(6423): p. 857-60.
24. Barak, Y., et al., *mdm2 expression is induced by wild type p53 activity.* EMBO J, 1993. **12**(2): p. 461-8.
25. Perry, M.E., et al., *The mdm-2 gene is induced in response to UV light in a p53-dependent manner.* Proc Natl Acad Sci U S A, 1993. **90**(24): p. 11623-7.
26. Montes de Oca Luna, R., D.S. Wagner, and G. Lozano, *Rescue of early embryonic lethality in mdm2-deficient mice by deletion of p53.* Nature, 1995. **378**(6553): p. 203-6.
27. Zhang, Y. and Y. Xiong, *Control of p53 ubiquitination and nuclear export by MDM2 and ARF.* Cell Growth Differ, 2001. **12**(4): p. 175-86.
28. Honda, R. and H. Yasuda, *Association of p19(ARF) with Mdm2 inhibits ubiquitin ligase activity of Mdm2 for tumor suppressor p53.* EMBO J, 1999. **18**(1): p. 22-7.
29. Weber, J.D., et al., *Nucleolar Arf sequesters Mdm2 and activates p53.* Nat Cell Biol, 1999. **1**(1): p. 20-6.
30. Kastan, M.B. and J. Bartek, *Cell-cycle checkpoints and cancer.* Nature, 2004. **432**(7015): p. 316-23.
31. Chehab, N.H., et al., *Phosphorylation of Ser-20 mediates stabilization of human p53 in response to DNA damage.* Proc Natl Acad Sci U S A, 1999. **96**(24): p. 13777-82.
32. Shieh, S.Y., et al., *DNA damage-induced phosphorylation of p53 alleviates inhibition by MDM2.* Cell, 1997. **91**(3): p. 325-34.
33. Jenkins, L.M., et al., *p53 N-terminal phosphorylation: a defining layer of complex regulation.* Carcinogenesis, 2012. **33**(8): p. 1441-9.
34. Barlev, N.A., et al., *Acetylation of p53 activates transcription through recruitment of coactivators/histone acetyltransferases.* Mol Cell, 2001. **8**(6): p. 1243-54.
35. Espinosa, J.M. and B.M. Emerson, *Transcriptional regulation by p53 through intrinsic DNA/chromatin binding and site-directed cofactor recruitment.* Mol Cell, 2001. **8**(1): p. 57-69.
36. Liu, G., T. Xia, and X. Chen, *The activation domains, the proline-rich domain, and the C-terminal basic domain in p53 are necessary for acetylation of histones on the proximal p21 promoter and interaction with p300/CREB-binding protein.* J Biol Chem, 2003. **278**(19): p. 17557-65.
37. Avantaggiati, M.L., et al., *Recruitment of p300/CBP in p53-dependent signal pathways.* Cell, 1997. **89**(7): p. 1175-84.

38. Candau, R., et al., *Two tandem and independent sub-activation domains in the amino terminus of p53 require the adaptor complex for activity.* Oncogene, 1997. **15**(7): p. 807-16.
39. Gevry, N., et al., *p21 transcription is regulated by differential localization of histone H2A.Z.* Genes Dev, 2007. **21**(15): p. 1869-81.
40. Gu, W. and R.G. Roeder, *Activation of p53 sequence-specific DNA binding by acetylation of the p53 C-terminal domain.* Cell, 1997. **90**(4): p. 595-606.
41. Lill, N.L., et al., *Binding and modulation of p53 by p300/CBP coactivators.* Nature, 1997. **387**(6635): p. 823-7.
42. Scolnick, D.M., et al., *CREB-binding protein and p300/CBP-associated factor are transcriptional coactivators of the p53 tumor suppressor protein.* Cancer Res, 1997. **57**(17): p. 3693-6.
43. Grossman, S.R., *p300/CBP/p53 interaction and regulation of the p53 response.* Eur J Biochem, 2001. **268**(10): p. 2773-8.
44. Rodriguez, M.S., et al., *Multiple C-terminal lysine residues target p53 for ubiquitin-proteasome-mediated degradation.* Mol Cell Biol, 2000. **20**(22): p. 8458-67.
45. An, W., J. Kim, and R.G. Roeder, *Ordered cooperative functions of PRMT1, p300, and CARM1 in transcriptional activation by p53.* Cell, 2004. **117**(6): p. 735-48.
46. Lee, D., et al., *SWI/SNF complex interacts with tumor suppressor p53 and is necessary for the activation of p53-mediated transcription.* J Biol Chem, 2002. **277**(25): p. 22330-7.
47. Gu, W., et al., *A novel human SRB/MED-containing cofactor complex, SMCC, involved in transcription regulation.* Mol Cell, 1999. **3**(1): p. 97-108.
48. Zhang, X., et al., *MED1/TRAP220 exists predominantly in a TRAP/ Mediator subpopulation enriched in RNA polymerase II and is required for ER-mediated transcription.* Mol Cell, 2005. **19**(1): p. 89-100.
49. Chen, X., et al., *Cooperative DNA binding of p53 with TFIID (TBP): a possible mechanism for transcriptional activation.* Genes Dev, 1993. **7**(10): p. 1837-49.
50. Farmer, G., et al., *Functional interaction between p53, the TATA-binding protein (TBP), andTBP-associated factors in vivo.* Mol Cell Biol, 1996. **16**(8): p. 4295-304.
51. Ko, L.J. and C. Prives, *p53: puzzle and paradigm.* Genes Dev, 1996. **10**(9): p. 1054-72.
52. Liu, X., et al., *The p53 activation domain binds the TATA box-binding polypeptide in Holo-TFIID, and a neighboring p53 domain inhibits transcription.* Mol Cell Biol, 1993. **13**(6): p. 3291-300.
53. Seto, E., et al., *Wild-type p53 binds to the TATA-binding protein and represses transcription.* Proc Natl Acad Sci U S A, 1992. **89**(24): p. 12028-32.
54. Thut, C.J., et al., *p53 transcriptional activation mediated by coactivators TAFII40 and TAFII60.* Science, 1995. **267**(5194): p. 100-4.
55. Xing, J., et al., *p53 Stimulates TFIID-TFIIA-promoter complex assembly, and p53-T antigen complex inhibits TATA binding protein-TATA interaction.* Mol Cell Biol, 2001. **21**(11): p. 3652-61.
56. el-Deiry, W.S., et al., *Definition of a consensus binding site for p53.* Nat Genet, 1992. **1**(1): p. 45-9.

57. Funk, W.D., et al., *A transcriptionally active DNA-binding site for human p53 protein complexes.* Mol Cell Biol, 1992. **12**(6): p. 2866-71.
58. Riley, T., et al., *Transcriptional control of human p53-regulated genes.* Nat Rev Mol Cell Biol, 2008. **9**(5): p. 402-12.
59. Bieging, K.T., S.S. Mello, and L.D. Attardi, *Unravelling mechanisms of p53-mediated tumour suppression.* Nat Rev Cancer, 2014. **14**(5): p. 359-70.
60. Rinn, J.L. and M. Huarte, *To repress or not to repress: this is the guardian's question.* Trends Cell Biol, 2011. **21**(6): p. 344-53.
61. Godar, S., et al., *Growth-inhibitory and tumor- suppressive functions of p53 depend on its repression of CD44 expression.* Cell, 2008. **134**(1): p. 62-73.
62. Johnson, R.A., T.A. Ince, and K.W. Scotto, *Transcriptional repression by p53 through direct binding to a novel DNA element.* J Biol Chem, 2001. **276**(29): p. 27716-20.
63. Wang, B., Z. Xiao, and E.C. Ren, *Redefining the p53 response element.* Proc Natl Acad Sci U S A, 2009. **106**(34): p. 14373-8.
64. Wang, B., et al., *The p53 response element and transcriptional repression.* Cell Cycle, 2010. **9**(5): p. 870-9.
65. Nikulenkov, F., et al., *Insights into p53 transcriptional function via genome-wide chromatin occupancy and gene expression analysis.* Cell Death Differ, 2012. **19**(12): p. 1992-2002.
66. Budhram-Mahadeo, V., et al., *p53 suppresses the activation of the Bcl-2 promoter by the Brn-3a POU family transcription factor.* J Biol Chem, 1999. **274**(21): p. 15237-44.
67. Hoffman, W.H., et al., *Transcriptional repression of the anti-apoptotic survivin gene by wild type p53.* J Biol Chem, 2002. **277**(5): p. 3247-57.
68. Ho, J.S., et al., *p53-Dependent transcriptional repression of c-myc is required for G1 cell cycle arrest.* Mol Cell Biol, 2005. **25**(17): p. 7423-31.
69. Maiyar, A.C., et al., *Repression of glucocorticoid receptor transactivation and DNA binding of a glucocorticoid response element within the serum/glucocorticoid-inducible protein kinase (sgk) gene promoter by the p53 tumor suppressor protein.* Mol Endocrinol, 1997. **11**(3): p. 312-29.
70. Kanaya, T., et al., *Adenoviral expression of p53 represses telomerase activity through down-regulation of human telomerase reverse transcriptase transcription.* Clin Cancer Res, 2000. **6**(4): p. 1239-47.
71. Barsotti, A.M. and C. Prives, *Pro-proliferative FoxM1 is a target of p53-mediated repression.* Oncogene, 2009. **28**(48): p. 4295-305.
72. Gottifredi, V., et al., *p53 down-regulates CHK1 through p21 and the retinoblastoma protein.* Mol Cell Biol, 2001. **21**(4): p. 1066-76.
73. Lohr, K., et al., *p21/CDKN1A mediates negative regulation of transcription by p53.* J Biol Chem, 2003. **278**(35): p. 32507-16.
74. Lander, E.S., et al., *Initial sequencing and analysis of the human genome.* Nature, 2001. **409**(6822): p. 860-921.
75. Derrien, T., et al., *The GENCODE v7 catalog of human long noncoding RNAs: analysis of their gene structure, evolution, and expression.* Genome Res, 2012. **22**(9): p. 1775-89.
76. Djebali, S., et al., *Landscape of transcription in human cells.* Nature, 2012. **489**(7414): p. 101-8.

77. Hermeking, H., *p53 enters the microRNA world.* Cancer Cell, 2007. **12**(5): p. 414-8.
78. Esquela-Kerscher, A. and F.J. Slack, *Oncomirs - microRNAs with a role in cancer.* Nat Rev Cancer, 2006. **6**(4): p. 259-69.
79. Caldas, C. and J.D. Brenton, *Sizing up miRNAs as cancer genes.* Nat Med, 2005. **11**(7): p. 712-4.
80. Calin, G.A. and C.M. Croce, *MicroRNA signatures in human cancers.* Nat Rev Cancer, 2006. **6**(11): p. 857-66.
81. Kent, O.A. and J.T. Mendell, *A small piece in the cancer puzzle: microRNAs as tumor suppressors and oncogenes.* Oncogene, 2006. **25**(46): p. 6188-96.
82. Lu, J., et al., *MicroRNA expression profiles classify human cancers.* Nature, 2005. **435**(7043): p. 834-8.
83. Kumar, M.S., et al., *Impaired microRNA processing enhances cellular transformation and tumorigenesis.* Nat Genet, 2007. **39**(5): p. 673-7.
84. Friedman, R.C., et al., *Most mammalian mRNAs are conserved targets of microRNAs.* Genome Res, 2009. **19**(1): p. 92-105.
85. Kim, V.N., J. Han, and M.C. Siomi, *Biogenesis of small RNAs in animals.* Nat Rev Mol Cell Biol, 2009. **10**(2): p. 126-39.
86. Rokavec, M., et al., *The p53/microRNA connection in gastrointestinal cancer.* Clin Exp Gastroenterol, 2014. **7**: p. 395-413.
87. Bartel, D.P., *MicroRNAs: target recognition and regulatory functions.* Cell, 2009. **136**(2): p. 215-33.
88. Pillai, R.S., S.N. Bhattacharyya, and W. Filipowicz, *Repression of protein synthesis by miRNAs: how many mechanisms?* Trends Cell Biol, 2007. **17**(3): p. 118-26.
89. Bommer, G.T., et al., *p53-mediated activation of miRNA34 candidate tumor-suppressor genes.* Curr Biol, 2007. **17**(15): p. 1298-307.
90. Chang, T.C., et al., *Transactivation of miR-34a by p53 broadly influences gene expression and promotes apoptosis.* Mol Cell, 2007. **26**(5): p. 745-52.
91. Corney, D.C., et al., *MicroRNA-34b and MicroRNA-34c are targets of p53 and cooperate in control of cell proliferation and adhesion-independent growth.* Cancer Res, 2007. **67**(18): p. 8433-8.
92. He, L., et al., *A microRNA component of the p53 tumour suppressor network.* Nature, 2007. **447**(7148): p. 1130-4.
93. Raver-Shapira, N., et al., *Transcriptional activation of miR-34a contributes to p53-mediated apoptosis.* Mol Cell, 2007. **26**(5): p. 731-43.
94. Tarasov, V., et al., *Differential regulation of microRNAs by p53 revealed by massively parallel sequencing: miR-34a is a p53 target that induces apoptosis and G1-arrest.* Cell Cycle, 2007. **6**(13): p. 1586-93.
95. Tazawa, H., et al., *Tumor-suppressive miR-34a induces senescence-like growth arrest through modulation of the E2F pathway in human colon cancer cells.* Proc Natl Acad Sci U S A, 2007. **104**(39): p. 15472-7.
96. Rokavec, M., et al., *The p53/miR-34 axis in development and disease.* J Mol Cell Biol, 2014. **6**(3): p. 214-30.
97. Gregory, P.A., et al., *The miR-200 family and miR-205 regulate epithelial to mesenchymal transition by targeting ZEB1 and SIP1.* Nat Cell Biol, 2008. **10**(5): p. 593-601.

98. Kim, T., et al., *p53 regulates epithelial-mesenchymal transition through microRNAs targeting ZEB1 and ZEB2.* J Exp Med, 2011. **208**(5): p. 875-83.
99. Dong, P., et al., *MicroRNA-194 inhibits epithelial to mesenchymal transition of endometrial cancer cells by targeting oncogene BMI-1.* Mol Cancer, 2011. **10**: p. 99.
100. Geng, L., et al., *MicroRNA-192 suppresses liver metastasis of colon cancer.* Oncogene, 2013.
101. Braun, C.J., et al., *p53-Responsive micrornas 192 and 215 are capable of inducing cell cycle arrest.* Cancer Res, 2008. **68**(24): p. 10094-104.
102. Georges, S.A., et al., *Coordinated regulation of cell cycle transcripts by p53-Inducible microRNAs, miR-192 and miR-215.* Cancer Res, 2008. **68**(24): p. 10105-12.
103. Pichiorri, F., et al., *Downregulation of p53-inducible microRNAs 192, 194, and 215 impairs the p53/MDM2 autoregulatory loop in multiple myeloma development.* Cancer Cell, 2010. **18**(4): p. 367-81.
104. Bohlig, L., M. Friedrich, and K. Engeland, *p53 activates the PANK1/miRNA-107 gene leading to downregulation of CDK6 and p130 cell cycle proteins.* Nucleic Acids Res, 2011. **39**(2): p. 440-53.
105. Yamakuchi, M., et al., *P53-induced microRNA-107 inhibits HIF-1 and tumor angiogenesis.* Proc Natl Acad Sci U S A, 2010. **107**(14): p. 6334-9.
106. Sachdeva, M., et al., *p53 represses c-Myc through induction of the tumor suppressor miR-145.* Proc Natl Acad Sci U S A, 2009. **106**(9): p. 3207-12.
107. Xu, N., et al., *MicroRNA-145 regulates OCT4, SOX2, and KLF4 and represses pluripotency in human embryonic stem cells.* Cell, 2009. **137**(4): p. 647-58.
108. Kent, O.A., et al., *Repression of the miR-143/145 cluster by oncogenic Ras initiates a tumor-promoting feed-forward pathway.* Genes Dev, 2010. **24**(24): p. 2754-9.
109. Fabbri, M., et al., *Association of a microRNA/TP53 feedback circuitry with pathogenesis and outcome of B-cell chronic lymphocytic leukemia.* JAMA, 2011. **305**(1): p. 59-67.
110. Shi, L., et al., *p53-induced miR-15a/16-1 and AP4 form a double-negative feedback loop to regulate epithelial-mesenchymal transition and metastasis in colorectal cancer.* Cancer Res, 2014. **74**(2): p. 532-42.
111. Bonci, D., et al., *The miR-15a-miR-16-1 cluster controls prostate cancer by targeting multiple oncogenic activities.* Nat Med, 2008. **14**(11): p. 1271-7.
112. Cimmino, A., et al., *miR-15 and miR-16 induce apoptosis by targeting BCL2.* Proc Natl Acad Sci U S A, 2005. **102**(39): p. 13944-9.
113. Liu, Q., et al., *miR-16 family induces cell cycle arrest by regulating multiple cell cycle genes.* Nucleic Acids Res, 2008. **36**(16): p. 5391-404.
114. Ugalde, A.P., et al., *Aging and chronic DNA damage response activate a regulatory pathway involving miR-29 and p53.* EMBO J, 2011. **30**(11): p. 2219-32.
115. Xiao, J., et al., *miR-605 joins p53 network to form a p53:miR-605:Mdm2 positive feedback loop in response to stress.* EMBO J, 2011. **30**(3): p. 524-32.
116. Jin, L., et al., *MicroRNA-149*, a p53-responsive microRNA, functions as an oncogenic regulator in human melanoma.* Proc Natl Acad Sci U S A, 2011. **108**(38): p. 15840-5.

117. Lin, J., et al., *A novel p53/microRNA-22/Cyr61 axis in synovial cells regulates inflammation in rheumatoid arthritis.* Arthritis Rheumatol, 2014. **66**(1): p. 49-59.
118. Au Yeung, C.L., et al., *Human papillomavirus type 16 E6 induces cervical cancer cell migration through the p53/microRNA-23b/urokinase-type plasminogen activator pathway.* Oncogene, 2011. **30**(21): p. 2401-10.
119. Zhang, Y., et al., *p53 downregulates Down syndrome-associated DYRK1A through miR-1246.* EMBO Rep, 2011. **12**(8): p. 811-7.
120. Barsotti, A.M., et al., *p53-Dependent induction of PVT1 and miR-1204.* J Biol Chem, 2012. **287**(4): p. 2509-19.
121. Olive, V., I. Jiang, and L. He, *mir-17-92, a cluster of miRNAs in the midst of the cancer network.* Int J Biochem Cell Biol, 2010. **42**(8): p. 1348-54.
122. Tsuchida, A., et al., *miR-92 is a key oncogenic component of the miR-17-92 cluster in colon cancer.* Cancer Sci, 2011. **102**(12): p. 2264-71.
123. Yan, H.L., et al., *Repression of the miR-17-92 cluster by p53 has an important function in hypoxia-induced apoptosis.* EMBO J, 2009. **28**(18): p. 2719-32.
124. Zhai, H., et al., *Inhibition of autophagy and tumor growth in colon cancer by miR-502.* Oncogene, 2013. **32**(12): p. 1570-9.
125. Liang, M., et al., *Transcriptional cooperation between p53 and NF-kappaB p65 regulates microRNA-224 transcription in mouse ovarian granulosa cells.* Mol Cell Endocrinol, 2013. **370**(1-2): p. 119-29.
126. Suzuki, H.I., et al., *Modulation of microRNA processing by p53.* Nature, 2009. **460**(7254): p. 529-33.
127. Mudhasani, R., et al., *Loss of miRNA biogenesis induces p19Arf-p53 signaling and senescence in primary cells.* J Cell Biol, 2008. **181**(7): p. 1055-63.
128. Su, X., et al., *TAp63 suppresses metastasis through coordinate regulation of Dicer and miRNAs.* Nature, 2010. **467**(7318): p. 986-90.
129. Leveille, N., et al., *Selective inhibition of microRNA accessibility by RBM38 is required for p53 activity.* Nat Commun, 2011. **2**: p. 513.
130. Le, M.T., et al., *MicroRNA-125b is a novel negative regulator of p53.* Genes Dev, 2009. **23**(7): p. 862-76.
131. Nishida, N., et al., *MicroRNA miR-125b is a prognostic marker in human colorectal cancer.* Int J Oncol, 2011. **38**(5): p. 1437-43.
132. Hu, W., et al., *Negative regulation of tumor suppressor p53 by microRNA miR-504.* Mol Cell, 2010. **38**(5): p. 689-99.
133. Li, N., et al., *A combined array-based comparative genomic hybridization and functional library screening approach identifies mir-30d as an oncomir in cancer.* Cancer Res, 2012. **72**(1): p. 154-64.
134. Li, X., et al., *The expression of miR-25 is increased in colorectal cancer and is associated with patient prognosis.* Med Oncol, 2014. **31**(1): p. 781.
135. Kumar, M., et al., *Negative regulation of the tumor suppressor p53 gene by microRNAs.* Oncogene, 2011. **30**(7): p. 843-53.
136. Swarbrick, A., et al., *miR-380-5p represses p53 to control cellular survival and is associated with poor outcome in MYCN-amplified neuroblastoma.* Nat Med, 2010. **16**(10): p. 1134-40.
137. Herrera-Merchan, A., et al., *miR-33-mediated downregulation of p53 controls hematopoietic stem cell self-renewal.* Cell Cycle, 2010. **9**(16): p. 3277-85.

138. Tian, S., et al., *MicroRNA-1285 inhibits the expression of p53 by directly targeting its 3' untranslated region.* Biochem Biophys Res Commun, 2010. **396**(2): p. 435-9.
139. Zhang, N., X. Wei, and L. Xu, *miR-150 promotes the proliferation of lung cancer cells by targeting P53.* FEBS Lett, 2013. **587**(15): p. 2346-51.
140. Xu, C.X., et al., *MicroRNA miR-214 regulates ovarian cancer cell stemness by targeting p53/Nanog.* J Biol Chem, 2012. **287**(42): p. 34970-8.
141. Liu, Y., et al., *miR-375 targets the p53 gene to regulate cellular response to ionizing radiation and etoposide in gastric cancer cells.* DNA Repair (Amst), 2013. **12**(9): p. 741-50.
142. Zhang, J., et al., *Loss of microRNA-143/145 disturbs cellular growth and apoptosis of human epithelial cancers by impairing the MDM2-p53 feedback loop.* Oncogene, 2013. **32**(1): p. 61-9.
143. Fornari, F., et al., *MiR-122/cyclin G1 interaction modulates p53 activity and affects doxorubicin sensitivity of human hepatocarcinoma cells.* Cancer Res, 2009. **69**(14): p. 5761-7.
144. Okamoto, K., et al., *Cyclin G recruits PP2A to dephosphorylate Mdm2.* Mol Cell, 2002. **9**(4): p. 761-71.
145. Luo, J., et al., *Negative control of p53 by Sir2alpha promotes cell survival under stress.* Cell, 2001. **107**(2): p. 137-48.
146. Yamakuchi, M., M. Ferlito, and C.J. Lowenstein, *miR-34a repression of SIRT1 regulates apoptosis.* Proc Natl Acad Sci U S A, 2008. **105**(36): p. 13421-6.
147. Zhou, X., et al., *Inhibition of Na,K-ATPase activates PI3 kinase and inhibits apoptosis in LLC-PK1 cells.* Biochem Biophys Res Commun, 2001. **285**(1): p. 46-51.
148. Bu, D., et al., *NONCODE v3.0: integrative annotation of long noncoding RNAs.* Nucleic Acids Res, 2012. **40**(Database issue): p. D210-5.
149. Guttman, M., et al., *Chromatin signature reveals over a thousand highly conserved large non-coding RNAs in mammals.* Nature, 2009. **458**(7235): p. 223-7.
150. Prensner, J.R. and A.M. Chinnaiyan, *The emergence of lncRNAs in cancer biology.* Cancer Discov, 2011. **1**(5): p. 391-407.
151. Khalil, A.M., et al., *Many human large intergenic noncoding RNAs associate with chromatin-modifying complexes and affect gene expression.* Proc Natl Acad Sci U S A, 2009. **106**(28): p. 11667-72.
152. Natoli, G. and J.C. Andrau, *Noncoding transcription at enhancers: general principles and functional models.* Annu Rev Genet, 2012. **46**: p. 1-19.
153. Huarte, M., et al., *A large intergenic noncoding RNA induced by p53 mediates global gene repression in the p53 response.* Cell, 2010. **142**(3): p. 409-19.
154. Yap, K.L., et al., *Molecular interplay of the noncoding RNA ANRIL and methylated histone H3 lysine 27 by polycomb CBX7 in transcriptional silencing of INK4a.* Mol Cell, 2010. **38**(5): p. 662-74.
155. Bernard, D., et al., *A long nuclear-retained non-coding RNA regulates synaptogenesis by modulating gene expression.* EMBO J, 2010. **29**(18): p. 3082-93.

156. Tripathi, V., et al., *The nuclear-retained noncoding RNA MALAT1 regulates alternative splicing by modulating SR splicing factor phosphorylation.* Mol Cell, 2010. **39**(6): p. 925-38.
157. Salmena, L., et al., *A ceRNA hypothesis: the Rosetta Stone of a hidden RNA language?* Cell, 2011. **146**(3): p. 353-8.
158. Kim, K., et al., *Isolation and characterization of a novel H1.2 complex that acts as a repressor of p53-mediated transcription.* J Biol Chem, 2008. **283**(14): p. 9113-26.
159. Yoon, J.H., et al., *LincRNA-p21 suppresses target mRNA translation.* Mol Cell, 2012. **47**(4): p. 648-55.
160. Hung, T., et al., *Extensive and coordinated transcription of noncoding RNAs within cell-cycle promoters.* Nat Genet, 2011. **43**(7): p. 621-9.
161. Liu, Q., et al., *LncRNA loc285194 is a p53-regulated tumor suppressor.* Nucleic Acids Res, 2013. **41**(9): p. 4976-87.
162. Pasic, I., et al., *Recurrent focal copy-number changes and loss of heterozygosity implicate two noncoding RNAs and one tumor suppressor gene at chromosome 3q13.31 in osteosarcoma.* Cancer Res, 2010. **70**(1): p. 160-71.
163. Zhang, A., et al., *The human long non-coding RNA-RoR is a p53 repressor in response to DNA damage.* Cell Res, 2013. **23**(3): p. 340-50.
164. Dugimont, T., et al., *The H19 TATA-less promoter is efficiently repressed by wild-type tumor suppressor gene product p53.* Oncogene, 1998. **16**(18): p. 2395-401.
165. Matouk, I.J., et al., *The H19 non-coding RNA is essential for human tumor growth.* PLoS One, 2007. **2**(9): p. e845.
166. Yoshimizu, T., et al., *The H19 locus acts in vivo as a tumor suppressor.* Proc Natl Acad Sci U S A, 2008. **105**(34): p. 12417-22.
167. Tripathi, V., et al., *Long noncoding RNA MALAT1 controls cell cycle progression by regulating the expression of oncogenic transcription factor B-MYB.* PLoS Genet, 2013. **9**(3): p. e1003368.
168. Zhou, Y., et al., *Activation of p53 by MEG3 non-coding RNA.* J Biol Chem, 2007. **282**(34): p. 24731-42.
169. Mahmoudi, S., et al., *Wrap53, a natural p53 antisense transcript required for p53 induction upon DNA damage.* Mol Cell, 2009. **33**(4): p. 462-71.
170. Melo, C.A., et al., *eRNAs are required for p53-dependent enhancer activity and gene transcription.* Mol Cell, 2013. **49**(3): p. 524-35.
171. Yang, J. and R.A. Weinberg, *Epithelial-mesenchymal transition: at the crossroads of development and tumor metastasis.* Dev Cell, 2008. **14**(6): p. 818-29.
172. Arnoux, V., et al., *Erk5 controls Slug expression and keratinocyte activation during wound healing.* Mol Biol Cell, 2008. **19**(11): p. 4738-49.
173. Zeisberg, E.M., et al., *Endothelial-to-mesenchymal transition contributes to cardiac fibrosis.* Nat Med, 2007. **13**(8): p. 952-61.
174. Thiery, J.P., *Epithelial-mesenchymal transitions in tumour progression.* Nat Rev Cancer, 2002. **2**(6): p. 442-54.
175. Lamouille, S., J. Xu, and R. Derynck, *Molecular mechanisms of epithelial-mesenchymal transition.* Nat Rev Mol Cell Biol, 2014. **15**(3): p. 178-96.

176. Sanchez-Tillo, E., et al., *EMT-activating transcription factors in cancer: beyond EMT and tumor invasiveness.* Cell Mol Life Sci, 2012. **69**(20): p. 3429-56.
177. Giroldi, L.A., et al., *Role of E boxes in the repression of E-cadherin expression.* Biochem Biophys Res Commun, 1997. **241**(2): p. 453-8.
178. Kim, N.H., et al., *A p53/miRNA-34 axis regulates Snail1-dependent cancer cell epithelial-mesenchymal transition.* J Cell Biol, 2011. **195**(3): p. 417-33.
179. Brabletz, T., et al., *Invasion and metastasis in colorectal cancer: epithelial-mesenchymal transition, mesenchymal-epithelial transition, stem cells and beta-catenin.* Cells Tissues Organs, 2005. **179**(1-2): p. 56-65.
180. Mani, S.A., et al., *The epithelial-mesenchymal transition generates cells with properties of stem cells.* Cell, 2008. **133**(4): p. 704-15.
181. Wellner, U., et al., *The EMT-activator ZEB1 promotes tumorigenicity by repressing stemness-inhibiting microRNAs.* Nat Cell Biol, 2009. **11**(12): p. 1487-95.
182. Scheel, C. and R.A. Weinberg, *Cancer stem cells and epithelial-mesenchymal transition: concepts and molecular links.* Semin Cancer Biol, 2012. **22**(5-6): p. 396-403.
183. Jones, G., D.E. Prosser, and M. Kaufmann, *Cytochrome P450-mediated metabolism of vitamin D.* J Lipid Res, 2014. **55**(1): p. 13-31.
184. Zehnder, D., et al., *Extrarenal expression of 25-hydroxyvitamin d(3)-1 alpha-hydroxylase.* J Clin Endocrinol Metab, 2001. **86**(2): p. 888-94.
185. Holick, M.F., *Vitamin D and bone health.* J Nutr, 1996. **126**(4 Suppl): p. 1159S-64S.
186. Deeb, K.K., D.L. Trump, and C.S. Johnson, *Vitamin D signalling pathways in cancer: potential for anticancer therapeutics.* Nat Rev Cancer, 2007. **7**(9): p. 684-700.
187. Feldman, D., et al., *The role of vitamin D in reducing cancer risk and progression.* Nat Rev Cancer, 2014. **14**(5): p. 342-57.
188. Schwartz, G.G., et al., *Human prostate cells synthesize 1,25-dihydroxyvitamin D3 from 25-hydroxyvitamin D3.* Cancer Epidemiol Biomarkers Prev, 1998. **7**(5): p. 391-5.
189. Townsend, K., et al., *Autocrine metabolism of vitamin D in normal and malignant breast tissue.* Clin Cancer Res, 2005. **11**(9): p. 3579-86.
190. Bareis, P., et al., *25-hydroxy-vitamin d metabolism in human colon cancer cells during tumor progression.* Biochem Biophys Res Commun, 2001. **285**(4): p. 1012-7.
191. Bises, G., et al., *25-hydroxyvitamin D3-1alpha-hydroxylase expression in normal and malignant human colon.* J Histochem Cytochem, 2004. **52**(7): p. 985-9.
192. Cross, H.S., et al., *25-Hydroxyvitamin D(3)-1alpha-hydroxylase and vitamin D receptor gene expression in human colonic mucosa is elevated during early cancerogenesis.* Steroids, 2001. **66**(3-5): p. 287-92.
193. Cross, H.S., et al., *The Vitamin D endocrine system of the gut--its possible role in colorectal cancer prevention.* J Steroid Biochem Mol Biol, 2005. **97**(1-2): p. 121-8.

194. Friedrich, M., et al., *Analysis of the vitamin D system in cervical carcinomas, breast cancer and ovarian cancer.* Recent Results Cancer Res, 2003. **164**: p. 239-46.
195. Anderson, M.G., et al., *Expression of VDR and CYP24A1 mRNA in human tumors.* Cancer Chemother Pharmacol, 2006. **57**(2): p. 234-40.
196. Ly, L.H., et al., *Liarozole acts synergistically with 1alpha,25-dihydroxyvitamin D3 to inhibit growth of DU 145 human prostate cancer cells by blocking 24-hydroxylase activity.* Endocrinology, 1999. **140**(5): p. 2071-6.
197. Peehl, D.M., et al., *Preclinical activity of ketoconazole in combination with calcitriol or the vitamin D analogue EB 1089 in prostate cancer cells.* J Urol, 2002. **168**(4 Pt 1): p. 1583-8.
198. Zhao, J., et al., *Enhancement of antiproliferative activity of 1alpha,25-dihydroxyvitamin D3 (analogs) by cytochrome P450 enzyme inhibitors is compound- and cell-type specific.* J Steroid Biochem Mol Biol, 1996. **57**(3-4): p. 197-202.
199. Pereira, F., M.J. Larriba, and A. Munoz, *Vitamin D and colon cancer.* Endocr Relat Cancer, 2012. **19**(3): p. R51-71.
200. Alvarez-Diaz, S., et al., *Cystatin D is a candidate tumor suppressor gene induced by vitamin D in human colon cancer cells.* J Clin Invest, 2009. **119**(8): p. 2343-58.
201. Larriba, M.J., et al., *Vitamin D Is a Multilevel Repressor of Wnt/b-Catenin Signaling in Cancer Cells.* Cancers (Basel), 2013. **5**(4): p. 1242-60.
202. Palmer, H.G., et al., *Vitamin D(3) promotes the differentiation of colon carcinoma cells by the induction of E-cadherin and the inhibition of beta-catenin signaling.* J Cell Biol, 2001. **154**(2): p. 369-87.
203. Aguilera, O., et al., *The Wnt antagonist DICKKOPF-1 gene is induced by 1alpha,25-dihydroxyvitamin D3 associated to the differentiation of human colon cancer cells.* Carcinogenesis, 2007. **28**(9): p. 1877-84.
204. Grant, W.B., *Ecological studies of the UVB-vitamin D-cancer hypothesis.* Anticancer Res, 2012. **32**(1): p. 223-36.
205. Lee, J.E., et al., *Circulating levels of vitamin D and colon and rectal cancer: the Physicians' Health Study and a meta-analysis of prospective studies.* Cancer Prev Res (Phila), 2011. **4**(5): p. 735-43.
206. Fedirko, V., et al., *Prediagnostic 25-hydroxyvitamin D, VDR and CASR polymorphisms, and survival in patients with colorectal cancer in western European ppulations.* Cancer Epidemiol Biomarkers Prev, 2012. **21**(4): p. 582-93.
207. Fang, F., et al., *Prediagnostic plasma vitamin D metabolites and mortality among patients with prostate cancer.* PLoS One, 2011. **6**(4): p. e18625.
208. Chlebowski, R.T., et al., *Calcium plus vitamin D supplementation and the risk of breast cancer.* J Natl Cancer Inst, 2008. **100**(22): p. 1581-91.
209. Brandstedt, J., et al., *Vitamin D, PTH, and calcium and the risk of prostate cancer: a prospective nested case-control study.* Cancer Causes Control, 2012. **23**(8): p. 1377-85.
210. Bjelakovic, G., et al., *Vitamin D supplementation for prevention of cancer in adults.* Cochrane Database Syst Rev, 2014. **6**: p. CD007469.

211. Bjelakovic, G., et al., *Vitamin D supplementation for prevention of mortality in adults.* Cochrane Database Syst Rev, 2014. **1**: p. CD007470.
212. Maalmi, H., et al., *Serum 25-hydroxyvitamin D levels and survival in colorectal and breast cancer patients: systematic review and meta-analysis of prospective cohort studies.* Eur J Cancer, 2014. **50**(8): p. 1510-21.
213. Mohr, S.B., et al., *Meta-analysis of vitamin D sufficiency for improving survival of patients with breast cancer.* Anticancer Res, 2014. **34**(3): p. 1163-6.
214. Wei, M.Y., et al., *Vitamin D and prevention of colorectal adenoma: a meta-analysis.* Cancer Epidemiol Biomarkers Prev, 2008. **17**(11): p. 2958-69.
215. Kupferschmidt, K., *Uncertain verdict as vitamin D goes on trial.* Science, 2012. **337**(6101): p. 1476-8.
216. He, T.C., et al., *PPARdelta is an APC-regulated target of nonsteroidal anti-inflammatory drugs.* Cell, 1999. **99**(3): p. 335-45.
217. Kaller, M., et al., *Genome-wide characterization of miR-34a induced changes in protein and mRNA expression by a combined pulsed SILAC and microarray analysis.* Mol Cell Proteomics, 2011. **10**(8): p. M111 010462.
218. Welch, C., Y. Chen, and R.L. Stallings, *MicroRNA-34a functions as a potential tumor suppressor by inducing apoptosis in neuroblastoma cells.* Oncogene, 2007. **26**(34): p. 5017-22.
219. Pillai, R.S., et al., *Inhibition of translational initiation by Let-7 MicroRNA in human cells.* Science, 2005. **309**(5740): p. 1573-6.
220. Jackstadt, R., et al., *AP4 is a mediator of epithelial-mesenchymal transition and metastasis in colorectal cancer.* J Exp Med, 2013. **210**(7): p. 1331-50.
221. Amati, B., et al., *Function of the c-Myc oncoprotein in chromatin remodeling and transcription.* Biochim Biophys Acta, 2001. **1471**(3): p. M135-45.
222. Cristodero, M., et al., *Mitochondrial translation factors of Trypanosoma brucei: elongation factor-Tu has a unique subdomain that is essential for its function.* Mol Microbiol, 2013. **90**(4): p. 744-55.
223. Cox, J. and M. Mann, *MaxQuant enables high peptide identification rates, individualized p.p.b.-range mass accuracies and proteome-wide protein quantification.* Nat Biotechnol, 2008. **26**(12): p. 1367-72.
224. Cox, J., et al., *Andromeda: a peptide search engine integrated into the MaxQuant environment.* J Proteome Res, 2011. **10**(4): p. 1794-805.
225. UniProt, C., *Activities at the Universal Protein Resource (UniProt).* Nucleic Acids Res, 2014. **42**(Database issue): p. D191-8.
226. Vizcaino, J.A., et al., *ProteomeXchange provides globally coordinated proteomics data submission and dissemination.* Nat Biotechnol, 2014. **32**(3): p. 223-6.
227. Windhager, L., et al., *Ultrashort and progressive 4sU-tagging reveals key characteristics of RNA processing at nucleotide resolution.* Genome Res, 2012. **22**(10): p. 2031-42.
228. Langmead, B., et al., *Ultrafast and memory-efficient alignment of short DNA sequences to the human genome.* Genome Biol, 2009. **10**(3): p. R25.
229. Mortazavi, A., et al., *Mapping and quantifying mammalian transcriptomes by RNA-Seq.* Nat Methods, 2008. **5**(7): p. 621-8.
230. Dueck, A., et al., *A miR-155-dependent microRNA hierarchy in dendritic cell maturation and macrophage activation.* FEBS Lett, 2014. **588**(4): p. 632-40.

231. Ho, C.K. and S. Shuman, *Bacteriophage T4 RNA ligase 2 (gp24.1) exemplifies a family of RNA ligases found in all phylogenetic domains.* Proc Natl Acad Sci U S A, 2002. **99**(20): p. 12709-14.
232. Griffiths-Jones, S., et al., *miRBase: microRNA sequences, targets and gene nomenclature.* Nucleic Acids Res, 2006. **34**(Database issue): p. D140-4.
233. Feng, J., T. Liu, and Y. Zhang, *Using MACS to identify peaks from ChIP-Seq data.* Curr Protoc Bioinformatics, 2011. **Chapter 2**: p. Unit 2 14.
234. Bailey, T.L., et al., *MEME SUITE: tools for motif discovery and searching.* Nucleic Acids Res, 2009. **37**(Web Server issue): p. W202-8.
235. Whitington, T., et al., *Inferring transcription factor complexes from ChIP-seq data.* Nucleic Acids Res, 2011. **39**(15): p. e98.
236. Sandelin, A., et al., *JASPAR: an open-access database for eukaryotic transcription factor binding profiles.* Nucleic Acids Res, 2004. **32**(Database issue): p. D91-4.
237. Rhodes, D.R., et al., *ONCOMINE: a cancer microarray database and integrated data-mining platform.* Neoplasia, 2004. **6**(1): p. 1-6.
238. Goswami, C.P. and H. Nakshatri, *PROGgene: gene expression based survival analysis web application for multiple cancers.* J Clin Bioinforma, 2013. **3**(1): p. 22.
239. Grimson, A., et al., *MicroRNA targeting specificity in mammals: determinants beyond seed pairing.* Mol Cell, 2007. **27**(1): p. 91-105.
240. Krek, A., et al., *Combinatorial microRNA target predictions.* Nat Genet, 2005. **37**(5): p. 495-500.
241. Huang da, W., B.T. Sherman, and R.A. Lempicki, *Systematic and integrative analysis of large gene lists using DAVID bioinformatics resources.* Nat Protoc, 2009. **4**(1): p. 44-57.
242. Huang da, W., B.T. Sherman, and R.A. Lempicki, *Bioinformatics enrichment tools: paths toward the comprehensive functional analysis of large gene lists.* Nucleic Acids Res, 2009. **37**(1): p. 1-13.
243. Kent, W.J., et al., *The human genome browser at UCSC.* Genome Res, 2002. **12**(6): p. 996-1006.
244. Cancer Genome Atlas, N., *Comprehensive molecular characterization of human colon and rectal cancer.* Nature, 2012. **487**(7407): p. 330-7.
245. Chang, C.J., et al., *p53 regulates epithelial-mesenchymal transition and stem cell properties through modulating miRNAs.* Nat Cell Biol, 2011. **13**(3): p. 317-23.
246. Bunz, F., et al., *Requirement for p53 and p21 to sustain G2 arrest after DNA damage.* Science, 1998. **282**(5393): p. 1497-501.
247. Vassilev, L.T., et al., *In vivo activation of the p53 pathway by small-molecule antagonists of MDM2.* Science, 2004. **303**(5659): p. 844-8.
248. Wang, S.P., et al., *p53 controls cancer cell invasion by inducing the MDM2-mediated degradation of Slug.* Nat Cell Biol, 2009. **11**(6): p. 694-704.
249. John, B., et al., *Human MicroRNA targets.* PLoS Biol, 2004. **2**(11): p. e363.
250. Liu, C., et al., *The microRNA miR-34a inhibits prostate cancer stem cells and metastasis by directly repressing CD44.* Nat Med, 2011. **17**(2): p. 211-5.
251. Cannell, I.G. and M. Bushell, *Regulation of Myc by miR-34c: A mechanism to prevent genomic instability?* Cell Cycle, 2010. **9**(14): p. 2726-30.

252. Christoffersen, N.R., et al., *p53-independent upregulation of miR-34a during oncogene-induced senescence represses MYC.* Cell Death Differ, 2010. **17**(2): p. 236-45.
253. Shimono, Y., et al., *Downregulation of miRNA-200c links breast cancer stem cells with normal stem cells.* Cell, 2009. **138**(3): p. 592-603.
254. Bracken, C.P., et al., *A double-negative feedback loop between ZEB1-SIP1 and the microRNA-200 family regulates epithelial-mesenchymal transition.* Cancer Res, 2008. **68**(19): p. 7846-54.
255. Burk, U., et al., *A reciprocal repression between ZEB1 and members of the miR-200 family promotes EMT and invasion in cancer cells.* EMBO Rep, 2008. **9**(6): p. 582-9.
256. Selbach, M., et al., *Widespread changes in protein synthesis induced by microRNAs.* Nature, 2008. **455**(7209): p. 58-63.
257. Maire, V., et al., *TTK/hMPS1 is an attractive therapeutic target for triple-negative breast cancer.* PLoS One, 2013. **8**(5): p. e63712.
258. Ambrosini, G., C. Adida, and D.C. Altieri, *A novel anti-apoptosis gene, survivin, expressed in cancer and lymphoma.* Nat Med, 1997. **3**(8): p. 917-21.
259. Liu, P., T.P. Kao, and H. Huang, *CDK1 promotes cell proliferation and survival via phosphorylation and inhibition of FOXO1 transcription factor.* Oncogene, 2008. **27**(34): p. 4733-44.
260. Yu, H., *Cdc20: a WD40 activator for a cell cycle degradation machine.* Mol Cell, 2007. **27**(1): p. 3-16.
261. Yu, M., Q. Zhan, and O.J. Finn, *Immune recognition of cyclin B1 as a tumor antigen is a result of its overexpression in human tumors that is caused by non-functional p53.* Mol Immunol, 2002. **38**(12-13): p. 981-7.
262. Piovan, C., et al., *Oncosuppressive role of p53-induced miR-205 in triple negative breast cancer.* Mol Oncol, 2012. **6**(4): p. 458-72.
263. Wang, J., et al., *Downregulation of miR-486-5p contributes to tumor progression and metastasis by targeting protumorigenic ARHGAP5 in lung cancer.* Oncogene, 2014. **33**(9): p. 1181-9.
264. Chen, L., et al., *miR-1207-5p and miR-1266 suppress gastric cancer growth and invasion by targeting telomerase reverse transcriptase.* Cell Death Dis, 2014. **5**: p. e1034.
265. Gao, X. and W. Jin, *The emerging role of tumor-suppressive microRNA-218 in targeting glioblastoma stemness.* Cancer Lett, 2014. **353**(1): p. 25-31.
266. Li, M., et al., *miR-92a family and their target genes in tumorigenesis and metastasis.* Exp Cell Res, 2014. **323**(1): p. 1-6.
267. Hwang, M.S., et al., *miR-221/222 targets adiponectin receptor 1 to promote the epithelial-to-mesenchymal transition in breast cancer.* PLoS One, 2013. **8**(6): p. e66502.
268. Menendez, D., et al., *Diverse stresses dramatically alter genome-wide p53 binding and transactivation landscape in human cancer cells.* Nucleic Acids Res, 2013. **41**(15): p. 7286-301.
269. Idogawa, M., et al., *Identification and analysis of large intergenic non-coding RNAs regulated by p53 family members through a genome-wide analysis of p53-binding sites.* Hum Mol Genet, 2014. **23**(11): p. 2847-57.

270. Takei, Y., et al., *Isolation of a novel TP53 target gene from a colon cancer cell line carrying a highly regulated wild-type TP53 expression system.* Genes Chromosomes Cancer, 1998. **23**(1): p. 1-9.
271. Chien, C.H., et al., *Identifying transcriptional start sites of human microRNAs based on high-throughput sequencing data.* Nucleic Acids Res, 2011. **39**(21): p. 9345-56.
272. Chang, G.S., et al., *A comprehensive and high-resolution genome-wide response of p53 to stress.* Cell Rep, 2014. **8**(2): p. 514-27.
273. Schlereth, K., et al., *Characterization of the p53 cistrome--DNA binding cooperativity dissects p53's tumor suppressor functions.* PLoS Genet, 2013. **9**(8): p. e1003726.
274. Subramanian, A., et al., *Gene set enrichment analysis: a knowledge-based approach for interpreting genome-wide expression profiles.* Proc Natl Acad Sci U S A, 2005. **102**(43): p. 15545-50.
275. Liberzon, A., et al., *Molecular signatures database (MSigDB) 3.0.* Bioinformatics, 2011. **27**(12): p. 1739-40.
276. Pulikkan, J.A., et al., *C/EBPalpha regulated microRNA-34a targets E2F3 during granulopoiesis and is down-regulated in AML with CEBPA mutations.* Blood, 2010. **116**(25): p. 5638-49.
277. Zauli, G., et al., *miR-34a induces the downregulation of both E2F1 and B-Myb oncogenes in leukemic cells.* Clin Cancer Res, 2011. **17**(9): p. 2712-24.
278. Leone, G., et al., *E2F3 activity is regulated during the cell cycle and is required for the induction of S phase.* Genes Dev, 1998. **12**(14): p. 2120-30.
279. Ohtani, K., et al., *Cell growth-regulated expression of mammalian MCM5 and MCM6 genes mediated by the transcription factor E2F.* Oncogene, 1999. **18**(14): p. 2299-309.
280. Tsuruga, H., et al., *HsMCM6: a new member of the human MCM/P1 family encodes a protein homologous to fission yeast Mis5.* Genes Cells, 1997. **2**(6): p. 381-99.
281. Kel, A.E., et al., *Computer-assisted identification of cell cycle-related genes: new targets for E2F transcription factors.* J Mol Biol, 2001. **309**(1): p. 99-120.
282. Ma, Y., et al., *Identification of novel E2F1-regulated genes by microarray.* Arch Biochem Biophys, 2002. **399**(2): p. 212-24.
283. Alon, U., *Network motifs: theory and experimental approaches.* Nat Rev Genet, 2007. **8**(6): p. 450-61.
284. Liu, K., et al., *regulates autophagy and apoptosis by targeting in the retinoblastoma cell.* Autophagy, 2014. **10**(3).
285. Alon, U., et al., *Broad patterns of gene expression revealed by clustering analysis of tumor and normal colon tissues probed by oligonucleotide arrays.* Proc Natl Acad Sci U S A, 1999. **96**(12): p. 6745-50.
286. Buchholz, M., et al., *Transcriptome analysis of microdissected pancreatic intraepithelial neoplastic lesions.* Oncogene, 2005. **24**(44): p. 6626-36.
287. Tomlins, S.A., et al., *Integrative molecular concept modeling of prostate cancer progression.* Nat Genet, 2007. **39**(1): p. 41-51.
288. Finak, G., et al., *Stromal gene expression predicts clinical outcome in breast cancer.* Nat Med, 2008. **14**(5): p. 518-27.

289. Badea, L., et al., *Combined gene expression analysis of whole-tissue and microdissected pancreatic ductal adenocarcinoma identifies genes specifically overexpressed in tumor epithelia.* Hepatogastroenterology, 2008. **55**(88): p. 2016-27.
290. Cho, J.Y., et al., *Gene expression signature-based prognostic risk score in gastric cancer.* Clin Cancer Res, 2011. **17**(7): p. 1850-7.
291. Hong, Y., et al., *A susceptibility gene set for early onset colorectal cancer that integrates diverse signaling pathways: implication for tumorigenesis.* Clin Cancer Res, 2007. **13**(4): p. 1107-14.
292. Richardson, A.L., et al., *X chromosomal abnormalities in basal-like human breast cancer.* Cancer Cell, 2006. **9**(2): p. 121-32.
293. Iacobuzio-Donahue, C.A., et al., *Exploration of global gene expression patterns in pancreatic adenocarcinoma using cDNA microarrays.* Am J Pathol, 2003. **162**(4): p. 1151-62.
294. Maruyama, R., et al., *Comparative genome analysis identifies the vitamin D receptor gene as a direct target of p53-mediated transcriptional activation.* Cancer Res, 2006. **66**(9): p. 4574-83.
295. Thiery, J.P., et al., *Epithelial-mesenchymal transitions in development and disease.* Cell, 2009. **139**(5): p. 871-90.
296. Roy, H.K., et al., *The transcriptional repressor SNAIL is overexpressed in human colon cancer.* Dig Dis Sci, 2005. **50**(1): p. 42-6.
297. Polyak, K. and R.A. Weinberg, *Transitions between epithelial and mesenchymal states: acquisition of malignant and stem cell traits.* Nat Rev Cancer, 2009. **9**(4): p. 265-73.
298. Zhu, L.F., et al., *Snail overexpression induces an epithelial to mesenchymal transition and cancer stem cell-like properties in SCC9 cells.* Lab Invest, 2012. **92**(5): p. 744-52.
299. Lu, Z.Y., et al., *SNAI1 overexpression induces stemness and promotes ovarian cancer cell invasion and metastasis.* Oncol Rep, 2012. **27**(5): p. 1587-91.
300. Zhou, W., et al., *Snail contributes to the maintenance of stem cell-like phenotype cells in human pancreatic cancer.* PLoS One, 2014. **9**(1): p. e87409.
301. Han, X.Y., et al., *Epithelial-mesenchymal transition associates with maintenance of stemness in spheroid-derived stem-like colon cancer cells.* PLoS One, 2013. **8**(9): p. e73341.
302. Hwang, W.L., et al., *SNAIL regulates interleukin-8 expression, stem cell-like activity, and tumorigenicity of human colorectal carcinoma cells.* Gastroenterology, 2011. **141**(1): p. 279-91, 291 e1-5.
303. Horvay, K., et al., *Wnt signaling regulates Snai1 expression and cellular localization in the mouse intestinal epithelial stem cell niche.* Stem Cells Dev, 2011. **20**(4): p. 737-45.
304. Bu, P., et al., *A microRNA miR-34a-regulated bimodal switch targets Notch in colon cancer stem cells.* Cell Stem Cell, 2013. **12**(5): p. 602-15.
305. Siemens, H., et al., *Repression of c-Kit by p53 is mediated by miR-34 and is associated with reduced chemoresistance, migration and stemness.* Oncotarget, 2013. **4**(9): p. 1399-415.
306. Zhao, J., et al., *TP53-independent function of miR-34a via HDAC1 and p21(CIP1/WAF1.).* Mol Ther, 2013. **21**(9): p. 1678-86.

307. Peinado, H., et al., *Snail mediates E-cadherin repression by the recruitment of the Sin3A/histone deacetylase 1 (HDAC1)/HDAC2 complex.* Mol Cell Biol, 2004. **24**(1): p. 306-19.
308. Ren, D., et al., *Wild-type p53 suppresses the epithelial-mesenchymal transition and stemness in PC-3 prostate cancer cells by modulating miR145.* Int J Oncol, 2013. **42**(4): p. 1473-81.
309. Dong, P., et al., *Mutant p53 gain-of-function induces epithelial-mesenchymal transition through modulation of the miR-130b-ZEB1 axis.* Oncogene, 2013. **32**(27): p. 3286-95.
310. Lim, S.O., H. Kim, and G. Jung, *p53 inhibits tumor cell invasion via the degradation of snail protein in hepatocellular carcinoma.* FEBS Lett, 2010. **584**(11): p. 2231-6.
311. Mehta, S.A., et al., *Negative regulation of chemokine receptor CXCR4 by tumor suppressor p53 in breast cancer cells: implications of p53 mutation or isoform expression on breast cancer cell invasion.* Oncogene, 2007. **26**(23): p. 3329-37.
312. Lu, M., et al., *MicroRNA-based regulation of epithelial-hybrid-mesenchymal fate determination.* Proc Natl Acad Sci U S A, 2013. **110**(45): p. 18144-9.
313. Moes, M., et al., *A novel network integrating a miRNA-203/SNAI1 feedback loop which regulates epithelial to mesenchymal transition.* PLoS One, 2012. **7**(4): p. e35440.
314. Nieto, M.A., *Epithelial plasticity: a common theme in embryonic and cancer cells.* Science, 2013. **342**(6159): p. 1234850.
315. Brabletz, T., et al., *Variable beta-catenin expression in colorectal cancers indicates tumor progression driven by the tumor environment.* Proc Natl Acad Sci U S A, 2001. **98**(18): p. 10356-61.
316. Peinado, H., M. Quintanilla, and A. Cano, *Transforming growth factor beta-1 induces snail transcription factor in epithelial cell lines: mechanisms for epithelial mesenchymal transitions.* J Biol Chem, 2003. **278**(23): p. 21113-23.
317. Vega, S., et al., *Snail blocks the cell cycle and confers resistance to cell death.* Genes Dev, 2004. **18**(10): p. 1131-43.
318. Lodygin, D., et al., *Inactivation of miR-34a by aberrant CpG methylation in multiple types of cancer.* Cell Cycle, 2008. **7**(16): p. 2591-600.
319. Toyota, M., et al., *Epigenetic silencing of microRNA-34b/c and B-cell translocation gene 4 is associated with CpG island methylation in colorectal cancer.* Cancer Res, 2008. **68**(11): p. 4123-32.
320. Vogt, M., et al., *Frequent concomitant inactivation of miR-34a and miR-34b/c by CpG methylation in colorectal, pancreatic, mammary, ovarian, urothelial, and renal cell carcinomas and soft tissue sarcomas.* Virchows Arch, 2011. **458**(3): p. 313-22.
321. Siemens, H., et al., *Detection of miR-34a promoter methylation in combination with elevated expression of c-Met and beta-catenin predicts distant metastasis of colon cancer.* Clin Cancer Res, 2013. **19**(3): p. 710-20.
322. Wei, J.S., et al., *The MYCN oncogene is a direct target of miR-34a.* Oncogene, 2008. **27**(39): p. 5204-13.
323. Chen, Y., et al., *Nanoparticles modified with tumor-targeting scFv deliver siRNA and miRNA for cancer therapy.* Mol Ther, 2010. **18**(9): p. 1650-6.

324. Pramanik, D., et al., *Restitution of tumor suppressor microRNAs using a systemic nanovector inhibits pancreatic cancer growth in mice.* Mol Cancer Ther, 2011. **10**(8): p. 1470-80.
325. Wiggins, J.F., et al., *Development of a lung cancer therapeutic based on the tumor suppressor microRNA-34.* Cancer Res, 2010. **70**(14): p. 5923-30.
326. Bader, A.G., *miR-34 - a microRNA replacement therapy is headed to the clinic.* Front Genet, 2012. **3**: p. 120.
327. Ling, H., M. Fabbri, and G.A. Calin, *MicroRNAs and other non-coding RNAs as targets for anticancer drug development.* Nat Rev Drug Discov, 2013. **12**(11): p. 847-65.
328. Botcheva, K., et al., *Distinct p53 genomic binding patterns in normal and cancer-derived human cells.* Cell Cycle, 2011. **10**(24): p. 4237-49.
329. Wei, C.L., et al., *A global map of p53 transcription-factor binding sites in the human genome.* Cell, 2006. **124**(1): p. 207-19.
330. Zheng, R. and G.A. Blobel, *GATA Transcription Factors and Cancer.* Genes Cancer, 2010. **1**(12): p. 1178-88.
331. Bartunek, P., et al., *GATA-1 and c-myb crosstalk during red blood cell differentiation through GATA-1 binding sites in the c-myb promoter.* Oncogene, 2003. **22**(13): p. 1927-35.
332. Munugalavadla, V., et al., *Repression of c-kit and its downstream substrates by GATA-1 inhibits cell proliferation during erythroid maturation.* Mol Cell Biol, 2005. **25**(15): p. 6747-59.
333. Rylski, M., et al., *GATA-1-mediated proliferation arrest during erythroid maturation.* Mol Cell Biol, 2003. **23**(14): p. 5031-42.
334. Trainor, C.D., et al., *GATA-1 associates with and inhibits p53.* Blood, 2009. **114**(1): p. 165-73.
335. Gregory, T., et al., *GATA-1 and erythropoietin cooperate to promote erythroid cell survival by regulating bcl-xL expression.* Blood, 1999. **94**(1): p. 87-96.
336. Yan, W., et al., *GATA3 inhibits breast cancer metastasis through the reversal of epithelial-mesenchymal transition.* J Biol Chem, 2010. **285**(18): p. 14042-51.
337. van Hamburg, J.P., et al., *Cooperation of Gata3, c-Myc and Notch in malignant transformation of double positive thymocytes.* Mol Immunol, 2008. **45**(11): p. 3085-95.
338. Li, M., et al., *Distinct regulatory mechanisms and functions for p53-activated and p53-repressed DNA damage response genes in embryonic stem cells.* Mol Cell, 2012. **46**(1): p. 30-42.
339. Hermeking, H., *MicroRNAs in the p53 network: micromanagement of tumour suppression.* Nat Rev Cancer, 2012. **12**(9): p. 613-26.
340. Yu, J., et al., *Identification and classification of p53-regulated genes.* Proc Natl Acad Sci U S A, 1999. **96**(25): p. 14517-22.
341. Zhao, R., et al., *Analysis of p53-regulated gene expression patterns using oligonucleotide arrays.* Genes Dev, 2000. **14**(8): p. 981-93.
342. Oh, H.K., et al., *Genomic loss of miR-486 regulates tumor progression and the OLFM4 antiapoptotic factor in gastric cancer.* Clin Cancer Res, 2011. **17**(9): p. 2657-67.

343. Pang, W., et al., *Pim-1 kinase is a target of miR-486-5p and eukaryotic translation initiation factor 4E, and plays a critical role in lung cancer.* Mol Cancer, 2014. **13**: p. 240.
344. Zhang, G., et al., *MicroRNA-486-5p targeting PIM-1 suppresses cell proliferation in breast cancer cells.* Tumour Biol, 2014. **35**(11): p. 11137-45.
345. Huang, X.P., et al., *Microrna-486-5p, downregulated in hepatocelluar carcinoma, suppresses tumor growth by targeting p85alpha.* FEBS J, 2014.
346. Sanchez, Y., et al., *Genome-wide analysis of the human p53 transcriptional network unveils a lncRNA tumour suppressor signature.* Nat Commun, 2014. **5**: p. 5812.
347. Huarte, M. and J.L. Rinn, *Large non-coding RNAs: missing links in cancer?* Hum Mol Genet, 2010. **19**(R2): p. R152-61.
348. Lee, G.L., A. Dobi, and S. Srivastava, *Prostate cancer: diagnostic performance of the PCA3 urine test.* Nat Rev Urol, 2011. **8**(3): p. 123-4.
349. Tomlins, S.A., et al., *Urine TMPRSS2:ERG fusion transcript stratifies prostate cancer risk in men with elevated serum PSA.* Sci Transl Med, 2011. **3**(94): p. 94ra72.
350. Xie, H., H. Ma, and D. Zhou, *Plasma HULC as a promising novel biomarker for the detection of hepatocellular carcinoma.* Biomed Res Int, 2013. **2013**: p. 136106.
351. Castanotto, D. and J.J. Rossi, *The promises and pitfalls of RNA-interference-based therapeutics.* Nature, 2009. **457**(7228): p. 426-33.
352. Davis, M.E., et al., *Evidence of RNAi in humans from systemically administered siRNA via targeted nanoparticles.* Nature, 2010. **464**(7291): p. 1067-70.
353. Li, C.H. and Y. Chen, *Targeting long non-coding RNAs in cancers: progress and prospects.* Int J Biochem Cell Biol, 2013. **45**(8): p. 1895-910.
354. Kolfschoten, I.G., et al., *A genetic screen identifies PITX1 as a suppressor of RAS activity and tumorigenicity.* Cell, 2005. **121**(6): p. 849-58.
355. Ohta, M., et al., *Decreased expression of the RAS-GTPase activating protein RASAL1 is associated with colorectal tumor progression.* Gastroenterology, 2009. **136**(1): p. 206-16.
356. Chen, H., et al., *Hypermethylation and clinicopathological significance of RASAL1 gene in gastric cancer.* Asian Pac J Cancer Prev, 2013. **14**(11): p. 6261-5.
357. Chen, H., et al., *In vivo and in vitro expression of the RASAL1 gene in human gastric adenocarcinoma and its clinicopathological significance.* Oncol Lett, 2012. **3**(3): p. 535-540.
358. Liu, D., et al., *Identification of RASAL1 as a major tumor suppressor gene in thyroid cancer.* J Natl Cancer Inst, 2013. **105**(21): p. 1617-27.
359. Qiao, F., et al., *Enforced expression of RASAL1 suppresses cell proliferation and the transformation ability of gastric cancer cells.* Oncol Rep, 2012. **28**(4): p. 1475-81.
360. Seto, M., et al., *Reduced expression of RAS protein activator like-1 in gastric cancer.* Int J Cancer, 2011. **128**(6): p. 1293-302.
361. Chen, H., et al., *RASAL1 Attenuates Gastric Carcinogenesis in Nude Mice by Blocking RAS/ERK Signaling.* Asian Pac J Cancer Prev, 2015. **16**(3): p. 1077-82.

362. Kosa, P., et al., *Suppression of Tumorigenicity-14, encoding matriptase, is a critical suppressor of colitis and colitis-associated colon carcinogenesis.* Oncogene, 2012. **31**(32): p. 3679-95.
363. Wang, Y., et al., *ST14 (suppression of tumorigenicity 14) gene is a target for miR-27b, and the inhibitory effect of ST14 on cell growth is independent of miR-27b regulation.* J Biol Chem, 2009. **284**(34): p. 23094-106.
364. Lin, P.C., et al., *Clinical Relevance of Plasma DNA Methylation in Colorectal Cancer Patients Identified by Using a Genome-Wide High-Resolution Array.* Ann Surg Oncol, 2014.
365. Omura, N., et al., *Genome-wide profiling of methylated promoters in pancreatic adenocarcinoma.* Cancer Biol Ther, 2008. **7**(7): p. 1146-56.
366. Deisenroth, C., et al., *Mitochondrial Hep27 is a c-Myb target gene that inhibits Mdm2 and stabilizes p53.* Mol Cell Biol, 2010. **30**(16): p. 3981-93.
367. Hibino, S., et al., *Reduced expression of DENND2D through promoter hypermethylation is an adverse prognostic factor in squamous cell carcinoma of the esophagus.* Oncol Rep, 2014. **31**(2): p. 693-700.
368. Kanda, M., et al., *Downregulation of DENND2D by promoter hypermethylation is associated with early recurrence of hepatocellular carcinoma.* Int J Oncol, 2014. **44**(1): p. 44-52.
369. Ling, B., et al., *Suppression of non-small cell lung cancer proliferation and tumorigenicity by DENND2D.* Lung Cancer, 2013. **79**(2): p. 104-10.
370. Li, B., et al., *The role of TGFBI in mesothelioma and breast cancer: association with tumor suppression.* BMC Cancer, 2012. **12**: p. 239.
371. Wen, G., et al., *Transforming growth factor-beta-induced protein (TGFBI) suppresses mesothelioma progression through the Akt/mTOR pathway.* Int J Oncol, 2011. **39**(4): p. 1001-9.
372. Wen, G., et al., *TGFBI expression reduces in vitro and in vivo metastatic potential of lung and breast tumor cells.* Cancer Lett, 2011. **308**(1): p. 23-32.
373. Irigoyen, M., et al., *TGFBI expression is associated with a better response to chemotherapy in NSCLC.* Mol Cancer, 2010. **9**: p. 130.
374. Zhang, Y., et al., *TGFBI deficiency predisposes mice to spontaneous tumor development.* Cancer Res, 2009. **69**(1): p. 37-44.
375. Zhu, J., et al., *TGFBI protein high expression predicts poor prognosis in colorectal cancer patients.* Int J Clin Exp Pathol, 2015. **8**(1): p. 702-10.
376. Ma, C., et al., *Extracellular matrix protein betaig-h3/TGFBI promotes metastasis of colon cancer by enhancing cell extravasation.* Genes Dev, 2008. **22**(3): p. 308-21.
377. Nummela, P., et al., *Transforming growth factor beta-induced (TGFBI) is an anti-adhesive protein regulating the invasive growth of melanoma cells.* Am J Pathol, 2012. **180**(4): p. 1663-74.
378. Wu, G., et al., *LOXL1 and LOXL4 are epigenetically silenced and can inhibit ras/extracellular signal-regulated kinase signaling pathway in human bladder cancer.* Cancer Res, 2007. **67**(9): p. 4123-9.
379. Gorogh, T., et al., *Selective upregulation and amplification of the lysyl oxidase like-4 (LOXL4) gene in head and neck squamous cell carcinoma.* J Pathol, 2007. **212**(1): p. 74-82.

380. Holtmeier, C., et al., *Overexpression of a novel lysyl oxidase-like gene in human head and neck squamous cell carcinomas.* Anticancer Res, 2003. **23**(3B): p. 2585-91.
381. Li, R.K., et al., *Lysyl oxidase-like 4 (LOXL4) promotes proliferation and metastasis of gastric cancer via FAK/Src pathway.* J Cancer Res Clin Oncol, 2015. **141**(2): p. 269-81.
382. Kirschmann, D.A., et al., *A molecular role for lysyl oxidase in breast cancer invasion.* Cancer Res, 2002. **62**(15): p. 4478-83.
383. Yang, H., et al., *Effect of over-expressed LRIG3 on cell cycle and survival of glioma cells.* J Huazhong Univ Sci Technolog Med Sci, 2011. **31**(5): p. 667-72.
384. Qi, Y., et al., *Over-expression of LRIG3 suppresses growth and invasion of bladder cancer cells.* J Huazhong Univ Sci Technolog Med Sci, 2013. **33**(1): p. 111-6.
385. Yuan, X., et al., *Effect of silencing LRIG3 gene on the proliferation and apoptosis of bladder cancer T24 cells.* J Huazhong Univ Sci Technolog Med Sci, 2011. **31**(2): p. 220-5.
386. Kim, D.H., et al., *The E2F1 oncogene transcriptionally regulates NELL2 in cancer cells.* DNA Cell Biol, 2013. **32**(9): p. 517-23.
387. Alvarez-Diaz, S., et al., *MicroRNA-22 is induced by vitamin D and contributes to its antiproliferative, antimigratory and gene regulatory effects in colon cancer cells.* Hum Mol Genet, 2012. **21**(10): p. 2157-65.
388. Nasarre, P., et al., *Neuropilin-2 Is upregulated in lung cancer cells during TGF-beta1-induced epithelial-mesenchymal transition.* Cancer Res, 2013. **73**(23): p. 7111-21.
389. Grandclement, C., et al., *Neuropilin-2 expression promotes TGF-beta1-mediated epithelial to mesenchymal transition in colorectal cancer cells.* PLoS One, 2011. **6**(7): p. e20444.
390. Hayden Gephart, M.G., et al., *Neuropilin-2 contributes to tumorigenicity in a mouse model of Hedgehog pathway medulloblastoma.* J Neurooncol, 2013. **115**(2): p. 161-8.
391. Chen, T.M., et al., *Overexpression of FGF9 in colon cancer cells is mediated by hypoxia-induced translational activation.* Nucleic Acids Res, 2014. **42**(5): p. 2932-44.
392. Teishima, J., et al., *Accumulation of FGF9 in prostate cancer correlates with epithelial-to-mesenchymal transition and induction of VEGF-A expression.* Anticancer Res, 2014. **34**(2): p. 695-700.
393. Ohgino, K., et al., *Expression of fibroblast growth factor 9 is associated with poor prognosis in patients with resected non-small cell lung cancer.* Lung Cancer, 2014. **83**(1): p. 90-6.
394. Tang, D., et al., *High-mobility group box 1 and cancer.* Biochim Biophys Acta, 2010. **1799**(1-2): p. 131-40.
395. Kang, R., et al., *HMGB1 in cancer: good, bad, or both?* Clin Cancer Res, 2013. **19**(15): p. 4046-57.
396. Lotze, M.T. and R.A. DeMarco, *Dealing with death: HMGB1 as a novel target for cancer therapy.* Curr Opin Investig Drugs, 2003. **4**(12): p. 1405-9.
397. Uramoto, H., et al., *Physical interaction of tumour suppressor p53/p73 with CCAAT-binding transcription factor 2 (CTF2) and differential regulation of*

human high-mobility group 1 (HMG1) gene expression. Biochem J, 2003. **371**(Pt 2): p. 301-10.
398. Livesey, K.M., et al., *p53/HMGB1 complexes regulate autophagy and apoptosis.* Cancer Res, 2012. **72**(8): p. 1996-2005.
399. Livesey, K.M., et al., *Autophagy inhibition in combination cancer treatment.* Curr Opin Investig Drugs, 2009. **10**(12): p. 1269-79.
400. Chang, B.P., et al., *miR-200c inhibits metastasis of breast cancer cells by targeting HMGB1.* J Huazhong Univ Sci Technolog Med Sci, 2014. **34**(2): p. 201-6.
401. Nakamura, Y., et al., *Kruppel-like factor 12 plays a significant role in poorly differentiated gastric cancer progression.* Int J Cancer, 2009. **125**(8): p. 1859-67.
402. Fu, Y., et al., *RNA interference targeting CITRON can significantly inhibit the proliferation of hepatocellular carcinoma cells.* Mol Biol Rep, 2011. **38**(2): p. 693-702.
403. Whitworth, H., et al., *Identification of kinases regulating prostate cancer cell growth using an RNAi phenotypic screen.* PLoS One, 2012. **7**(6): p. e38950.
404. Ehrlichova, M., et al., *The association of taxane resistance genes with the clinical course of ovarian carcinoma.* Genomics, 2013. **102**(2): p. 96-101.
405. Xing, Z., et al., *lncRNA Directs Cooperative Epigenetic Regulation Downstream of Chemokine Signals.* Cell, 2014. **159**(5): p. 1110-25.
406. Merkel, A.L., E. Meggers, and M. Ocker, *PIM1 kinase as a target for cancer therapy.* Expert Opin Investig Drugs, 2012. **21**(4): p. 425-36.
407. Fearon, E.R. and B. Vogelstein, *A genetic model for colorectal tumorigenesis.* Cell, 1990. **61**(5): p. 759-67.
408. Vassilev, L.T., *Small-molecule antagonists of p53-MDM2 binding: research tools and potential therapeutics.* Cell Cycle, 2004. **3**(4): p. 419-21.
409. Issaeva, N., et al., *Small molecule RITA binds to p53, blocks p53-HDM-2 interaction and activates p53 function in tumors.* Nat Med, 2004. **10**(12): p. 1321-8.
410. Lehmann, S., et al., *Targeting p53 in vivo: a first-in-human study with p53-targeting compound APR-246 in refractory hematologic malignancies and prostate cancer.* J Clin Oncol, 2012. **30**(29): p. 3633-9.
411. Bykov, V.J., et al., *Restoration of the tumor suppressor function to mutant p53 by a low-molecular-weight compound.* Nat Med, 2002. **8**(3): p. 282-8.
412. Gu, S., et al., *Global investigation of p53-induced apoptosis through quantitative proteomic profiling using comparative amino acid-coded tagging.* Mol Cell Proteomics, 2004. **3**(10): p. 998-1008.
413. Jenkins, L.M., et al., *Quantitative proteomics analysis of the effects of ionizing radiation in wild type and p53 K317R knock-in mouse thymocytes.* Mol Cell Proteomics, 2008. **7**(4): p. 716-27.
414. Nicholson, J., et al., *An iTRAQ proteomics screen reveals the effects of the MDM2 binding ligand Nutlin-3 on cellular proteostasis.* J Proteome Res, 2012. **11**(11): p. 5464-78.
415. Tay, Y., J. Rinn, and P.P. Pandolfi, *The multilayered complexity of ceRNA crosstalk and competition.* Nature, 2014. **505**(7483): p. 344-52.

416. Dimri, G.P., et al., *Inhibition of E2F activity by the cyclin-dependent protein kinase inhibitor p21 in cells expressing or lacking a functional retinoblastoma protein.* Mol Cell Biol, 1996. **16**(6): p. 2987-97.
417. Sherr, C.J., *Cancer cell cycles.* Science, 1996. **274**(5293): p. 1672-7.
418. Dimova, D.K. and N.J. Dyson, *The E2F transcriptional network: old acquaintances with new faces.* Oncogene, 2005. **24**(17): p. 2810-26.
419. Joyce, J.A. and D. Hanahan, *Multiple roles for cysteine cathepsins in cancer.* Cell Cycle, 2004. **3**(12): p. 1516-619.
420. Gocheva, V. and J.A. Joyce, *Cysteine cathepsins and the cutting edge of cancer invasion.* Cell Cycle, 2007. **6**(1): p. 60-4.
421. Yan, S., M. Sameni, and B.F. Sloane, *Cathepsin B and human tumor progression.* Biol Chem, 1998. **379**(2): p. 113-23.
422. Mohamed, M.M. and B.F. Sloane, *Cysteine cathepsins: multifunctional enzymes in cancer.* Nat Rev Cancer, 2006. **6**(10): p. 764-75.
423. Foekens, J.A., et al., *Prognostic significance of cathepsins B and L in primary human breast cancer.* J Clin Oncol, 1998. **16**(3): p. 1013-21.
424. Lah, T.T., et al., *Cathepsin B, a prognostic indicator in lymph node-negative breast carcinoma patients: comparison with cathepsin D, cathepsin L, and other clinical indicators.* Clin Cancer Res, 2000. **6**(2): p. 578-84.
425. Joyce, J.A., et al., *Cathepsin cysteine proteases are effectors of invasive growth and angiogenesis during multistage tumorigenesis.* Cancer Cell, 2004. **5**(5): p. 443-53.
426. Gocheva, V., et al., *Distinct roles for cysteine cathepsin genes in multistage tumorigenesis.* Genes Dev, 2006. **20**(5): p. 543-56.
427. Schagdarsurengin, U., G.P. Pfeifer, and R. Dammann, *Frequent epigenetic inactivation of cystatin M in breast carcinoma.* Oncogene, 2007. **26**(21): p. 3089-94.
428. Zhang, J., et al., *Cystatin m: a novel candidate tumor suppressor gene for breast cancer.* Cancer Res, 2004. **64**(19): p. 6957-64.
429. Shridhar, R., et al., *Cystatin M suppresses the malignant phenotype of human MDA-MB-435S cells.* Oncogene, 2004. **23**(12): p. 2206-15.
430. Vigneswaran, N., et al., *Silencing of cystatin M in metastatic oral cancer cell line MDA-686Ln by siRNA increases cysteine proteinases and legumain activities, cell proliferation and in vitro invasion.* Life Sci, 2006. **78**(8): p. 898-907.
431. Coulibaly, S., et al., *Modulation of invasive properties of murine squamous carcinoma cells by heterologous expression of cathepsin B and cystatin C.* Int J Cancer, 1999. **83**(4): p. 526-31.
432. Cox, J.L., et al., *Inhibition of B16 melanoma metastasis by overexpression of the cysteine proteinase inhibitor cystatin C.* Melanoma Res, 1999. **9**(4): p. 369-74.
433. Ervin, H. and J.L. Cox, *Late stage inhibition of hematogenous melanoma metastasis by cystatin C over-expression.* Cancer Cell Int, 2005. **5**(1): p. 14.
434. Sexton, P.S. and J.L. Cox, *Inhibition of motility and invasion of B16 melanoma by the overexpression of cystatin C.* Melanoma Res, 1997. **7**(2): p. 97-101.
435. Holick, M.F. and T.C. Chen, *Vitamin D deficiency: a worldwide problem with health consequences.* Am J Clin Nutr, 2008. **87**(4): p. 1080S-6S.

436. Clemens, T.L., et al., *Increased skin pigment reduces the capacity of skin to synthesise vitamin D3.* Lancet, 1982. **1**(8263): p. 74-6.
437. Matsuoka, L.Y., et al., *Sunscreens suppress cutaneous vitamin D3 synthesis.* J Clin Endocrinol Metab, 1987. **64**(6): p. 1165-8.
438. Webb, A.R., L. Kline, and M.F. Holick, *Influence of season and latitude on the cutaneous synthesis of vitamin D3: exposure to winter sunlight in Boston and Edmonton will not promote vitamin D3 synthesis in human skin.* J Clin Endocrinol Metab, 1988. **67**(2): p. 373-8.
439. Holick, M.F., L.Y. Matsuoka, and J. Wortsman, *Age, vitamin D, and solar ultraviolet.* Lancet, 1989. **2**(8671): p. 1104-5.
440. Wortsman, J., et al., *Decreased bioavailability of vitamin D in obesity.* Am J Clin Nutr, 2000. **72**(3): p. 690-3.
441. Selivanova, G. and K.G. Wiman, *Reactivation of mutant p53: molecular mechanisms and therapeutic potential.* Oncogene, 2007. **26**(15): p. 2243-54.
442. Matusiak, D., et al., *Expression of vitamin D receptor and 25-hydroxyvitamin D3-1{alpha}-hydroxylase in normal and malignant human colon.* Cancer Epidemiol Biomarkers Prev, 2005. **14**(10): p. 2370-6.
443. Sheinin, Y., et al., *In situ mRNA hybridization analysis and immunolocalization of the vitamin D receptor in normal and carcinomatous human colonic mucosa: relation to epidermal growth factor receptor expression.* Virchows Arch, 2000. **437**(5): p. 501-7.
444. Larriba, M.J. and A. Munoz, *SNAIL vs vitamin D receptor expression in colon cancer: therapeutics implications.* Br J Cancer, 2005. **92**(6): p. 985-9.
445. Stambolsky, P., et al., *Modulation of the vitamin D3 response by cancer-associated mutant p53.* Cancer Cell, 2010. **17**(3): p. 273-85.
446. Beer, T.M., et al., *Double-blinded randomized study of high-dose calcitriol plus docetaxel compared with placebo plus docetaxel in androgen-independent prostate cancer: a report from the ASCENT Investigators.* J Clin Oncol, 2007. **25**(6): p. 669-74.
447. Petrioli, R., et al., *Weekly high-dose calcitriol and docetaxel in patients with metastatic hormone-refractory prostate cancer previously exposed to docetaxel.* BJU Int, 2007. **100**(4): p. 775-9.
448. Kioulafa, M., et al., *Methylation of cystatin M promoter is associated with unfavorable prognosis in operable breast cancer.* Int J Cancer, 2009. **125**(12): p. 2887-92.
449. Lin, R., et al., *Expression profiling in squamous carcinoma cells reveals pleiotropic effects of vitamin D3 analog EB1089 signaling on cell proliferation, differentiation, and immune system regulation.* Mol Endocrinol, 2002. **16**(6): p. 1243-56.
450. Takahashi, H., et al., *1,25-dihydroxyvitamin D(3) increases human cystatin A expression by inhibiting the Raf-1/MEK1/ERK signaling pathway of keratinocytes.* Arch Dermatol Res, 2003. **295**(2): p. 80-7.
451. Palmer, H.G., et al., *Genetic signatures of differentiation induced by 1alpha,25-dihydroxyvitamin D3 in human colon cancer cells.* Cancer Res, 2003. **63**(22): p. 7799-806.

452. Wood, R.J., et al., *DNA microarray analysis of vitamin D-induced gene expression in a human colon carcinoma cell line.* Physiol Genomics, 2004. **17**(2): p. 122-9.
453. Barbachano, A., et al., *SPROUTY-2 and E-cadherin regulate reciprocally and dictate colon cancer cell tumourigenicity.* Oncogene, 2010. **29**(34): p. 4800-13.
454. Agger, K., et al., *The H3K27me3 demethylase JMJD3 contributes to the activation of the INK4A-ARF locus in response to oncogene- and stress-induced senescence.* Genes Dev, 2009. **23**(10): p. 1171-6.
455. De Santa, F., et al., *The histone H3 lysine-27 demethylase Jmjd3 links inflammation to inhibition of polycomb-mediated gene silencing.* Cell, 2007. **130**(6): p. 1083-94.
456. Pereira, F., et al., *KDM6B/JMJD3 histone demethylase is induced by vitamin D and modulates its effects in colon cancer cells.* Hum Mol Genet, 2011. **20**(23): p. 4655-65.
457. Palmer, H.G., et al., *The transcription factor SNAIL represses vitamin D receptor expression and responsiveness in human colon cancer.* Nat Med, 2004. **10**(9): p. 917-9.

11. ACKNOWLEDGMENT

I would like to thank a lot of people who accompanied and supported me during the last years.

First of all I am deeply grateful to my supervisor Prof. Dr. Heiko Hermeking for giving me the opportunity to perform my PhD studies in his lab. I would like to thank him for his constant support throughout my doctoral thesis, for his scientific input, ideas and helpful discussions. In addition, I would like to thank him for arranging helpful and successful collaborations.

Furthermore I would like to thank all former and present members of the AG Hermeking for their help and support over the past years. Especially I would like to thank Dr. Markus Kaller for his scientific support and helpfulness as well as for his steady motivation and encouragement. Moreover, I am grateful to Dr. Helge Siemens, Dr. Stefanie Hahn and Dr. René Jackstadt for constructive and interesting discussions and for giving me a helping hand whenever I needed it. I would also like to thank Uschi Götz for her great technical support and for her constant willingness to help with every problem in the lab.

I would like to thank the group of Prof. Dr. Bettina Warscheid, Prof. Dr. Ralf Zimmer and Prof. Dr. Gunter Meister for successful collaborations.

Additionally, I am so thankful to my family who always believed in me and who was always there. Thank you for helping me out with all the smaller and bigger problems, for your support and your never-ending encouragement!

And last but not least I would like to thank Volker for always being there and supporting me, no matter what. Thank you for your endless patience, your optimism and for always trying to put a smile on my face after a hard day in the lab!